



Faculty of Science and Technology
MASTER'S THESIS

Study program/ Specialization: Petroleum Geosciences Engineering	Spring semester, 2014 Open
Writer: Rizky Amanda Syahrul (Writer's signature)
Faculty supervisor: Chris Townsend External supervisor(s):	
Thesis title: Fault Controlled Sedimentation: A Case Study of the Kerpini Fault, Greece	
Credits (ECTS): 30	
Key words: Greece Gulf of Corinth Geology Structural Modelling Fault and Sedimentation	Pages: 112 + Enclosure: 6 + Front Page : 20 Stavanger, June 16 th , 2014

Copyright
by

Rizky Amanda Syahrul
2014

**Fault Controlled Sedimentation: A Case Study of the Kerpini Fault Block,
Greece**

By

Rizky Amanda Syahrul, BSc.

Master Thesis

Presented to the Faculty of Science and Technology

University of Stavanger

University of Stavanger

June, 2014

Acknowledgements

I would like to thank Chris Townsend for defined the problem of the thesis project, discussions and constructive critics together with Alejandro Escalona. All of the professors and staffs in Petroleum Geoscience section are thanked for all the knowledge that you share in the master study period, especially for Lisa Bingham and Andreas Habel for their full support regarding GIS program and IT in master thesis period. Thanks to for my field partner, Abder. A special mention for my entire fellow master student in University of Stavanger that makes this 2-year study was fun and interesting. Thanks to University of Stavanger for securing the funding and IGME for the permission to conduct the field works in Greece. Roxar is also thanked for the new version of RMS 2013 and YONG Technology Inc. for its free online rose diagram program which I used for my thesis project. Thanks to Indonesian community in Stavanger for their laughs and humors which make me feels like at home

Last, but not least, I would like to thank my family in Indonesia, especially for my father and brother, for their supports.

Abstract

Fault Controlled Sedimentation: A Case Study of the Kerpini Fault Block, Greece

Rizky Amanda Syahrul

University of Stavanger

Supervisor: Chris Townsend

The study area is located in Gulf of Corinth, Central Greece. The focus of the study is located in the Kerpini area. The objective of this study is to learn about fault controlled sedimentation which is related to their internal structures including sedimentary layers and facies distribution of sediments within the Kerpini Fault Block.

It has been previously proposed, based on the field observations that sedimentation occurred during faulting and that the main direction of deposition is perpendicular to the fault strike (Ford et al., 2013). However, dip of the sedimentary rocks seem to have consistent values within the half grabens which is in contrast with classical syn-sedimentary models where dips of younger rocks are lower than the older rocks as the fault increases displacement.

According to the field work observations, apart from the basement (unit 2), there are 3 syn-fault deposits package that can be distinguished in the Kerpini Fault Block: 1) Massive Conglomerate (unit 2), 2) Early Sandstone-Conglomerate (Unit 3), and 3) Late Sandstone-Conglomerate (Unit 4). Dips of the unit 2 and 3 of sedimentary rocks are almost constant with an average of 20° - 25° . The general dip directions (southeast) appear to be not directly perpendicular to the fault plane, but slightly oriented towards the maximum throw of the fault. Unit four has different bedding orientation (dipping north) and dips of the sedimentary rocks seem to have a gentler angle (some of them are almost horizontal) suggesting less influence of the fault movement. The sedimentation direction has been interpreted to have been sourced diagonal from both tips of the fault in the SW and SE as smaller grain sizes in the centre of the fault block are mapped. For the youngest sedimentary rocks (unit 4), the source has been interpreted coming from the E-W direction rivers.

A Number of modelling scenarios have been done and are suggesting the relationship between fault and sedimentation (sedimentary layers). Reverse drag would be an important factor to control the dip angles of sediments in syn-fault deposits. In addition to that, the fault evolution and its movement for each phase are important to control the sedimentary layers and sediments distribution, because it will bring an effect to the evolution of accommodation space. Although lack of decreasing dip angle of sediments towards the younger sediments can be explained by the distance of reverse drag which might be far away from the fault. It is still having slightly changes in dip angles (not completely consistent); therefore, another possibility has been proposed to explain this feature. Episodic movement of the fault is another possible answer to explain the consistent dip angles within the Kerpini Fault Block besides the classical and reverse drag controlled in syn-fault deposits configuration.

Grain size and clast components analysis in the sedimentary rocks within Kerpini Fault Block were used to compose the paleo-drainage map in the fault block. Most of the source sediments have been interpreted as coming from the south through the Vouraikos and Kerinitis River. There are smaller source sediments coming from the north due to the foot-wall uplift of the Dhoumena Fault Block. It has been interpreted that way to explain the grain size anomaly in the central part of the Kerpini Fault Block where several outcrops show bigger grains composition although it should be smaller if they follow the trend of the grain size in Kerpini Fault Block (fining to the N and WNW).

Table of Contents

<i>Table of Contents</i>	<i>i</i>
<i>List of Figures</i>	<i>iii</i>
<i>List of Tables</i>	<i>xv</i>
Chapter 1 : INTRODUCTION	1
1.1 Background	1
1.2 Problem	3
1.3 Aim and Objectives	6
1.4 Output	6
1.5 Data and Methodology	6
1.6 Previous Works	7
Chapter 2 : GEOLOGICAL SETTING	9
2.1 Regional Structural Framework	9
2.2 Regional Stratigraphy Framework	12
Chapter 3 : FAULT CONTROLLED SEDIMENTATION	14
3.1 Classical Extensional Tectono-stratigraphy Models	14
3.2 Growth Fault and Distribution of Displacements	15
3.2.1 Normal Fault Geometry	15
3.2.2 Normal Growth Fault	16
3.2.2 Reverse Drag	18
3.2.3 Sedimentation	20
Chapter 4 : FIELD WORK OBSERVATIONS	23
4.1 Stratigraphy	23
4.1.1 Pindos Carbonate Basement (Unit 1)	26
4.1.2 Massive Conglomerate (Unit 2)	27
4.1.3 Early Sandstone-Conglomerate (Unit 3)	29
4.1.4 Late Sandstone-Conglomerate (unit 4)	32
4.1.5 Relative Age of Sedimentary Units	36
4.1.5 Grain Size Distribution	36
4.2 Geomorphology	41
4.2.1 Lineament	41

4.2.2	Drainage Patterns	41
4.3	Structural Observation	43
4.3.1	Faults	43
4.3.1.1	Kerpini Fault	45
4.3.1.2	Dhoumena Fault	48
4.3.1.3	Vouraikos Fault	50
4.3.1.4	Kerinitis Fault	50
4.3.1.5	Kerpini Fault East	51
4.2.1.6	Intra Block faults	51
4.4	Kerpini Fault Block Sedimentary Layers	54
4.5	New Discoveries	56
Chapter 5 : MODEL CONSTRUCTION		57
5.1	RMS 2013	57
5.1.1	Fault Uncertainty	57
5.1.2	Fault Displacement Estimation	58
5.2	Preparation and Parameters	59
5.2.1	Faults	60
5.2.2	Horizons	60
5.2.3	Reverse Drag	60
5.2.4	Displacement Points Sets	60
5.3	Workflow	60
5.3.1	Problem and Solution	61
5.4	Models	62
5.4.1	Constant Fault Tip (Model 1)	62
5.4.2	Propagate Fault Tip (Model 2)	72
5.4.3	Propagate Fault Tip in One Direction (Model 3)	82
5.5	Kerpini Fault Block Model	92
5.6	Modelling Summary	96
Chapter 6 : DISCUSSION		98
6.1	Structural Model of the Kerpini Fault Block	98
6.1.1	Effect of reverse drag on sedimentary layers	98

6.1.2	Alternative Interpretations	98
6.2	Sedimentation of the Kerpini Fault Block	102
6.3	Evolution of the Study Area	106
Chapter 7 : CONCLUSIONS		112
REFERENCES		
APPENDIX		

List of Figures

Figure 1.1:	Location map of the studied area. (a) <i>The regional structural map of Central Greece, modified after: Moretti et al. (2003), (b) The geological map of Gulf of Corinth area from Kalavrita to Helike, modified after: Ford et al. (2013), and (c) The topographic map of study area.</i>	3
Figure 1.2:	Panoramic photograph looking west of Kerpini Fault Block. <i>Sedimentation in the Kerpini Fault Block is belongs to syn-fault succession which mostly composed by conglomerate and sandstone. The sedimentation layers in this fault block seem to have a constant value from the youngest to oldest rocks.</i>	6
Figure 1.3:	Regional crosssection from Kalavrita Fault to Helike Fault modified from Ford et al. (2013). <i>The regional cross-section showing series of normal faults in the Kalavrita area, they are dipping to north with similar dip angle. The red rectangle represents the thesis area. It is shows that the sediment in the Kerpini Fault Block deposited in the syn-sedimentary phase.</i>	8
Figure 1.4:	Schematic depositional model from Kalavrita to Helike Fault modified from Collier and Jones (2004). <i>Schematic depositional model showing that the sedimentation in the Kerpini Fault Block is started by the fluvial deposit (dark brown) and followed by the alluvial fan deposit (brown). They were deposited in the syn-sedimentary phase. The red rectangle shows the interest area.</i>	8
Figure 2.1:	Regional structural map of the Gulf of Corinth modified after: Moretti et al. (2003). <i>Gulf of Corinth is composed of series of normal faults dipping to northeast as a result of Neogene-Recent rifting deformation, they produce half grabens system. Red rectangle represents the location of study area.</i>	9

- Figure 2.2: Development of Corinth-Patras rift (Sorel, 2000). *This figure showing that the development of Conrint-Patras rift is started by the early rift along the active Chelmos Fault, the faults further north which come later are detaching.* 10
- Figure 2.3: Cross-sections showing the evolution of the rift (Ford et al., 2013). A) *N-S cross section of the elements from onshore and offshore incorporating seismic section of (Bell et al., 2008) and (Taylor et al., 2011). B) Cross-section to show the northward fault migration and the formation of Gilbert-type deltas. C) Cross-section of the initial rifting phases during the deposition of continental facies sediments.* 11
- Figure 2.4: Representative regional stratigraphy of studied are (Ford et al., 2013). *The stratigraphy in the studied area has been divided into three main groups which started from Pliocene to Upper Pliocene. The facies sediments are vary from continental facies (alluvial fan) sediments to the distal turbidite facies.* 13
- Figure 3.1: Normal fault configuration. *A schematic normal fault configuration showing that the displacement of the normal fault consists of throw (vertical) and heave (horizontal), classical tectono-stratigraphy also differentiated the sedimentation phases into three phases which are pre-fault, syn-fault, and post-fault deposit. Not only the hanging-wall move relatively down to the foot-wall, but also the foot-wall has a movement which is called as foot-wall uplift. In the direction perpendicular to the fault, the displacement tends to decrease towards zero; this point is called reverse drag.* 16
- Figure 3.2: Schematic of the fault evolutions (Gawthorpe and Leeder, 2000). *(A) fault initiation stage is marked by the several small faults in the area, (B) interaction and linkage stage is marked by the linkage of several fault and form one faults, (C) through-going fault zone is marked by the linkage most of the faults and evolved to be one big fault zone. The evolutions of the faults also bring an effect to the displacement and also the length of the faults.* 17
- Figure 3.3: Normal fault profile figures (modified after: Walsh and Watterson, 1988b). *(a) A schematic theoretical vertical profile of fault plane showing the changes of the dip angles in depth, (b) one of the examples that shows the coalfield fault with radial increase in dip, (c) dip contour map in Markham Colliery showing that the dip has different values, and (d) fault trace in plan view showing the changes of the strike towards the tip.* 18
- Figure 3.4: Cross-sections showing the reverse drag in Utah (modified after: Hamblin, 1965). *Cross-sections a and b show how the reverse drag look like based on the field observation in*

the north and south of Hurricane, Utah respectively. Figures shows that reverse drag point location can vary; it can be close to the fault or has a very far distance in the perpendicular direction to the fault. 19

Figure 3.5: One of the synthetic contours model with one single fault in the middle (modified after: Gibson et al., 1989). *The model has been setup with the initial horizontal horizon and one single fault in the middle of the horizon, and then after faulting, the contour shows that the horizon has a unique configuration where the largest displacement is located close to the fault, gradually decreasing in height in the direction perpendicular to the fault. 20*

Figure 3.6: A schematic conceptual drainage pattern in normal fault blocks (Råvnas and Steel, 1998). *The figure shows the morphology of normal fault blocks complex and the drainage pattern to transport the sediments into the basin have various possibility, some of them are coming from the perpendicular direction to the faults, parallel to the faults, and from the relay ramps. 21*

Figure 3.7: Illustration of the proposed model for the clastic sediments input (Gupta et al., 1999). *The illustrations shows the development of the faults, before the faults are linked to each other, the sediments were coming from the fault tip (relay zone) and being a source of prograding delta complex, and after that being the drowned delta complex since the faults are linked. 21*

Figure 3.8: The last stage of Tectono-sedimentary model in continental environments (Gawthorpe and Leeder, 2000). *The last stage of tectono-sedimentary model in continental environments shows there is uplift and incision of former foot-wall derived fan. It also shows how the source sediments flow through the fault, there are rivers with perpendicular direction to the faults and also parallel to the faults. 22*

Figure 4.1: Stratigraphic chart within Kerpini Fault Block. *Stratigraphic chart of 4 main units within the fault block, from oldest to youngest as the following: Pindos Carbonate, Massive Conglomerate, Early Sandstone-Conglomerate, and Late Sandstone-Conglomerate. The interpreted age is taken from Ford et al., 2013. 23*

Figure 4.2: Facies distribution map in the Kerpini Fault Block. *The map shows the distribution of sedimentary facies within the Kerpini Fault Block. The sedimentary rocks (syn-fault succession) are concentrated close to the Kerpini Fault while the Pindos Carbonate Basement (Pre-fault deposit) is located in the immediate foot-wall to the Dhoumena Fault*

and the relationship between those two types of rocks is unconformity. The syn-fault succession can be distinguished into 4 main units. The basement outcrops at the Vouraikos Valley align with the topographical expression indicate the presence of the normal fault. . 26

Figure 4.3: Photopgraph of basement lithology at the foot-wall of Kerpini Fault. *The basement in this area is Pindos Carbonate (Limestone) with a very massive and compact structure. The figure shows that the basement has chaotic layers because of the deformation. 26*

Figure 4.4: Photograph of conglomerate outcrop at the Roghi Mountain close to the Vouraikos Valley (unit 2). *The Roghi Mountain is composed of mostly conglomerates with very big boulder grains and massive structure, difficult to see the bedding up close, the red dashed line represents the bedding interpretation striking N140°E and dipping 28°SW..... 28*

Figure 4.5: Rose Diagram of sedimentary layers in Massive Conglomerate unit (unit 2). *(a) The trend of dip direction of Massive Conglomerate unit showing NE-SW (N230°E) trend with (b) an average dip angle of 20°-25°. 29*

Figure 4.6: A representative outcrop for the conglomerate in Early Sandstone-Conglomerate unit (unit 3). *The conglomerate of this unit is characterized by the massive structure, and big boulder grain size with some inclusion of sandstone insets. Chaotic conglomerate's grains organization suggest the debris flow mechanism sedimentation..... 30*

Figure 4.7: Photographs showing the sandstone character. *(a) the panoramic photograph showing the relationship between the conglomerate and sandstone facies in this unit. There are some of sandstone sheets with a channel shape surrounded by conglomerate. (b) The detail of sandstone succesion showing the graded bedding sediment structure with the variation of the grain size..... 31*

Figure 4.8: Rose Diagram of measured strikes and dips in Early Sandstone-Conglomerate unit. *(a) The dip direction of the sedimentary layers showing N165°E trend and (b) the dip angles of the sedimentary layers are mostly dipping 20°. 32*

Figure 4.9: Photograph looking east. *A photograph shows the sedimentary layers of unit 4 (a) and the interpretation (b). The sedimentary layers are dipping to the north with 5°-10° of dip angle. There is an onlap relationship between this sediment with the basement, where the conglomerate and sandstone is dying towards the basement, there is also unconformity between them. 34*

- Figure 4.10: A photograph looking east from Roghi to the Roghi Mountain. *It shows the relationship between Massive Conglomerate, Late Sandstone-Conglomerate, and Pindos Carbonate. In this picture there are two unconformities, first is the unconformity between Pindos Carbonate and Sediments, and last, is the unconformity between unit 2 and unit 4. It shows also the sedimentary layers, in unit 2 Deposit, the layers seem to have dipping to south, but in the last facies, the layers seem to be flat (it shows a clear dip angle change). This implies that it should be boundary between the unit 2 and 4, it may related to incised fault block and subsequent river channel flow and carry sediments, which might be an unconformity between them.* 35
- Figure 4.11: Rose diagram of sedimentary layers in Late Sandstone-Conglomerate unit. (a) *The rose diagram shows two trends of dip direction (NE-SW and close N-S).* (b) *North dipping layers have a average of dip angle from 3° - 15° , whilst south dipping layers have a trend 5° and there are also gentle layer sediments with dip angles less than 5° . Those steeper dips have been interpreted as the collapsed layer (not true dips).* 36
- Figure 4.12: Grain size map distribution of sediments within Kerpini Fault Block. *The grain size map distribution shows the general trend of fining northward for all of the sediments within the Kerpini Fault Block and coarsening upwards only can be observed in the Roghi Mountain section.* 38
- Figure 4.13: Cross-section P-Q shows south to north section. *This section is showing that the general trend of grain size within the Kerpini Fault Block is fining northwards and coarsening upward, this interpretation is supported by the filed photo which may represent the real condition in the field.*..... 39
- Figure 4.14: Cross-section R-S shows west to east section of Roghi Mountain. *This Cross-section is showing the trend analysis for internal Roghi Mountain from west to north, the reconstruction reveals that the grain size of sediments in Roghi Mountain is tend to be smaller to the west and bigger to the east, it may implies to the paleo-drainage or source sediment analysis.*..... 40
- Figure 4.15: Digital Elevation Map (DEM) of the Kerpini Fault Block. *The map shows the elevation map of Kerpini Fault Block where it is bounded by the Kerpini and Dhoumena Fault at south and north, the Vouraikos and Kerinitis Rivers/Valleys at east and west parts. The rose diagram has been produced to show the lineament analysis using this map which*

tells the trend of lineament is striking $N280^{\circ} - 300^{\circ}E$ (the black lines represent lineaments). Green polygons represent dendritic river pattern while red polygons represent parallel river pattern..... 43

Figure 4.16: Structural map of the Kerpini Fault Block. *The geological map shows the distribution of basement (pre-fault deposit) and sedimentary rocks (syn-fault deposit) in the Kerpini Fault Block. Hanging-wall of the Kerpini Fault is consisted of mostly sedimentary rocks while the foot-wall is consisted of the basement. The basement exposure in foot-wall is the result of the foot-wall uplift erosion. In this fault block, there are 2 certain main faults and 4 interpreted faults. In addition to that, there are valleys at the eastern and western part that could be fault.* 45

Figure 4.17: Schematic figure to calculate throw of the fault. *Throw is calculated using the projected minimum surface of foot-wall uplift and sediments.....* 45

Figure 4.18: Photograph looking west of the Kerpini Fault Block. (a) *A panoramic photograph looking west of Kerpini Fault (taken from Souvardho Village). (b) Illustration of the interpretation from the photo, foot-wall of the Kerpini Fault is mostly composed of Pindos Carbonate Basement whilst the hanging-wall is composed of syn-fault succession (conglomerates and sandstones) with Pindos Carbonate Basement in the immediate foot-wall of Dhoumena Fault. There is an unconformity in this fault block which is related to the erosion of foot-wall uplift.* 48

Figure 4.19: Photograph looking west of the Dhoumena Fault. (a) *A panoramic photograph looking west of Kerpini Fault (taken from Monestary). (b) Illustration of the interpretation based on the photograph, Dhoumena Fault is striking NW-SW and dipping to NE. In the immediate footwal of Dhoumena Fault which is part of Kerpini Fault Block, there is an unconformity which marked by the syn-faul deposit on the top of Pindos Carbonate Basement. Moreover, the sediments are dipping to SW for except for the gentle layers of sediment at the top of syn-fault succession. Opposite to that, the sediments in Dhoumena Fault Block show the different dip direction, they are mostly dipping to NE.* 49

Figure 4.20: Cross sections through the Kerpini Fault Block. *Cross sections are showing the structural configuration within Kerpini Fault Block and their relationship between faults, basements, and sediments.* 54

- Figure 4.21: Rose diagram of the measured strikes and dips in the Kerpini Fault Block. (a) Rose diagram shows the distribution of dips direction in the kerpini Fault Block, it can be seen that most of the sediments are dipping to the SE. (b) Rose diagram shows the distribution of dips angle, most of the sediments have a dip angle around 20° - 25° 55
- Figure 5.1: Fault uncertainty tab in RMS 2013. The figure shows the interface of fault uncertainty module in RMS 2013, in this window, geo-modellers could change the position, dip, strike, throw of the faults. 58
- Figure 5.2: Schematic modelling preparation and parameters steps, figure shows the things that have done in preparation phase and all the parameters which used for the modeling..... 59
- Figure 5.3: Modelling workflow illustration, this illustrations shows how the modeling was conducted, it starts with figure 1) initial geological condition with horizontal surface and no fault is involved, move to number 2) fault was stars to move and create a depocentre and filled by the sediments, next to number 3) second phase of fault movement and sediments infill the space, last is number 4) fault was keep move and the space was filled by the sediments. 61
- Figure 5.4: Length Vs displacement plot of model 1. The plot shows relationship between length and displacement for each horizon in model 1, it shows that the fault tip is constant. 63
- Figure 5.5: Structural map of horizon 1 (model 1 - class 1). The structural map shows the structural configuration in the final evolution of model, the fault has 10000m in length with maximum throw (2000m) at the centre of the fault and gradually decreases towards the fault tip. 64
- Figure 5.6: Group of cross-sections of model 1 - class 1. This group of cross-sections shows variation in structural of sedimentary layers across the fault block. Cross-sections (perpendicular to the fault) bring an idea about the dip of sediment while the strike-sections show the sediments distribution. (VE= 1:1) 65
- Figure 5.7: Structural map of horizon 1 (model 1 - class 2). The structural map of horizon 1 shows the structural configuration of class 2, where the reverse drag distance was setup for 5000m, the fundamental difference compared to the class 1 is just the dimension of accommodation space and foot-wall uplift..... 66
- Figure 5.8: Group of cross-sections of model 1 - class 2. This group of cross-sections shows variation in structural of sedimentary layers across the fault block. Cross-sections

(perpendicular to the fault) bring an idea about the dip of sediment while the strike-sections show the sediments distribution. It shows the longer reverse drag distance will produce a bigger space for sediments and less decreasing dip angle towards the younger sediments. (VE= 1:1)..... 68

Figure 5.9: Structural map of horizon 1 (model 1 - class 3). *The structural map of horizon 1 shows the structural configuration of class 3, where the reverse drag distance was setup for 8000m, the fundamental difference compared to the class 1 and 2 is just the dimension of accommodation space and foot-wall uplift which can be observed from the structure maps. 69*

Figure 5.10: Group of cross-sections of model 1 - class 3. *This group of cross-sections shows variation in structural of sedimentary layers across the fault block. Cross-sections (perpendicular to the fault) bring an idea about the dip of sediment while the strike-sections show the sediments distribution. Comparing class 1, 2, and 3, it seems that the longer reverse drag distance will produce a bigger space for sediments and less decreasing dip angle towards the younger sediments. (VE= 1:1) 71*

Figure 5.11: Length (in X-axis) Vs displacement plot of model 2. *The plot shows relationship between length and displacement for each horizon in model 2, it shows that the fault tip are propagate to the west and east at the same propagation rate, and it is also constant in term of the fault development, there is no acceleration or slowness for the propagation rate when the fault starts to move and stops. 72*

Figure 5.12: Structural map of horizon 1 (model 2 - class 1). *The structural map shows the structural configuration in the final evolution of class 1, the fault has 8000m in length with maximum throw (2000m) at the centre of the fault and gradually decreases towards the fault tip. 73*

Figure 5.13: Group of cross-sections of model 2 - class 1. *This group of cross-sections shows variation in structural of sedimentary layers across the fault block. Cross-sections (perpendicular to the fault) bring an idea about the dips of sediments while the strike-sections show the sediments distribution. It shows unique results that not all the sediment packages can be found all over the area as the fault were propagating. (VE= 1:1) 75*

Figure 5.14: Structural map of horizon 1 (model 2 - class 2). *The structural map shows the structural configuration in the final evolution of class 2, the fault has 8000m in length with*

maximum throw (2000m) at the center of the fault and gradually decreases towards the fault tip. It seems similar with class 1..... 76

Figure 5.15: Group of cross-sections of model 2 - class 2. *This group of cross-sections shows variation in structural of sedimentary layers across the fault block. Cross-sections (perpendicular to the fault) bring an idea about the dip of sediment while the strike-sections show the sediments distribution. It shows unique results were not all the sediment packages can be found all over the area as the fault were propagating. It also showing bigger accommodation space compared to class 1. (VE= 1:1)..... 78*

Figure 5.16: Structural map of horizon 1 (model 2 - class 3). *The structural map shows the structural configuration in the final evolution of class 3, the fault has 8000m in length with maximum throw (2000m) at the centre of the fault and gradually decreases towards the fault tip. It seems similar with class 1 and 2 except the size of accommodation space and foot-wall uplift..... 79*

Figure 5.17: Group of cross-sections of model 2 - class 3. *This group of cross-sections shows variation in structural of sedimentary layers across the fault block. Cross-sections (perpendicular to the fault) bring an idea about the dip of sediment while the strike sections show the sediments distribution. It shows unique results that not all the sediment packages can be found all over the area as the fault were propagating (growth). It shows that this class has shallowest dip angles in model 2. (VE= 1:1)..... 81*

Figure 5.18: Length (in X-axis) Vs displacement plot of model 3. *The plot shows relationship between length and displacement for each horizon in model 3, it shows that the fault tip is propagating only to the east. The total propagation rate is the same as model 2. 82*

Figure 5.19: Structural map of horizon 1 (model 3 - class 1). *The structural map shows the structural configuration in the final evolution of class 1, the fault has 8000m in length with maximum throw (2000m) at the centre of the fault and gradually decreases towards the fault tip..... 83*

Figure 5.20: Group of cross-sections of model 3 - class 1. *This group of cross-sections shows variation in structural of sedimentary layers across the fault block. Cross-sections (perpendicular to the fault) bring an idea about the dip of sediment while the strike-sections show the sediments distribution. It shows unique results of sedimentary distribution and sedimentary layers dipping slightly dipping to the east. (VE= 1:1)..... 85*

- Figure 5.21: Structural map of horizon 1 (model 3 - class 2). *The structural map shows the structural configuration in the final evolution of class 2, the fault has 8000m in length with maximum throw (2000m) at the centre of the fault and gradually decreases towards the fault tip. It seems similar as model 3-class 1, while the basement structural configuration shows the structural high (foot-wall uplift) hanging-wall depocentre. Bigger accommodation space should be expected due to the longer reverse drag. 86*
- Figure 5.22: Group of cross-sections of model 3 - class 2. *This group of cross-sections shows variation in structural of sedimentary layers in the fault block. Cross-sections (perpendicular to the fault) show that the dip angles of the sediment is gentler than dip angles of sediments in class 1. It shows the different size of accommodation space which is created by different reverse drag distance represented by cross-sections P-Q. (VE= 1:1).. 88*
- Figure 5.23: Structural map of horizon 1 (model 3 - class 3). *The structural map shows the structural configuration in the final evolution of class 3, the fault has 8000m in length with maximum throw (2000m) at the centre of the fault and gradually decreases towards the fault tip. It seems similar as model 3-class 1 and 2. Bigger accommodation space than the class 1 and 2 should be expected because of the longer reverse drag. 89*
- Figure 5.24: Group of cross-sections of model 3 - class 3. *This group of cross-sections shows variation in structural of sedimentary layers in the fault block. Cross-sections (perpendicular to the fault) show the most shallow dip angle of model 3 compared to class 1 and 2. It shows the different size of accommodation space which created by different reverse drag distance represented by cross-sections P-Q and also the gentler dip configuration as compared to the other class in model 3. (VE= 1:1) 91*
- Figure 5.25: Length (in X-axis) Vs Displacement plot for Kerpini Fault Block Model. *The plot shows relationship between length and displacement for each horizon in the Kerpini Fault Block model, it shows that the fault tip is propagating only to the west and bounded to the structure to the east. 92*
- Figure 5.26: Structural map of Kerpini Fault Block (taken from the model). *A map showing the structural configuration of the basement in the Kerpini Fault Block, it shows that the maximum displacement is located at the eastern part of the area and decreases gradually to the west, the existence of the North-South Structure (Vouraikos Fault) is essential to build a*

reliable model of this block. (The model is simplified in term of the direction; it is not following the real field orientation). 94

Figure 5.27: Group of cross-sections within the model of the Kerpini Fault Block. *These cross-sections have been constructed to show the syn-fault deposits configuration within the Kerpini Fault Block. (VE= 1:1)..... 95*

Figure 5.28: Estimation calculation for dip of sediments. *The diagram shows the way to estimate the dip of sediments in faulted block using the simple mathematical and trigonometric equations, given the dip of the fault; reverse drag, total throw, and displacement fraction, the dip of sediments can be estimated. 96*

Figure 6.1: A schematic classical syn-faulting configuration. *The model shows the sharp decreasing dip angles of syn-fault deposits. (a) This figure is showing the first step of fault movement while (b) is showing the second step of fault movement..... 99*

Figure 6.2: A schematic syn-fault configuration with reverse drag controls. *This illustration is showing that with a longer reverse drag distance, the dip angles of syn-fault deposits are still decreasing towards the younger sediments. (a) The first step of fault movement and (b) the second step of the fault movement. 100*

Figure 6.3: The schematic syn-faulting configuration with an episodic movement. *A schematic model for consistent dip angle layers in syn-faulting phase, (a) first movement and (b) second movement. Syn-fault package 1 may represent the sediments in the Kerpini Fault Block, whilst the angular unconformity and package 2 may eroded due to significance exposure..... 102*

Figure 6.4: Paleo-drainage map based on facies, grain size, and clast components. *Reconstructed paleo-drainage map shows the schematic analysis of source sediments in Kerpini Fault Block is dominated by the south to north source. However, there is still minor sediments came from north suggested by the anomaly grain size distribution. 105*

Figure 6.5: Structural and Sedimentation model of the Kerpini Fault Block; initial fault stage (without scale). *The Kerpini Fault started to move and the Vouraikos River brought sediments to be deposited in the Kerpini Fault Block as alluvial fan deposits. 106*

Figure 6.6: Structural and Sedimentation model of the Kerpini Fault Block; Syn-fault and Roghi Fault South development (without scale). *The Kerpini Fault continuously propagated and*

provided a bigger accommodation space for the sediments, at this step also the Roghi Fault South started to move. 107

Figure 6.7: Structural and sedimentation model of the Kerpini Fault Block; syn-fault and western alluvial fan development phase (without scale). *In this phase, the Kerpini Fault continuously grew; resulting in the accommodation space was getting bigger. The river and alluvial fan in the Kalavrita Fault Block (behind the Kerpini Fault) brought sediments to the central and western part of the Kerpini Fault Block and were deposited as alluvial fan and deposits. 108*

Figure 6.8: Structural and sedimentation model of the Kerpini Fault Block; Fault climax phase and development of the next fault block (without scale). *The Kerpini Fault and Roghi Fault South together form a greater accommodation space for the alluvial fan deposits in the eastern part of the Kerpini Fault Block. In this step, the Dhoumena Fault and Roghi Fault West started to move and resulted in development of an alluvial fan from the northern part of the area. 109*

Figure 6.9: : Structural and sedimentation model of the Kerpini Fault Block; Late syn-fault and channel incision phase (without scale). *This is the end of early and peak syn-faulting period whilst there is a river that was trying to flow to the east and incise the sediments of unit 2 and 3 because of the foot-wall uplift of the Dhoumena Fault topographic expression which became a boundary for the river to flow straight to the north. The river also has a branch in the relay zone of the Dhoumena Fault which later became the source of sediments of alluvial fan deposits in the Dhoumena Fault Block. 110*

Figure 6.10: : Structural and sedimentation model of the Kerpini Fault Block; Post-fault phase (without scale). *This is the final step of syn-faulting period in the Kerpini Fault Block. The Kerpini Fault Block has been interpreted to stop its movement and later on this area has been exposed until today and start to have an erosional period the produce what can be seen today in the field. 111*

List of Tables

Table 4.1: Initial geological knowledge within the Kerpini Fault Block. _____	23
Table 4.2: New important findings in the field work compiled together with the initial knowledge. _____	56
Table 5.1: Modelling box for models construction, <i>Table shows the modeling box that which used for the models construction in this chapter.</i> _____	59
Table 5.2: Classification of the models based on the fault evolution and reverse drag distance. <i>The table shows the classification of model according to their reverse drag distance.</i> _____	62
Table 5.3: Table of estimated and determined dip observations of model 1 (class 1, 2, and 3). <i>The observations in the table show that it is possible to estimate the dip angle of the sediments with an uncertainty around 5°. The table also shows that the dip range of the oldest and youngest strata are getting smaller as the reverse drag distance is longer.</i> _____	97

Chapter 1 : INTRODUCTION

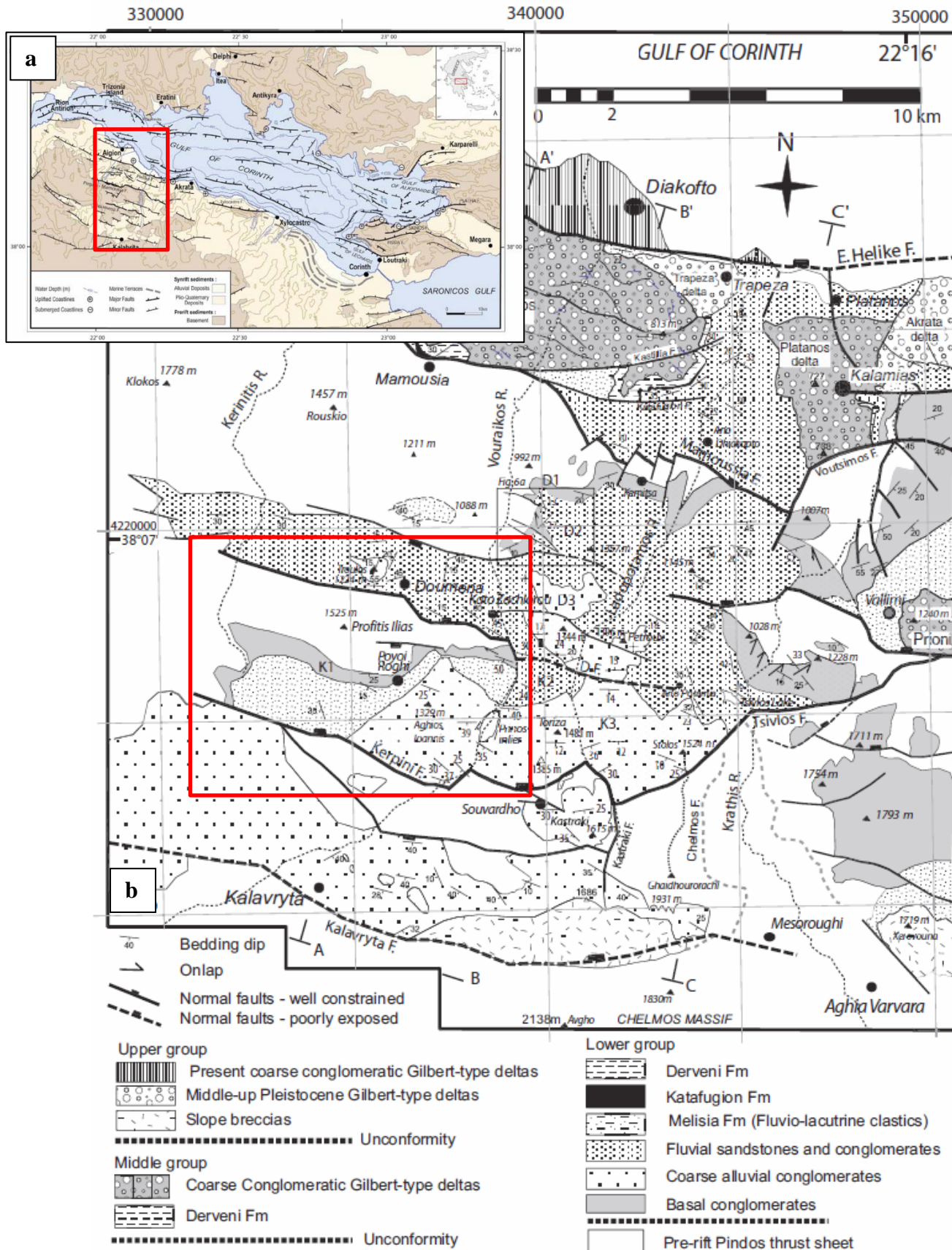
1.1 Background

To graduate with an MSc in Petroleum Geoscience Engineering, from the Department of Petroleum Engineering, University of Stavanger an independent, master research project must be designed, conducted and delivered in the form a written thesis. This thesis, titled “Fault Controlled Sedimentation: A Case Study of the Kerpini Fault Block, Greece”, involved field work, data analysis and interpretation components from which discussions were drawn and conclusions were made.

The study area for the surface study is located in Kalavrita-Helike area, Greece (Figure 1.1). This area has been influenced by the Gulf of Corinth rifting; therefore, normal fault setting would be expected. The Corinth Rift represents one of the most recent extensional features although the relationships between the Aegean Miocene extension and the evolution of the Gulf of Corinth itself are still debated (Moretti et al., 2003). This thesis is about fault controlled sedimentation; therefore, this study is more focused on the syn-fault sediments.

A series of normal faults, associated with rifting events can be seen in the Kalavrita-Helike region. Good exposure of outcrops in this area provides optimal observations for understanding fault controlled sedimentation. Regional structural style in this area is a series of normal faults striking NW-SE and dipping to the NE with several antithetic faults dipping to the south.

The primary focus of this study is on the Kerpini Fault Block, an area open to discussion regarding the relative age of faulting and of the sedimentary rocks. Some researchers (Ford et al., 2013, etc.) believe the sedimentary rocks above the basement were deposited during faulting (syn-fault); evidence in the field however does not completely comply with this.



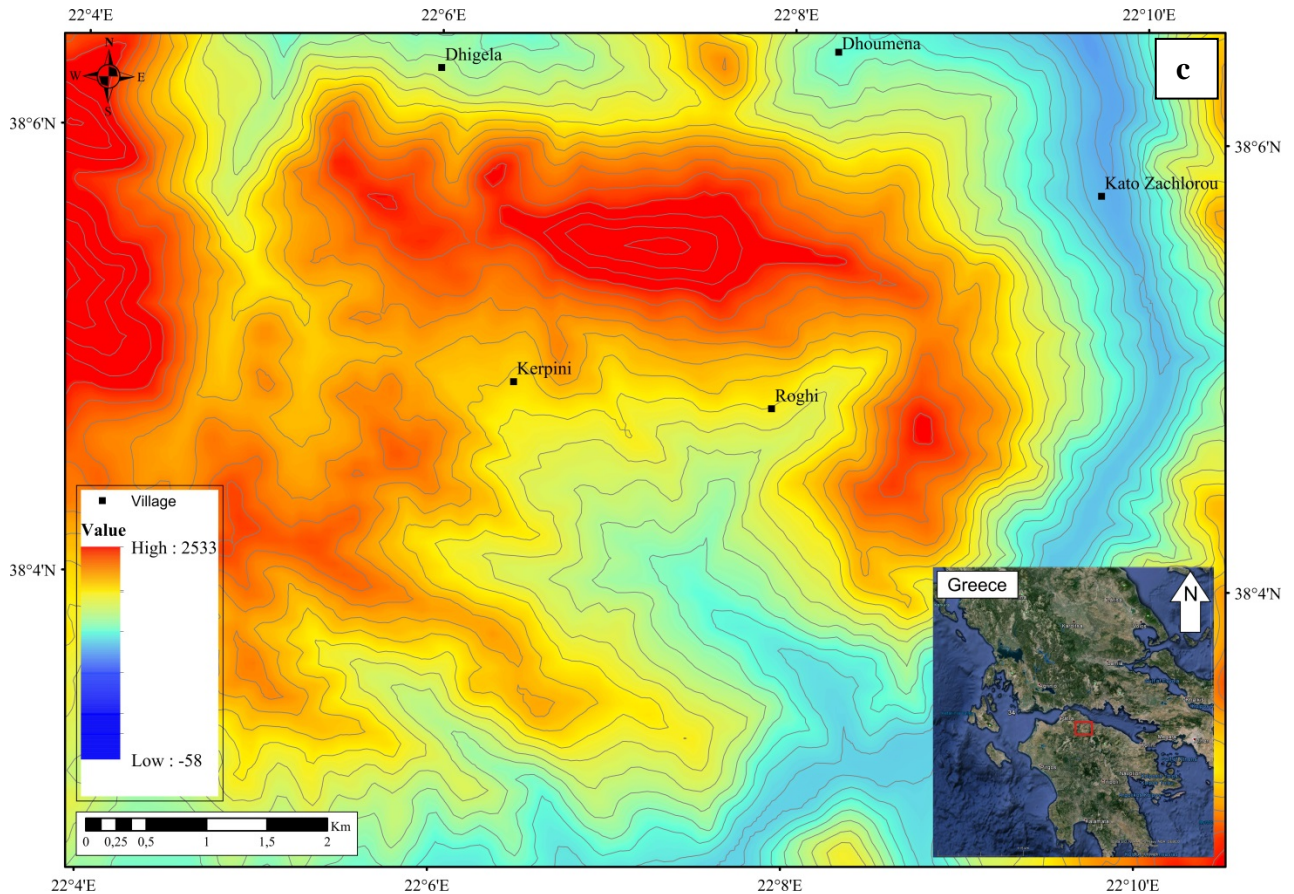


Figure 1.1: Location map of the studied area. (a) The regional structural map of Central Greece, modified after: Moretti et al. (2003), (b) The geological map of Gulf of Corinth area from Kalavrita to Helike, modified after: Ford et al. (2013), and (c) The topographic map of study area.

1.2 Problem

Normal faults in extensional settings often affect sedimentation patterns. Usually, it happens in syn-fault deposits while the sediments are coming in the same broad time with fault displacement. Fault displacement, geometry, relative movement, and age will be the main factors deforming deposited sedimentary units. Further factors may include; drainage systems, sea level fluctuation and sediment influx.

Using the Kerpini Fault Block, one of the faulted blocks in the Kalavrita-Helike region; it will attempt to explain how fault evolution controls sedimentation in an extensional setting. Previous studies have proposed, based on field observations that sedimentation occurred during faulting and that the main direction of deposition is towards NNE, perpendicular to the fault strike within syn-fault phase (Ford et al., 2013). However, the dip of the sedimentary rocks seems to have

constant values within the tilted fault block, in contrast to classical syn-fault depositional models where dips of younger rocks are shallower than those of older rocks (Figure 1.2).

The problem addressed in this thesis is to assess the influence of faulting on sedimentation. Implications may include; how the sedimentary layer patterns develop as a response to fault displacement and how the facies variation and distribution within the fault block are influenced by fault evolution.

This study can bring a better understanding related to the fault controlled sedimentation which can be used as an outcrop analogue for the similar geological setting since there are a lot of unexplored syn-fault deposit plays, for example, in North Sea. Conclusions from this study may therefore provide more ideas for the prediction of reservoir distribution in hydrocarbon exploration.

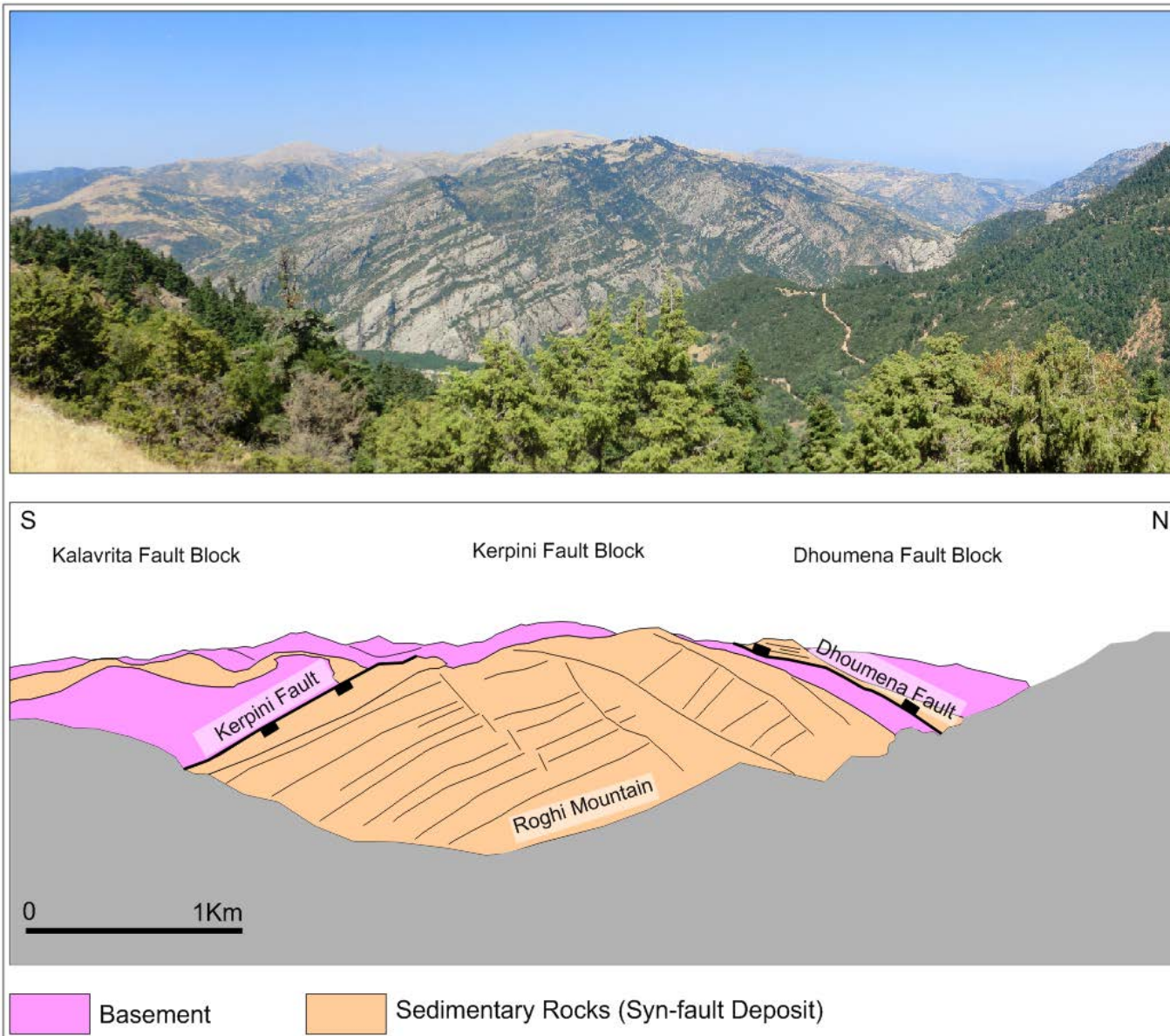


Figure 1.2: Panoramic photograph looking west of Kerpini Fault Block. *Sedimentation in the Kerpini Fault Block is belongs to syn-fault succession which mostly composed by conglomerate and sandstone. The sedimentation layers in this fault block seem to have a constant value from the youngest to oldest rocks.*

1.3 Aim and Objectives

The general objective of this study is to provide ideas about fault controlled sedimentation in the Kerpini Fault Block as an analogue model for reservoir models of similar geological setting. The main question answered is how the sedimentary layers and facies will change as a response to fault evolution.

1.4 Output

Key products of this research, used to achieve defined objectives include:

- Detailed geological and facies distribution map of the Kerpini Fault Block,
- Paleo-drainage analysis and map,
- Number of modelling scenarios that show the influence of the fault evolution towards the sedimentation.

1.5 Data and Methodology

Data used for this study are as the following:

- Observation collected during field work; strikes, dips, lithology description, photos, etc.
- Topographic map, Digital Elevation Map (DEM) and satellite imagery.

This study combines elements of both field work and structural modeling. In order to achieve the objectives, there are several methodologies that have been conducted. They are:

- Field work, which divided into two phases.
 - Preparation;
This stage included literature reviews about the study area. Sources included; books, journals, published papers, and other reports. DEM and topographic analysis also have been done in this stage. A thorough and well thought out background study is critical to establish a general picture of the geological setting, including lineaments and structural interpretation.

- Data gathering and observations;
Field data obtained includes; strike and dips of sedimentary layers and faults, lithology description and important photos to show the geological condition within the Kerpini Fault Block.
- Modelling
Several experiments were made in order to achieve a desired relationship between the fault evolution and the geometry of the sedimentary layering. Several scenarios have been provided to get a better understanding of this. Each scenario has unique parameters. Parameters that have been used in the construction of the fault displacement models include; reverse drag point and the displacement split between hanging-wall and foot-wall.
- Writing
This is the stage that all of the materials for the study have been done; therefore, writing thesis was ready to start. The thesis included regional geology, geological setting of studied area, modeling of fault controlled sedimentation, and sedimentation schematic model to explain the facies distribution.

In order to support the study, several software packages were utilized for data processing:

- Arc GIS 10: used for the database and geological map construction,
- RMS 2013: used to build geological model.

1.6 Previous Works

For many years, the Kalavrita area has been an interesting area to study normal fault block systems. This area has excellent outcrops due steep valley sides and the absence of any significant vegetation. From south to north (Gulf of Corinth), facies of sedimentary rocks display a general northward fining with typically cobble sized conglomerates in the south and mixed conglomerates, coarse to medium sands in the north. Moreover, the sorting also improves to the north. However, there is still a lack of detailed studies on the Kerpini Fault Block. Most of the studies that have been done in this area have focused on the structural evolution and sedimentation pattern of the Gilbert type delta situated (15 km) north of Kerpini Fault Block.

The Kerpini Fault is also interesting because of the uncertainty of the relative age of the fault and the sedimentation pattern in this fault block. Previous studies state that this fault has been displacing at the same time as the sedimentation periods (Figure 1.3) (Ford et al., 2013). Ford et al., (2004) state that drainage patterns, which become sediment sources for this fault block, might flow in a perpendicular direction to the fault. The Kerpini Fault has an estimated maximum throw of 2.5 Km (Collier and Jones, 2004) and a smaller offset of fault is also found within this fault block, this smaller fault buried deeply below the syn-fault package, could extend northward and westward (Collier and Jones, 2004). Collier and Jones (2004) published a schematic depositional model which proposed that the sedimentation in Kerpini Fault Block is related to syn-sedimentary phase which started by the fluvial deposit and was followed by an alluvial fan progradational conglomerate package deposited perpendicular to the fault (Figure 1.4).

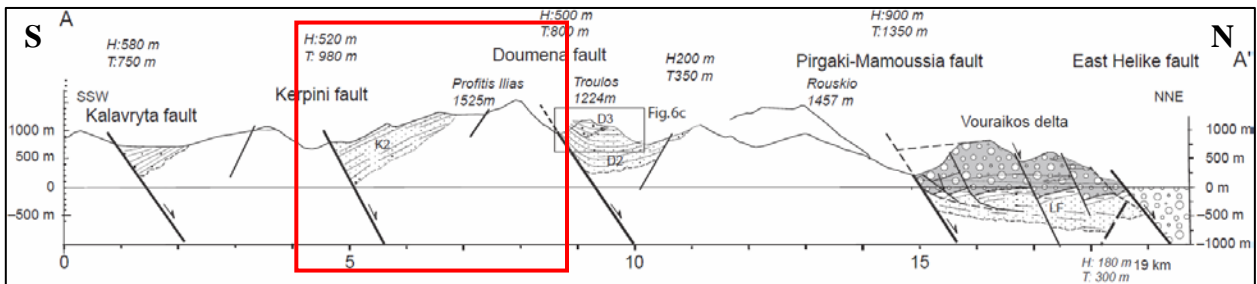


Figure 1.3: Regional cross-section from Kalavrita Fault to Helike Fault modified from Ford et al. (2013). The regional cross-section showing series of normal faults in the Kalavrita area, they are dipping to north with similar dip angle. The red rectangle represents the thesis area. It is shown that the sediment in the Kerpini Fault Block deposited in the syn-sedimentary phase.

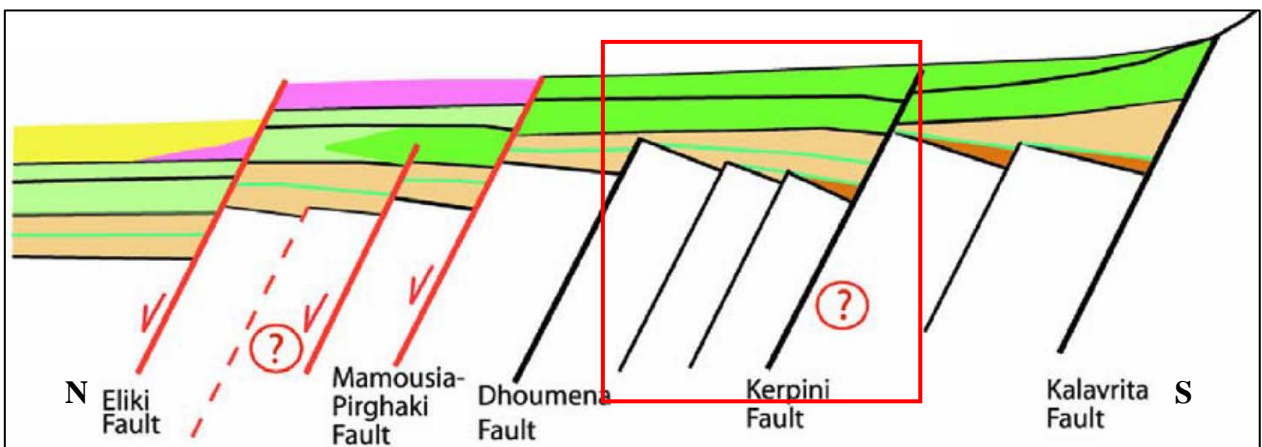


Figure 1.4: Schematic depositional model from Kalavrita to Helike Fault modified from Collier and Jones (2004). Schematic depositional model showing that the sedimentation in the Kerpini Fault Block is started by the fluvial deposit (dark brown) and followed by the alluvial fan deposit (brown). They were deposited in the syn-sedimentary phase. The red rectangle shows the interest area.

Chapter 2 : GEOLOGICAL SETTING

The Gulf of Corinth or known as Corinth Rift is located in Central Greece. This area has been studied for the last decades by many researchers. It becomes attractive for geological studies because of its well exposed outcrops. Most of the studies are related to the tectonic, structural, and stratigraphy frame work.

2.1 Regional Structural Framework

Corinth Rift represents a Miocene to Recent extensional rift system (Moretti et al., 2003) which structures are exposed in the south-western part of the Gulf, in what is known as the Kalavrita-Helike region (study area, Fig. 1). It consists of a series of rotated fault blocks dipping north forming half graben structures and filled by the Pliocene-Quaternary deposits above the basement (Moretti et al., 2003). In the northern part, most of the faults are dipping to the south. The half graben is bounded to the south by a major master fault, whereas the northern side of the basin affected by antithetic normal faults (Ori, 1989).

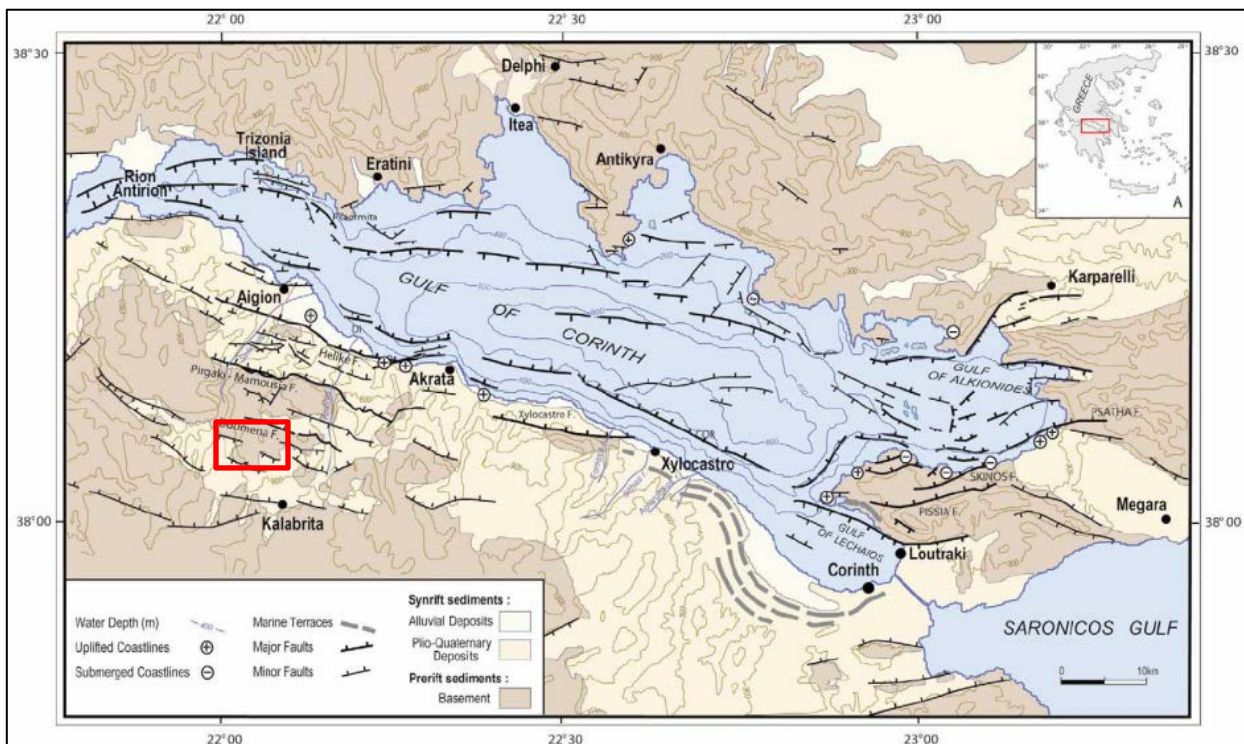


Figure 2.1: Regional structural map of the Gulf of Corinth modified after: Moretti et al. (2003). *Gulf of Corinth is composed of series of normal faults dipping to northeast as a result of Neogene-Recent rifting deformation, they produce half grabens system. Red rectangle represents the location of study area.*

The north dipping normal faults on the southern margin are dominant which cause the stratigraphy in Kalavrita-Helike area tilted to the south (Bell et al., 2008). The general southwards tilted of the foot-wall of the detachment reveal and incipient foot-wall uplift (Flotté and Sorel, 2001). There are several models to explain the structural pattern in Gulf of Corinth. One of them is detachment model of the Chelmos Fault which located further back to the southern Kerpini area (Sorel, 2000). The model shows that the Chelmos Fault is the biggest fault in this area and detached at depth, then all of the faults further north are detaching to this fault (Figure 2.2). The faults are getting younger to the north and the active faults are now located in the Gulf of Corinth.

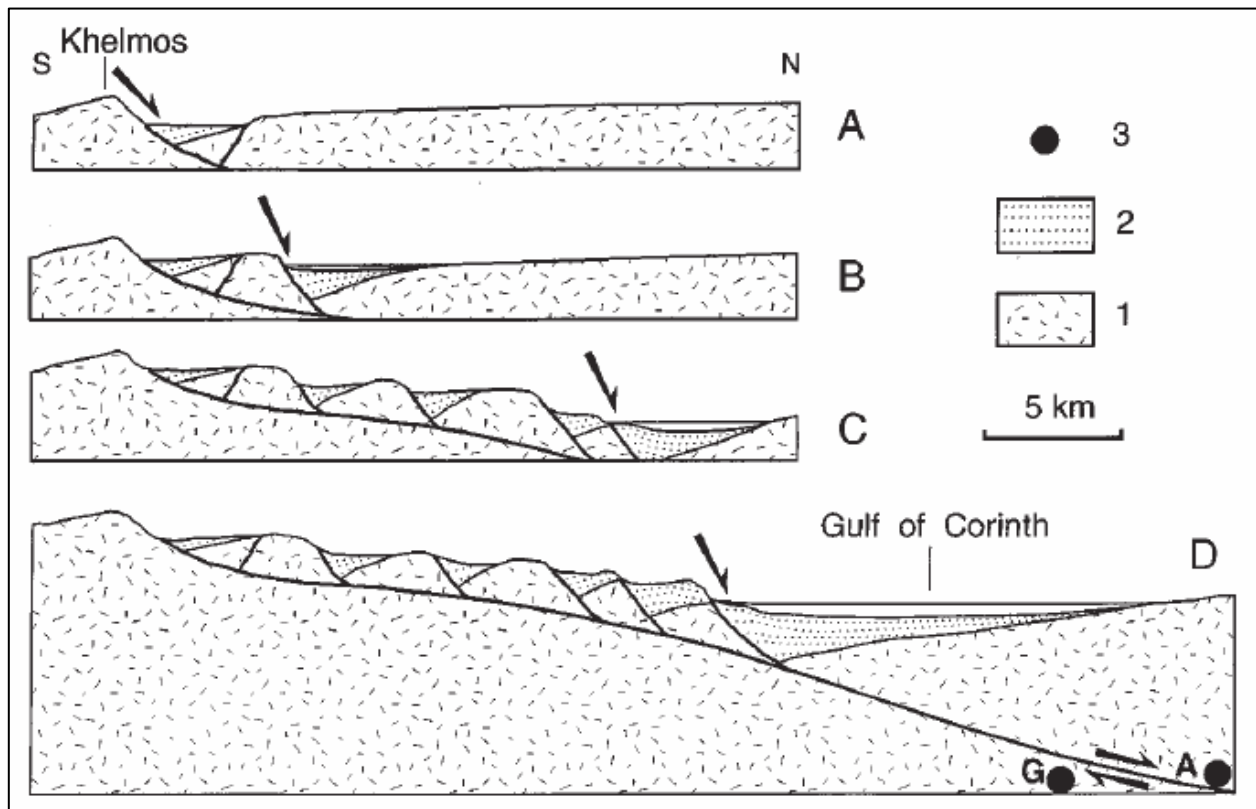


Figure 2.2: Development of Corinth-Patras rift (Sorel, 2000). This figure showing that the development of Corinth-Patras rift is started by the early rift along the active Chelmos Fault, the faults further north which come later are detaching.

This series of normal faults are the important role in sedimentation in this area. Basinward faults migration into hanging-walls has an effect on the evolution of syn-rift sediment patterns, through the sedimentation processes (erosion, deposition, etc.) which were influenced and by the faults evolution (Goldsworthy and Jackson, 2001). The faults displacement in this area vary from

hundreds to thousands meters with a 4-6km fault spacing. The fault displacement and spacing also bring strong effects on the sedimentation.

The latest study proposed a new model for evolution in Gulf of Corinth area (Ford et al., 2013). The model seems to be more complex than previous models. In their work, The Gulf of Corinth evolved in three phases, separated by distinct episodes of extension rate acceleration and northward fault and depocentre migration. The rift system was consistently asymmetrical and dominated by north-dipping fault, moreover, the sediments supply predominantly come from the south to southwest (Ford et al., 2013). The evolution began with the initial rifting in onshore and deposition of the continental facies sediment in the Kalavryta, Kerpini and Dhoumena Fault Blocks. Then, continued by the northward migration of fault and depocentre which make the southern faults stop to move, and produce Gilbert-type deltas in the hanging-wall of northern faults (for example Mamoussia and Pigarki Faults) and the last phase is the its Gulf of Configuration (Figure 2.3).

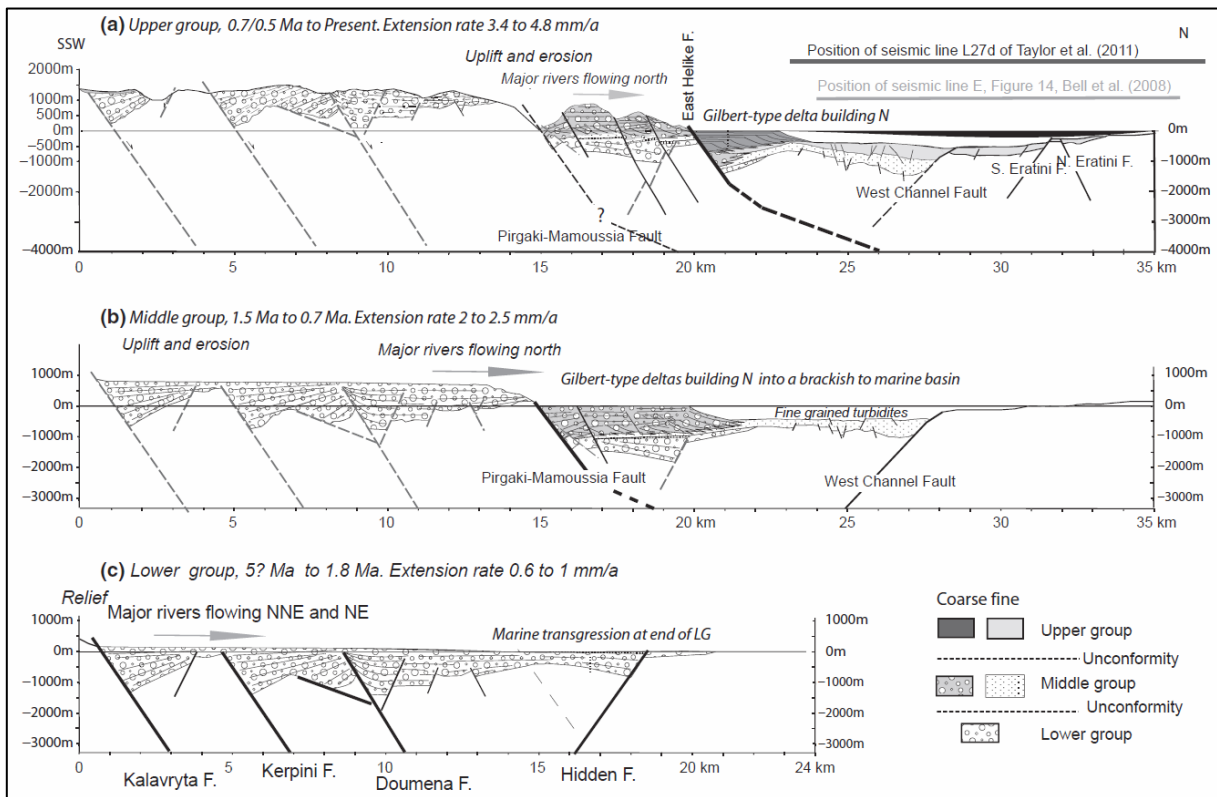


Figure 2.3: Cross-sections showing the evolution of the rift (Ford et al., 2013). A) N-S cross section of the elements from onshore and offshore incorporating seismic section of (Bell et al., 2008) and (Taylor et al., 2011). B) Cross-section to show the northward fault migration and the formation of Gilbert-type deltas. C) Cross-section of the initial rifting phases during the deposition of continental facies sediments.

2.2 Regional Stratigraphy Framework

Many authors have been published their research about the stratigraphy analysis from Gulf of Corinth Area (for example: Backert et al. (2010); Bell et al. (2008); Collier and Jones (2004); Doutsos and Piper (1990); Ghisetti and Vezzani (2005); Leeder et al. (2008); Ori (1989), etc.). The analysis includes the stratigraphy in Gulf of Corinth from the Ski Centre area which mostly comprised of the continental facies sediments until the sedimentation in the north with Gilbert-type deltas have been explained by the authors.

The history of Gulf of Corinth that can be divided into two phases based on their sedimentation (Ori, 1989). The first phase, the basin was filled with continental and shallow water deposits and was probably open to the east. It is maybe because of the extensive evidence of continental sediments in the southern which contain breccia and conglomerate. The second phase, the Gulf of Corinth assumed its present configuration.

The latest study about the stratigraphy in the southern part of Gulf of Corinth has been published by Ford et al. (2013). They have divided the stratigraphy in Kalavrita to Helike Fault Block into lower, middle, and upper groups (Figure 2.4). They used the palynological samples dating from Malartre et al. (2004) to constrain the stratigraphy analysis.

The lower group is dominated by the coarse alluvial conglomerates and fluvial sandstones, siltstones, and conglomerates (Ford et al., 2013). The relation between those two facies is inter-fingering. The grain sizes of the sediments are getting smaller towards the north. Middle group is sitting unconformably above the lower group. The unconformity has been interpreted as an erosional unconformity for the regional scale due to uplift. The middle group is composed of the inter-fingering Gilbert-types deltas conglomerates with mudstones, siltstones, fine sandstones (distal turbidite facies) in the north (Ford et al., 2013). This group has been deposited in the hanging-wall of Pigarki-Mamoussia Fault Blocks. Last, upper group, it is composed of the inter-fingering Gilbert-types deltas conglomerates in the north (Ford et al., 2013). At this time, the sedimentation is mostly taken place in Helike Fault Block and the Pigarki-Mamoussia is the marine terraces. Moreover, the source sediment is mostly coming from the south to north which might be a reason to have a fining northwards sedimentation patten in this area.

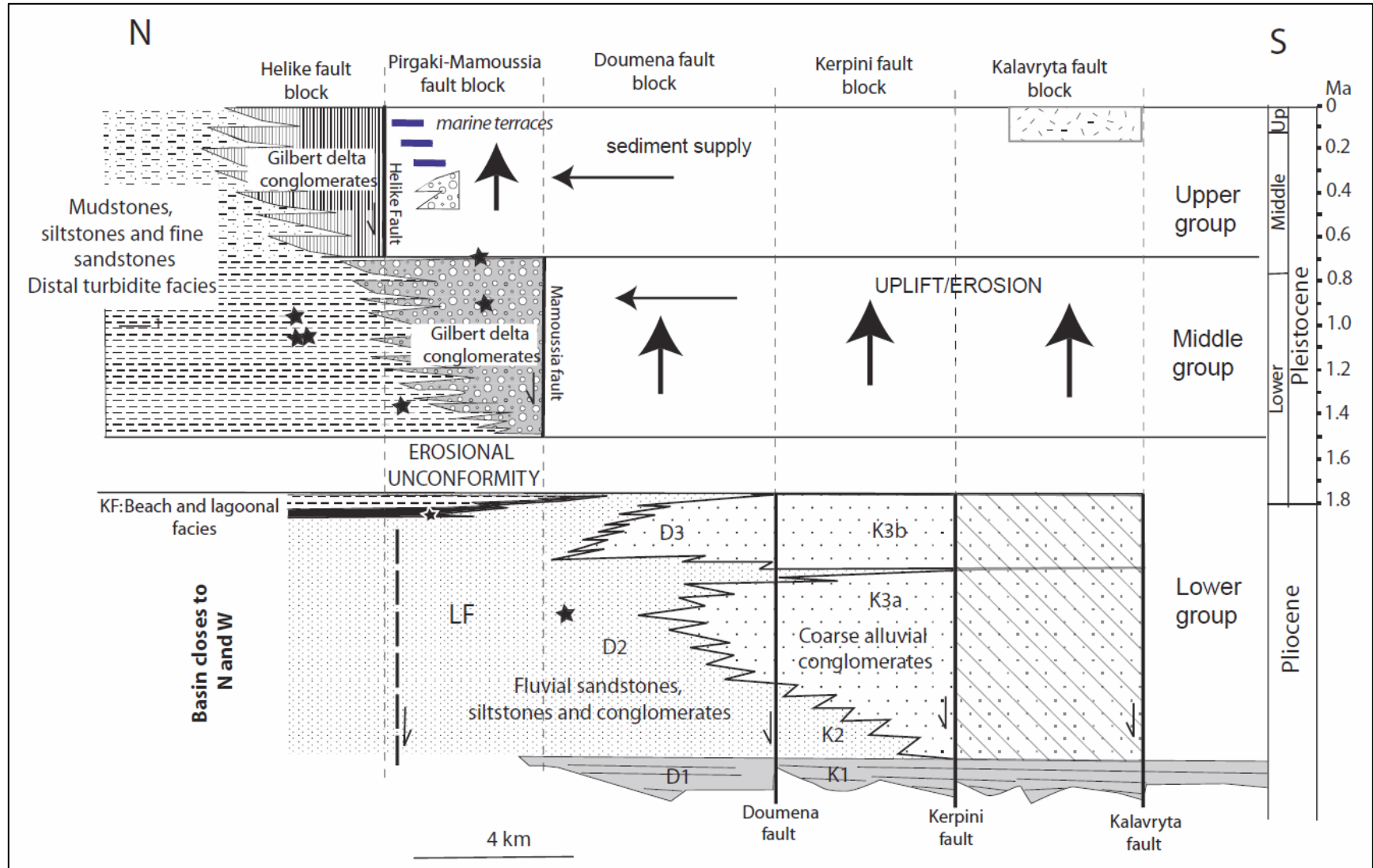


Figure 2.4: Representative regional stratigraphy of studied are (Ford et al., 2013). The stratigraphy in the studied area has been divided into three main groups which started from Pliocene to Upper Pliocene. The facies sediments are vary from continental facies (alluvial fan) sediments to the distal turbidite facies.

Chapter 3 : FAULT CONTROLLED SEDIMENTATION

Understanding about theoretical hypothesis related to the topic of study is important to produce a good work. This chapter is written to reveal the common knowledge related to fault controlled sedimentation.

3.1 Classical Extensional Tectono-stratigraphy Models

There are at least three factors effecting basin-filling: 1) eustasy (absolute sea level), 2) sediment influx, and 3) accommodation space. The last factor can be related to both regional (basin) and smaller scales (fault blocks).

Sedimentation in extensional settings areas is usually controlled by series of normal faults. Normal faults will create accommodation spaces in hanging-wall position for sediments to be deposited and uplifted foot-wall to create either condensed sequences or in extreme cases areas of erosion for sediment supply. Structures, facies, and variations of lithology are also expected in this kind of settings.

In the classical model of sedimentation in extensional settings, there are three phases commonly believed to be exist (Figure 3.1). They are:

- Pre-fault Deposit

Sediments in this phase are deposited before faulting. There are three criterias that can be expected to prove such sediment. 1) No facies changes related to fault geometry, 2) constant dip angles in rocks as the sediments may not be affected by the fault movements, and 3) consistency of sediment thickness.

- Syn-fault Deposit

Sediments in this phase are deposited in the same broad time as fault displacement. There are at least three criterias to identify such sediments: 1) facies lithology changing related to fault geometry, 2) decreasing dip angle upward as the sediments become younger, 3) thickness variation in the hanging-wall influenced by fault displacement (usually thinner towards fault tip and thicker at the maximum throw of faults), and 4) sediments thicker in the hanging-wall and are thinning towards the next foot-wall. In the foot-wall to the next fault, sediments can be thin, not deposited or eroded depending on conditions.

- Post-fault Deposit

Sediments in this phase are deposited after fault displacement has taken place. It means consistent dip angles would be expected. Subtle facies variations would be expected due to the shape of underlying post-rifting accommodation space.

3.2 Growth Fault and Distribution of Displacements

Extensional stress will ideally produce normal faults because of the horizontal stress is less than the vertical stress. It is assumed that the fault will move gradually, therefore the faults will move step by step even though the displacements are really large in present day. Several theories about the fault evolution have been proposed before, included fault geometries and evolutions.

3.2.1 Normal Fault Geometry

Faults are discontinued plane. There are displacements on both sides of the plane. They are generated as natural response to accommodate the stress. There are three types of faults based on the relative movement: normal, reverse, and strike-slip faults. For normal faults, the hanging-wall is displaced down with respect to the foot-wall in the opposite way of reverse fault (Groshong, 2006), and strike-slip faults, where the hanging-wall is displaced laterally either to the left or the right with respect to foot-wall.

As the faults are consisting of hanging-wall and foot-wall, they move relative to each other. There are three kinds of displacements that can be observed: slip, heave, and throw. Slip is the displacement of special (geological) features with relative movements; heave is simply horizontal component whilst throw is its vertical component of the displacement (Figure 3.1). Apart from the displacements, as the hanging-wall is move relatively down to the foot-wall, actually the foot-wall of the fault also move in the opposite direction as the hanging-wall does. The foot-wall tends to move up relatively to the hanging-wall, this is called foot-wall uplift, as the foot-wall actually looks higher than the initial position. It is also affecting sediment thicknesses; it should be expected to have sediment thickening in hanging-wall and thinning in foot-wall.

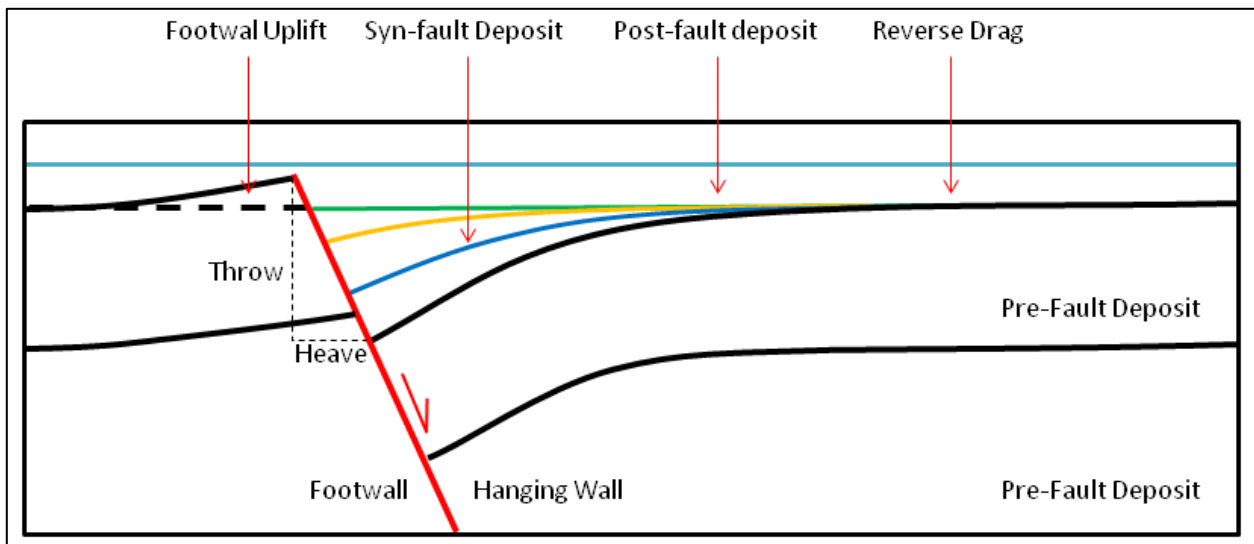


Figure 3.1: Normal fault configuration. A schematic normal fault configuration showing that the displacement of the normal fault consists of throw (vertical) and heave (horizontal), classical tectono-stratigraphy also differentiated the sedimentation phases into three phases which are pre-fault, syn-fault, and post-fault deposit. Not only the hanging-wall move relatively down to the foot-wall, but also the foot-wall has a movement which is called as foot-wall uplift. In the direction perpendicular to the fault, the displacement tends to decrease towards zero; this point is called reverse drag.

3.2.2 Normal Growth Fault

Normal growth faults exist in settings which have sedimentation rates higher than fault displacements rates, it can be supported by the presence of thickness and displacement variations within syn-faulting sequences (Walsh et al., 2001). Based on the field observations and seismic images, displacement on those faults are usually bigger at or near to the center of the faults and gradually decreasing to zero at the end of the faults (Barnett et al., 1987; Gibson et al., 1989; Walsh and Watterson, 1987; Walsh and Watterson, 1988a; Walsh and Watterson, 1989).

Single fault growth produces a large accommodation space (half graben), the filling of half graben depends on the fault movement and sedimentation rate (Schlische, 1991). The models show that if the sedimentation rate is high enough, the sediments can keep up with fault displacement and fill the half graben.

As the faults growth, the fault becomes larger and new faults turn up. Conventional fault growth models can be divided into three phases (Gawthorpe and Leeder, 2000). The three phases of fault development models are initiation, interaction and linkage, and through-going fault zone (Figure

3.2). The first phase, initiation, is marked by a couple of small faults. When they start to link to each other, it is said to be the interaction and linkage phase, where special structures will develop such as breached ramps. The final phase, through-going fault zone, is when most of the faults are connected to be one big fault or a fault zone. The idea of the models is that faults grow and propagate towards particular direction.

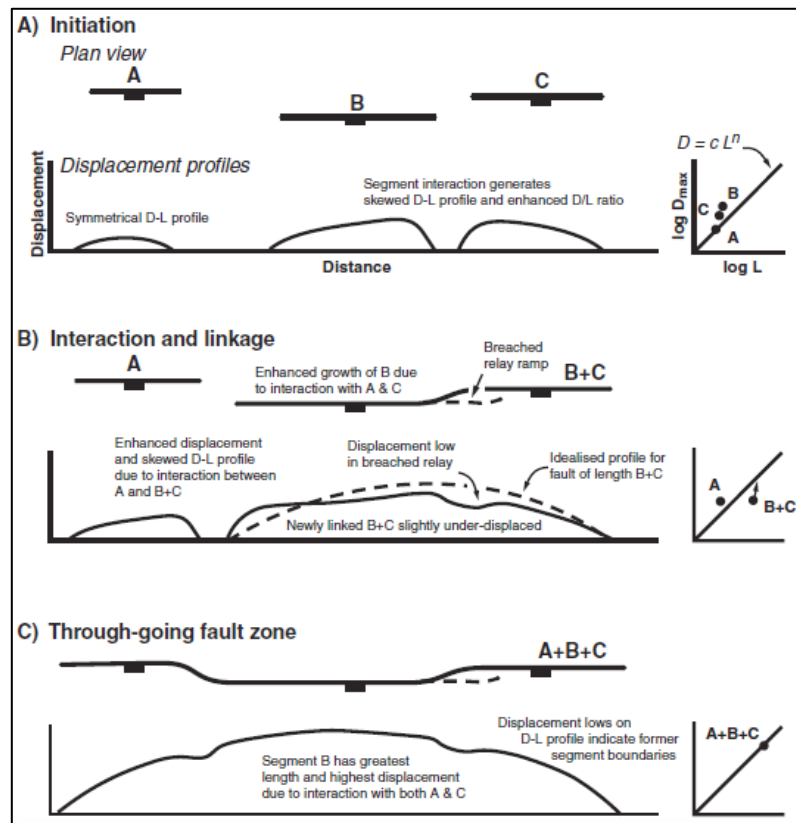


Figure 3.2: Schematic of the fault evolutions (Gawthorpe and Leeder, 2000). (A) fault initiation stage is marked by the several small faults in the area, (B) interaction and linkage stage is marked by the linkage of several fault and form one faults, (C) through-going fault zone is marked by the linkage most of the faults and evolved to be one big fault zone. The evolutions of the faults also bring an effect to the displacement and also the length of the faults.

Field observation in the UK coalfield found that the mean dip of the normal faults vary both on single faults and between faults, as a fault propagates deeper or lower the dip of the fault changes, it may present according to the hydrostatic pore fluid (Figure 3.3), but if they are independent of the propagation process, it may then related to the lithological changes (Walsh and Watterson, 1988b). A radial dip change on the fault plane in depth which can be taken to be elliptical (Barnett et al., 1987; Walsh and Watterson, 1988b).

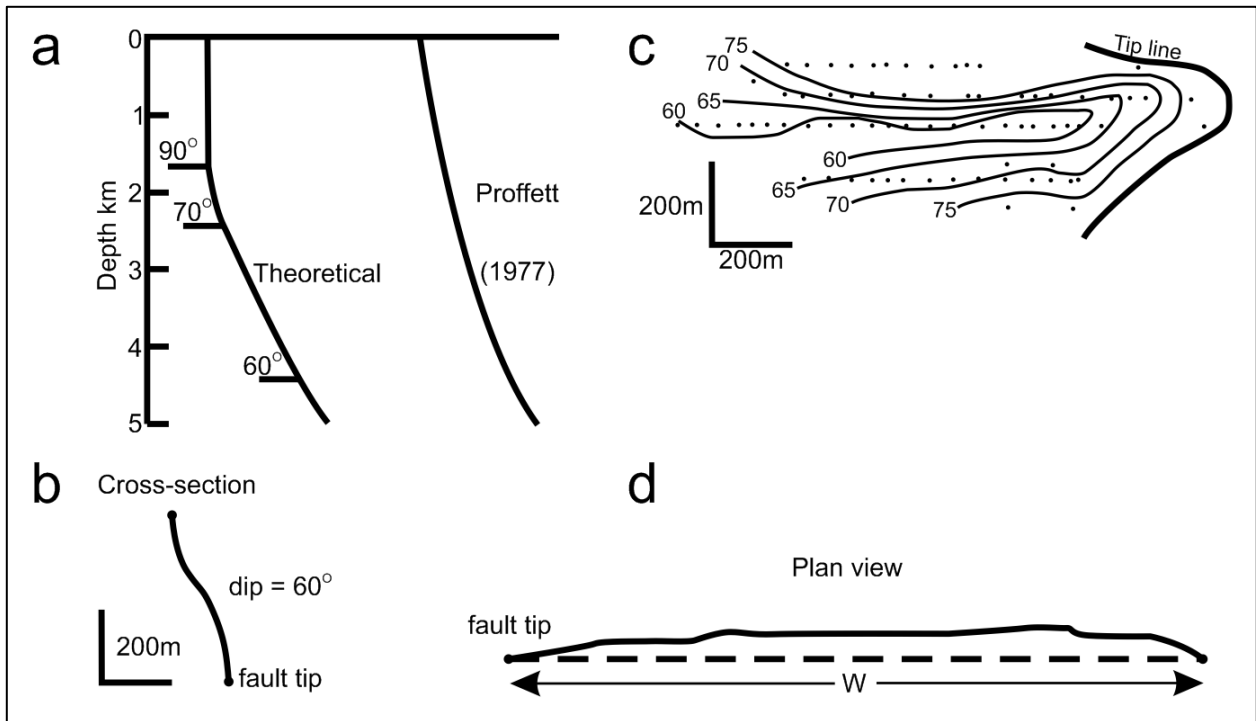


Figure 3.3: Normal fault profile figures (modified after: Walsh and Watterson, 1988b). (a) A schematic theoretical vertical profile of fault plane showing the changes of the dip angles in depth, (b) one of the examples that shows the coalfield fault with radial increase in dip, (c) dip contour map in Markham Colliery showing that the dip has different values, and (d) fault trace in plan view showing the changes of the strike towards the tip.

3.2.2 Reverse Drag

Faults have displacements along the strike of the fault plane. As discussed earlier, the displacements vary along the strike of the faults; ideally, they tend to be zero displacement close to the fault tip and maximum at the center of the faults. Moreover, the observations in UK coalfield and North Sea revealed that displacements will decrease systematically in the direction perpendicular or normal to the faults (Barnett et al., 1987). Decreasing displacement in local faults is called as reverse drag or down-bending or turnover (Hamblin, 1965). Even though the fault displacements are large, at some point a layer will reduce its displacement until the zero displacement is reached in the direction perpendicular to the fault (Figure 3.4). This distance is called as reverse drag.

The reverse drag term may refer to the rollover anticline structure in the hanging-wall (Barnett et al., 1987). In their paper is also said that the maximum distance of reverse drag in the fault-normal direction is ideally equal to the fault radius. It may also be affected by the mechanical

properties of the faulted rock itself. Therefore, the distance of zero displacement in the normal direction to the faults is difficult to predict.

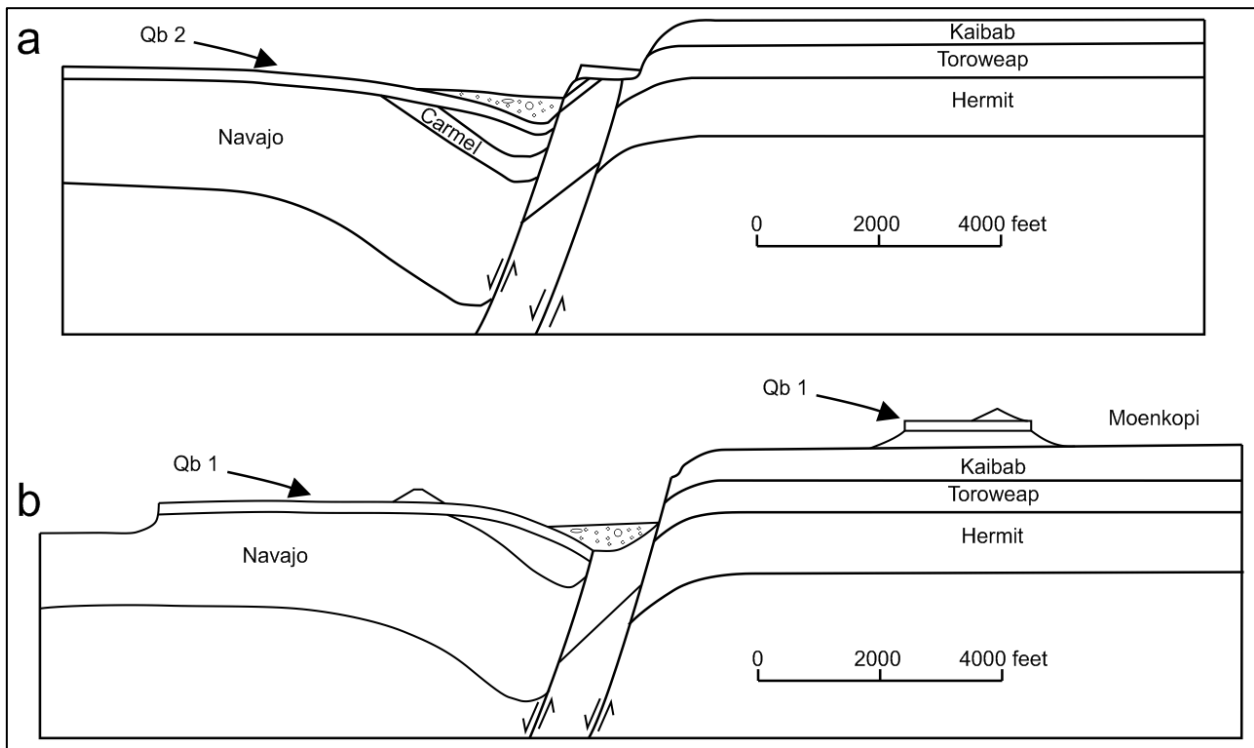


Figure 3.4: Cross-sections showing the reverse drag in Utah (modified after: Hamblin, 1965). Cross-sections *a* and *b* show how the reverse drag look like based on the field observation in the north and south of Hurricane, Utah respectively. Figures shows that reverse drag point location can vary; it can be close to the fault or has a very far distance in the perpendicular direction to the fault.

Gibson et al., (1989), explain how they constructed synthetic contour patterns and cross-sections. In their work, they tried to construct the displacement of hanging-wall and foot-wall and present them as the contour maps around the fault (Figure 3.5). They noted that there are several factors that bring effects to the displacements, they are: 1) width/displacement ratio, 2) variation in level of fault/horizon intersection, 3) variation of fault dip, and 4) variation of initial dip.

Their work is the only one single fault growth model that can be found (Figure 3.5). Another work that have found regarding to growth fault model including basin filling models is published by Schlische (1991). His work reveals that the sedimentary facies variations in numerous continental basins are best explained by the fault growth models.

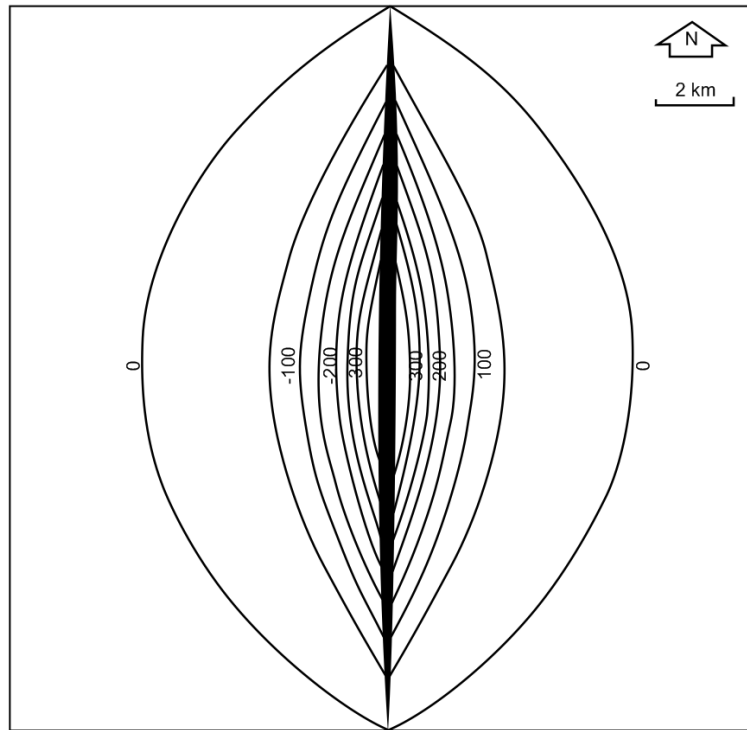


Figure 3.5: One of the synthetic contours model with one single fault in the middle (modified after: Gibson et al., 1989). *The model has been setup with the initial horizontal horizon and one single fault in the middle of the horizon, and then after faulting, the contour shows that the horizon has a unique configuration where the largest displacement is located close to the fault, gradually decreasing in height in the direction perpendicular to the fault.*

3.2.3 Sedimentation

Depositional environments in normal fault blocks can vary depending on whether the environment is terrestrial or marine environment. Sediments are deposited layer by layer as the faulting take place in the hanging-wall of the fault during syn-fault phase. Gross strata models of sedimentation show the fluvial and lacustrine sedimentation will generate the longitudinal onlap at side of the basin and transverse onlap at the hanging-wall (Schlische and Anders, 1996).

Drainage pattern will have a big influence for the sediment dispersal pattern. In non-marine environment particularly, the sedimentation dispersal pattern has been influenced by the drainage of rivers. In general, there are two conceptual models of river or channel direction which are perpendicular to the fault plane and parallel to the fault plane (Figure 3.6). Decreasing of displacement towards the fault tip, generating the typical half-graben accommodation space (Ravnås and Steel, 1998).

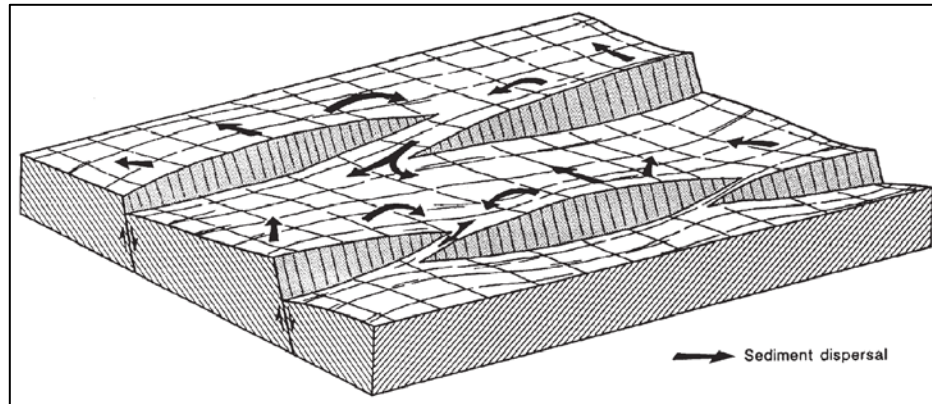


Figure 3.6: A schematic conceptual drainage pattern in normal fault blocks (Råvnas and Steel, 1998). The figure shows the morphology of normal fault blocks complex and the drainage pattern to transport the sediments into the basin have various possibility, some of them are coming from the perpendicular direction to the faults, parallel to the faults, and from the relay ramps.

Drainage point entry in a relay ramp zone is also possible in extensional setting, for example, in Sinai, Egypt (Gupta et al., 1999). The relay zone became an entry point for the sediments to be deposited in the hanging-wall (Figure 3.7). A thick pile of sediments produce a vertically stacked delta in Gebah-fault hanging-wall, Sinai, Egypt (Gupta et al., 1999).

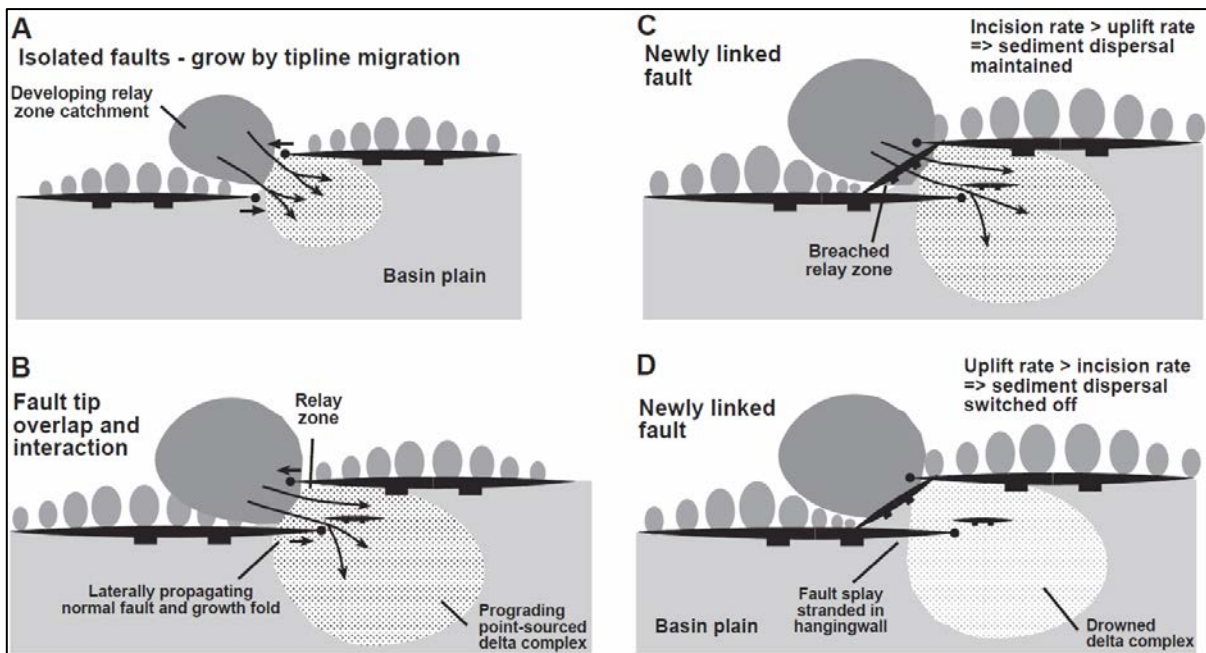


Figure 3.7: Illustration of the proposed model for the clastic sediments input (Gupta et al., 1999). The illustrations shows the development of the faults, before the faults are linked to each other, the sediments were coming from the fault tip (relay zone) and being a source of prograding delta complex, and after that being the drowned delta complex since the faults are linked.

Conceptual sedimentation and faulting relation has been proposed by Gawthorpe and Leeder (2000). They proposed the tectono-stratigraphy model in continental environments (Figure 3.8). The figure shows that in the latest stage of tectono-sedimentation, there is uplift and incision of former foot-wall fan and number of rivers that shift their drainage direction to be axial to the fault away from rift shoulder (Gawthorpe and Leeder, 2000).

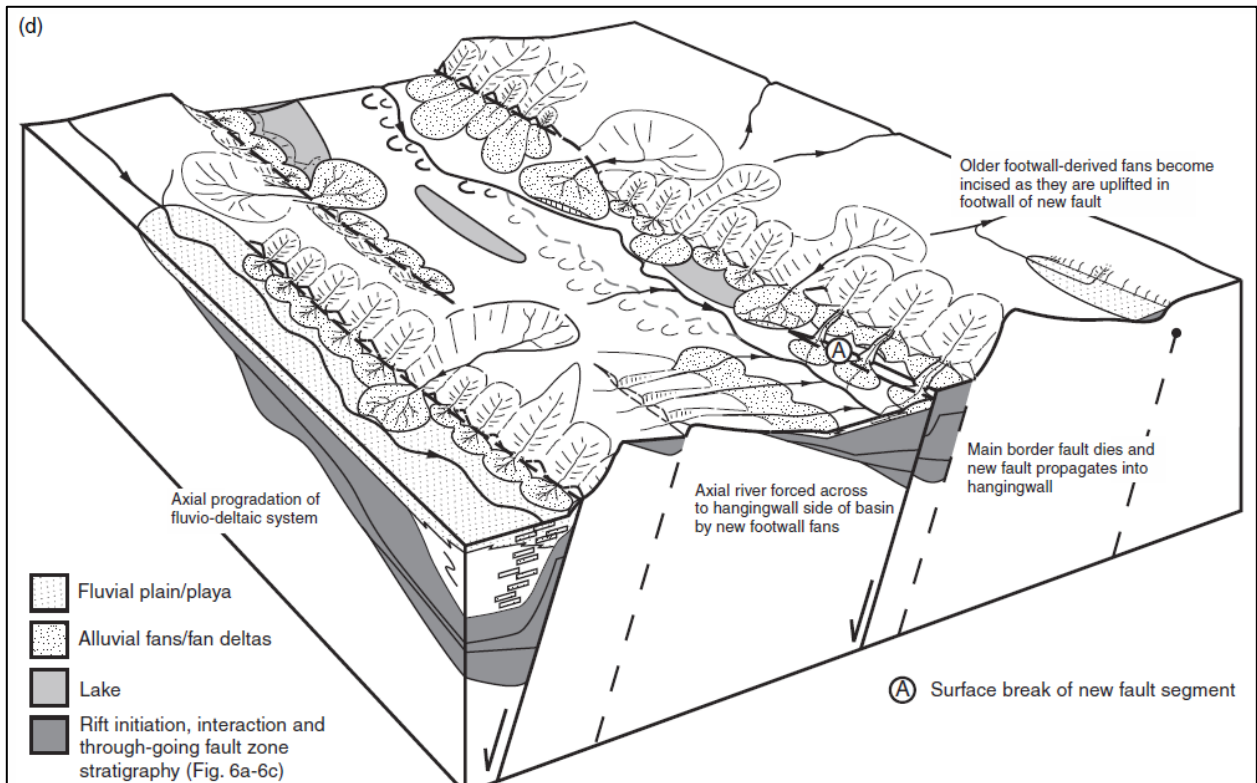


Figure 3.8: The last stage of Tectono-sedimentary model in continental environments (Gawthorpe and Leeder, 2000). *The last stage of tectono-sedimentary model in continental environments shows there is uplift and incision of former foot-wall derived fan. It also shows how the source sediments flow through the fault, there are rivers with perpendicular direction to the faults and also parallel to the faults.*

Chapter 4 : FIELD WORK OBSERVATIONS

This work is initiated by the initial field knowledge. There are 4 faults in the area and 2 simplified lithostratigraphy units.

Type	Name	Notes
Faults	Kerpini Fault	Regional Fault
	Dhoumena Fault 1	Regional Fault
	Dhoumena Fault 2	Regional Fault
	Vouraikos Fault	Interpreted Transfer Fault
Stratigraphy	Basement	Regional Basement (Limestone)
	Conglomerates	Syn-fault deposit dipping to the south

Table 4.1: Initial geological knowledge within the Kerpini Fault Block.

4.1 Stratigraphy

In General, there are two types of rocks within the Kerpini Fault Block, which are Pindos Carbonate Basement and sedimentary rocks. The basement has been interpreted as a pre-fault deposit whilst the sedimentary rocks as syn-fault deposits by many previous authors (Ford et al., 2013). The sediments are lying above the basement. Furthermore, the stratigraphic configuration in this fault block has been divided into 4 main units (Figure 4.1).

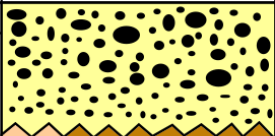
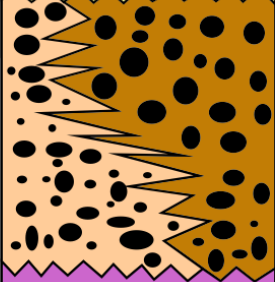

Age	Lithology	Tectono Stratigraphy	Facies Association
Pliocene		Late Syn-fault	Late Sandstone - Conglomerate
		Early Syn-fault	Early Sandstone - Conglomerate Massive Conglomerate
		Pre-fault	Pindos Carbonate

Figure 4.1: Stratigraphic chart within Kerpini Fault Block. Stratigraphic chart of 4 main units within the fault block, from oldest to youngest as the following: Pindos Carbonate, Massive Conglomerate, Early Sandstone-Conglomerate, and Late Sandstone-Conglomerate. The interpreted age is taken from Ford et al., 2013.

The units have been categorized based on their own characteristics, including the lithology characteristics and also their relative age. The lithology characteristics in this case refers to the type of sedimentary rocks (conglomerate, sandstone, etc.), and the interpreted depositional environment. The stratigraphic configuration in this area does not fit with the one from Ford et al. (2013). It seems that their work is too general; they tried to cover a bigger area. It may not apply if more detailed study in Kerpini Fault Block would be expected. Especially for the Late Sandstone-Conglomerate Unit, this unit was not described by them. Distribution of sediments within the Kerpini Fault Block can be seen in. Hanging-wall of the Kerpini Fault block mostly composed of the syn-fault deposits until close to the next foot-wall (Dhoumena Faults).

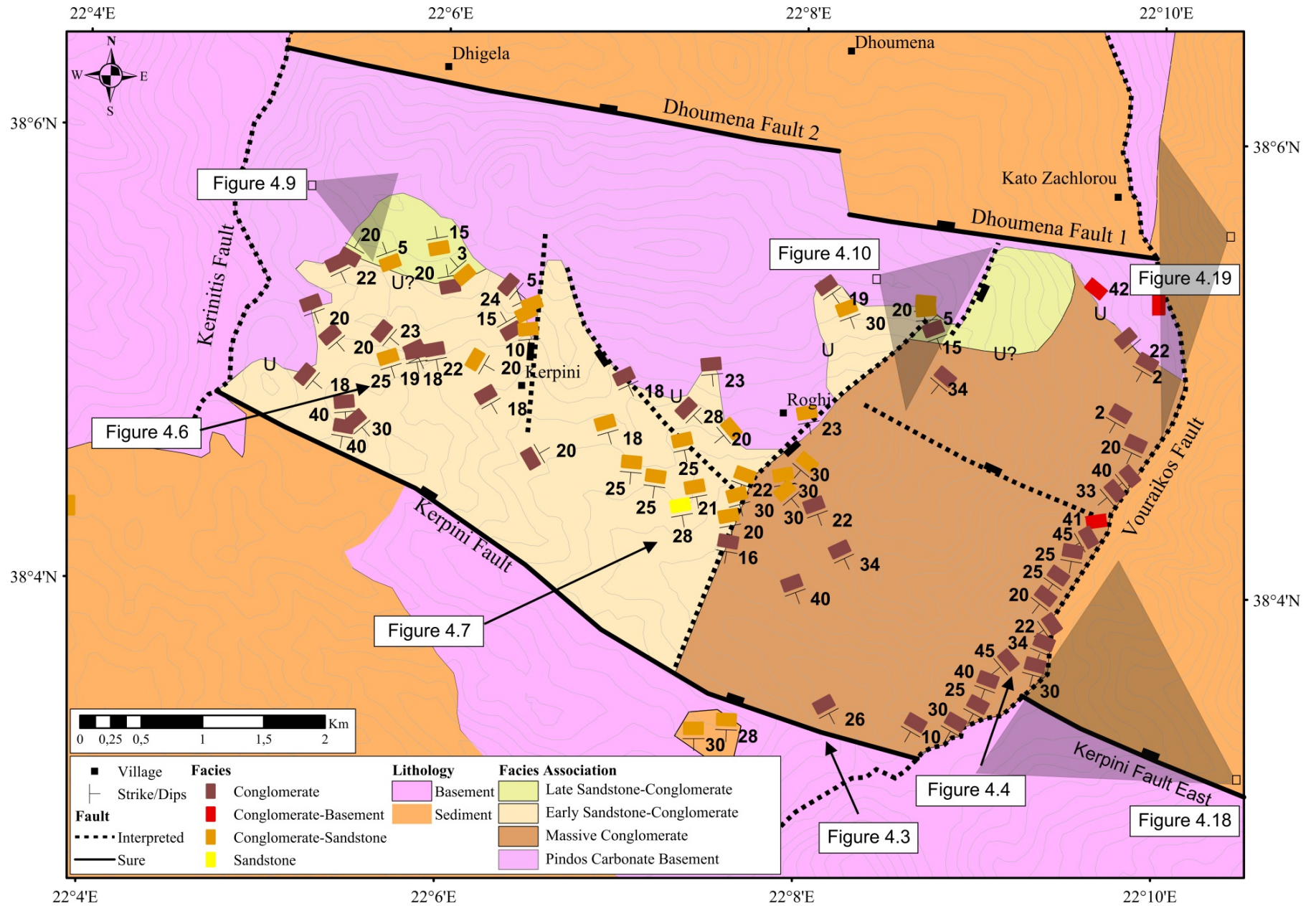


Figure 4.2: Facies distribution map in the Kerpini Fault Block. *The map shows the distribution of sedimentary facies within the Kerpini Fault Block. The sedimentary rocks (syn-fault succession) are concentrated close to the Kerpini Fault while the Pindos Carbonate Basement (Pre-fault deposit) is located in the immediate foot-wall to the Dhoumena Fault and the relationship between those two types of rocks is unconformity. The syn-fault succession can be distinguished into 4 main units. The basement outcrops at the Vouraikos Valley align with the topographical expression indicate the presence of the normal fault.*

4.1.1 Pindos Carbonate Basement (Unit 1)

The basement in this area is Pindos Carbonate. They are originally carbonate rocks (limestone) but considered to have slightly metamorphosed since they have a very massive and compact structure, with grey-yellow-red color. The layers of the basement rocks are very chaotic as they are folded, faulted, and fractured (Figure 4.3). It has been interpreted as a regional pre-rift deposit in this area (Ford et al., 2013).

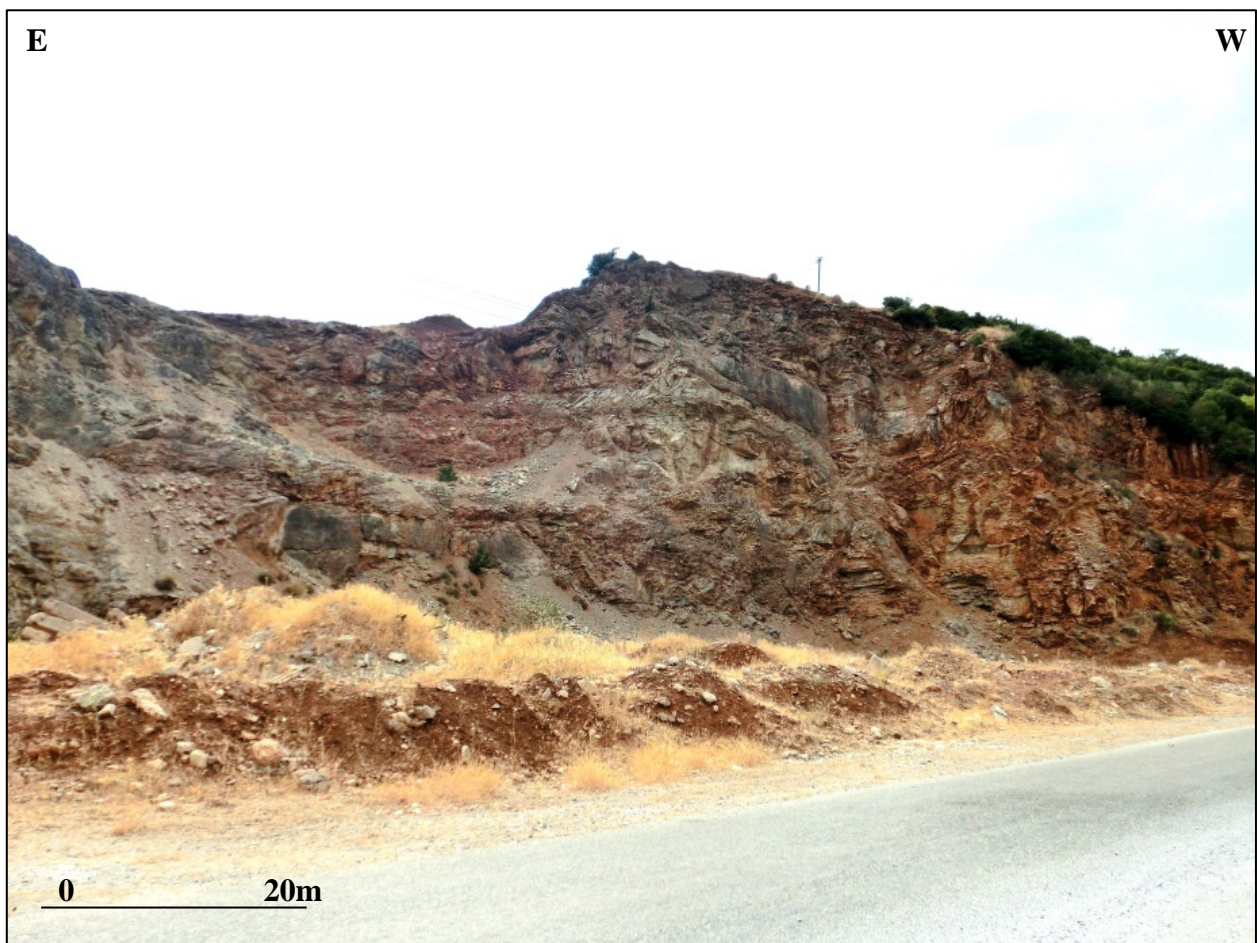


Figure 4.3: Photopgraph of basement lithology at the foot-wall of Kerpini Fault. *The basement in this area is Pindos Carbonate (Limestone) with a very massive and compact structure. The figure shows that the basement has chaotic layers because of the deformation.*

The Pindos Carbonate Basement is expanding on the northern edge of the Kerpini Fault Block close to the Dhoumena Fault. It forms a ridge of uplifted foot-wall basement. At the east side of Kerpini Fault Block, close to Vouraikos River, there is one outcrop of Pindos Carbonate, which is 72m in length with 11m as the maximum height. It is called as the Pindos Inlier (Ford et al., 2013).

The Pindos Inlier shows the unconformable relationship with the conglomerate above it. On the other side of the Kerpini Fault Block, the Pindos Inlier is also popping up to the surface with higher position. Changing height of the unconformity about 80-100m between the Pindos Inlier in the Kerpini Fault Block and on the other side of the block is suggesting existence of fault striking North-South in the Vouraikos Valley. The unconformity contact is striking N82°E and dipping 41°SE.

The Pindos Inlier is also interpreted to be an evidence for Inlier Fault existence. It has been supported by the photo of Roghi Mountain which has a lineament at the top of the mountain which aligns with it and supporting an appearance of faulted morphology (Figure 4.2).

4.1.2 Massive Conglomerate (Unit 2)

This unit is comprised of almost 100% conglomerates and is situated at the eastern part of the Kerpini Fault Block (Roghi Mountain). This unit is the dominant lithology unit that forms the Roghi Mountain.

The conglomerate, as the main lithology of this unit, can be characterized by boulder-cobble grain size (10-40cm, 30cm in average), grey-brown color, very massive structure with bedding structures that only can be seen from a distance because of its very thick nature (2m-10m), and occasional fine component beds are present (Figure 4.4). Its grains do not have a good orientation and it seems to be chaotic may suggest the debris flow mechanism.

Height of Roghi Mountain is approximately about 800m. Based on the observation, this mountain is mostly composed of the conglomerates. Clast components for this unit are mostly limestones (sub-rounded to rounded) with small amount of cherts (sub-rounded to sub-angular). Internally,

they seem to have a coarsening upward pattern and northward fining grain sizes variation (Grain size analysis section).

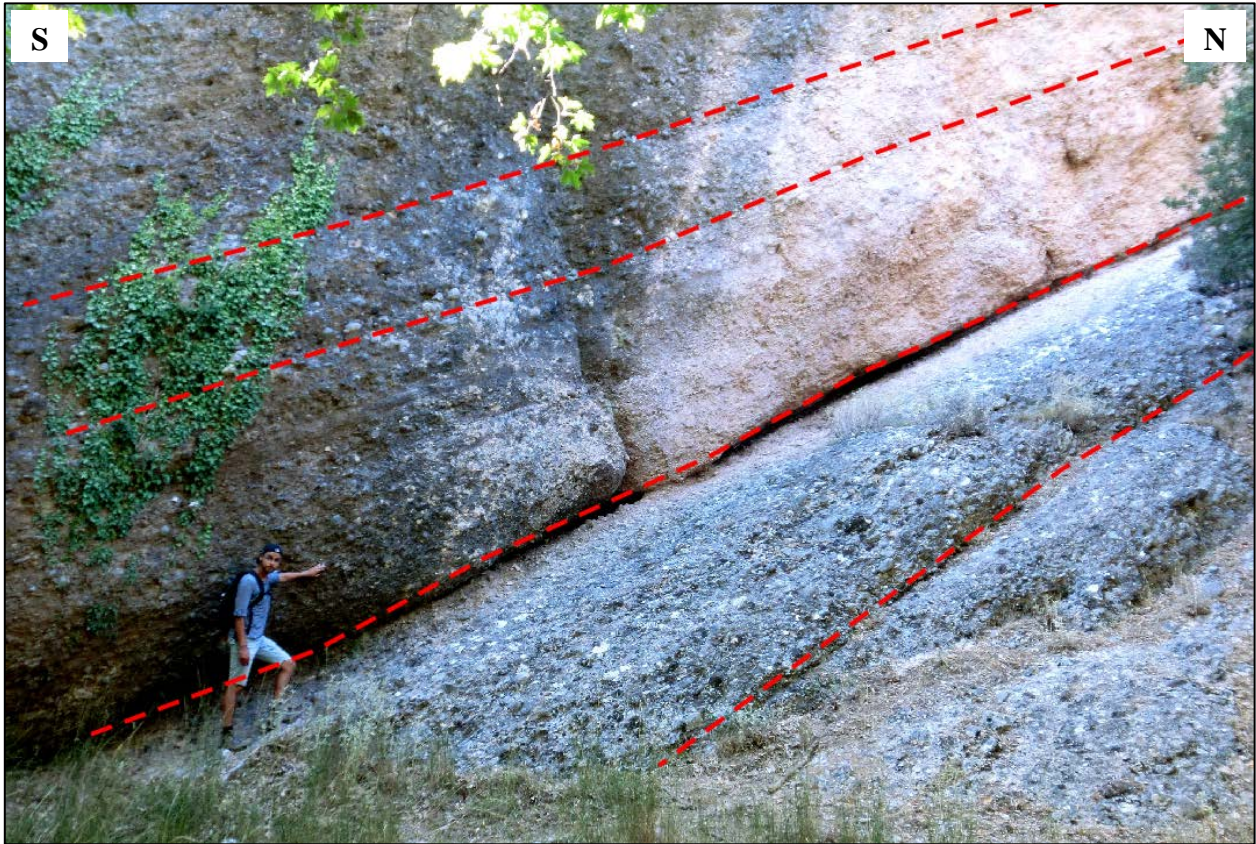


Figure 4.4: Photograph of conglomerate outcrop at the Roghi Mountain close to the Vouraikos Valley (unit 2). The Roghi Mountain is composed of mostly conglomerates with very big boulder grains and massive structure, difficult to see the bedding up close, the red dashed line represents the bedding interpretation striking $N140^{\circ}E$ and dipping $28^{\circ}SW$

Moreover, the sedimentary layers of this unit also have a special characteristic (Figure 4.5). They have a different trend of layering compared than the early Sandstone-Conglomerate unit. The orientation of dip direction is $N230^{\circ}E$ (make an angle of 20° with perpendicular direction to the Kerpini Fault) with an average dip angle of about 20° - 25° . Some of the measurements have been done by distance, it is difficult to measure the bedding up close to the outcrop because of its massive structure (difficult to see the bedding), and therefore, the bedding measurements for this unit are uncertain. The uncertainty of measurement is predicted to be around $\pm 10^{\circ}$ for dip direction and $\pm 5^{\circ}$ for dip angle measurements.

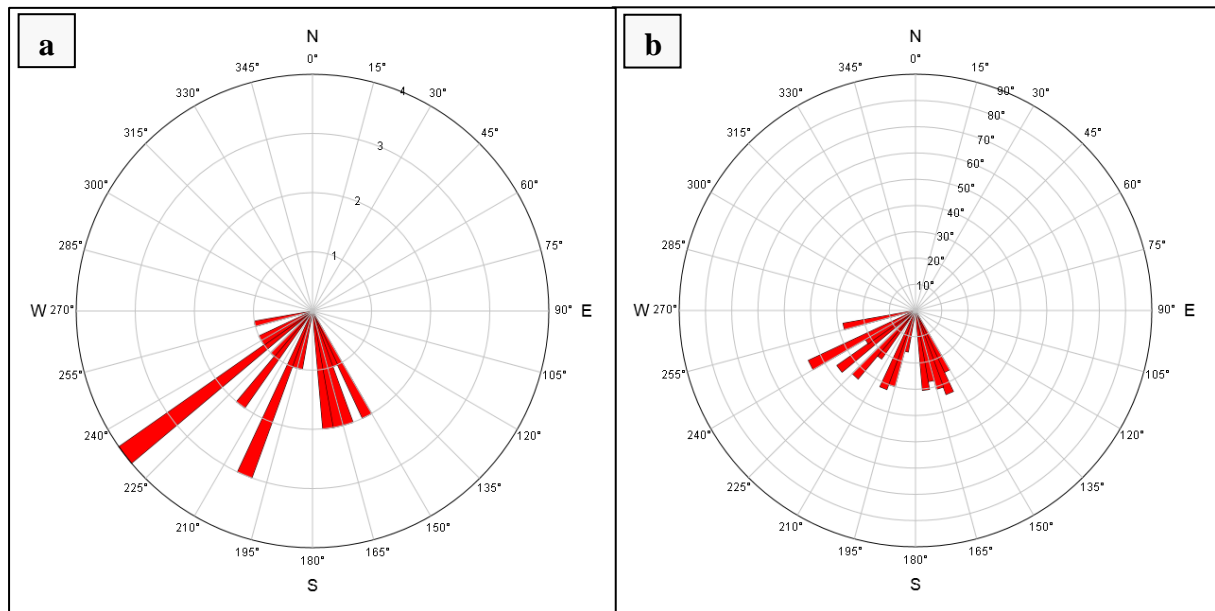


Figure 4.5: Rose Diagram of sedimentary layers in Massive Conglomerate unit (unit 2). (a) The trend of dip direction of Massive Conglomerate unit showing NE-SW ($N230^{\circ}E$) trend with (b) an average dip angle of 20° - 25° .

Depositional environment for unit 2 is interpreted to be alluvial fan. The coarsening upward general pattern and chaotic organization of grains within the beds are suggesting the debris flow mechanism of sedimentation. The southern part has bigger grains compared to the northern part are suggesting the sediments come from the south.

4.1.3 Early Sandstone-Conglomerate (Unit 3)

Early Sandstone-Conglomerate unit comprised of sandstones and conglomerates. The sandstones appear as a channelized sandstone facies whilst the conglomerates usually appear as the background lithology.

The conglomerates are widespread across the Kerpini Fault Block, and are most abundant in the western region of the fault block. The conglomerates are characterized by cobble to boulder grain size (10-40cm, 20cm in average) components slightly smaller than the unit 2, grey-brown color with in some outcrops sandstone insets, and a lack of any well-defined continuity of layers (Figure 4.6). The conglomerates are dominated by three 2 main types of clast components which are limestones, and cherts, but it also contains less amount of sandstones. Cherts appearance percentage is quite high in this unit; their clast size is usually bigger than limestone and sandstone

(they could reach 30-40cm). It is also can be easily recognized that most of the cherts have sub-rounded shape whilst limestone and sandstone clasts are more rounded.

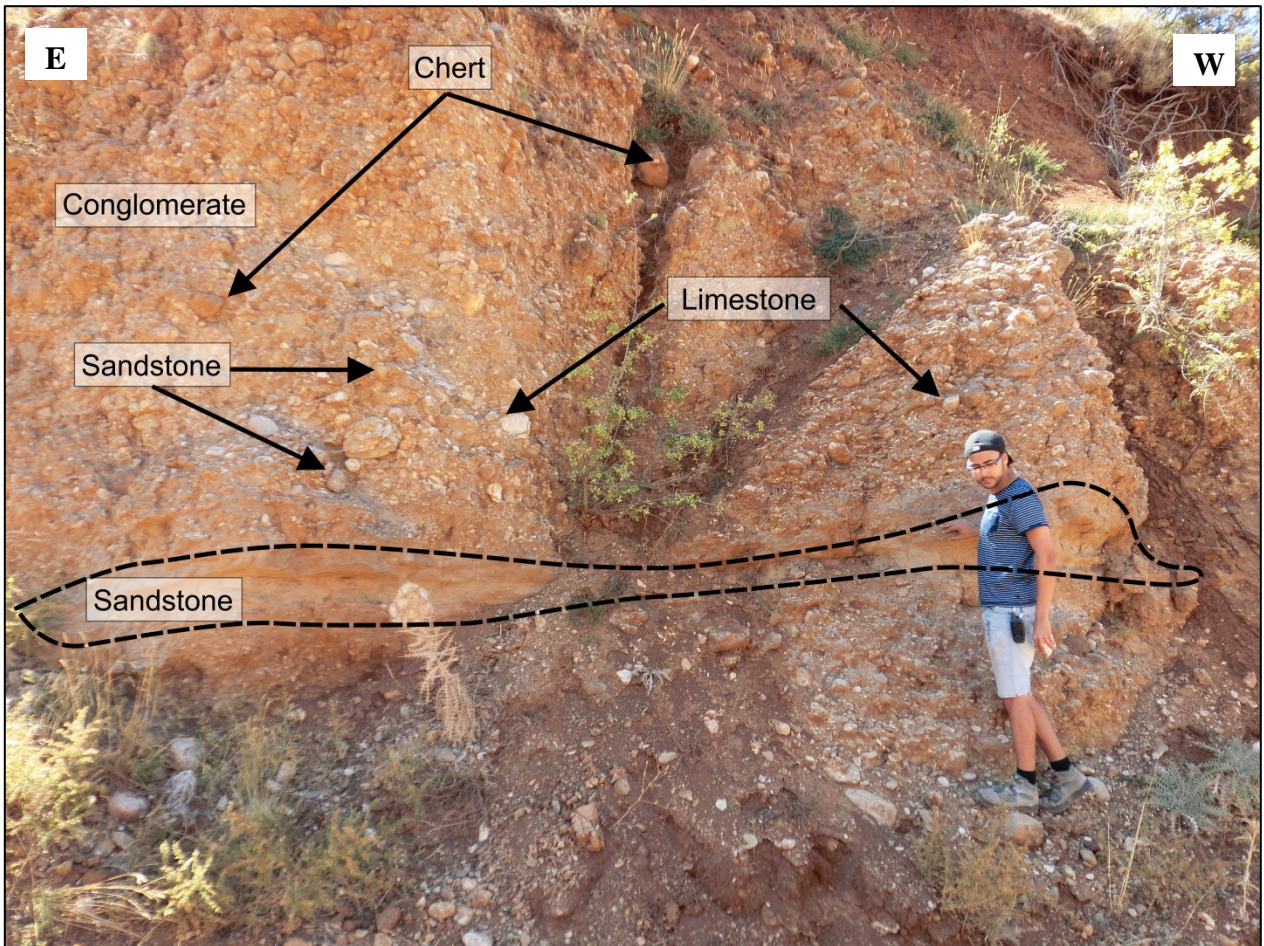


Figure 4.6: A representative outcrop for the conglomerate in Early Sandstone-Conglomerate unit (unit 3). The conglomerate of this unit is characterized by the massive structure, and big boulder grain size with some inclusion of sandstone insets. Chaotic conglomerate's grains organization suggest the debris flow mechanism sedimentation.

The sandstone facies mostly found in the middle of Kerpini Fault Block. It has been characterized by the lenses and graded bedding of the sediment structure. In Figure 4.7, there are some of sandstones facies with a channel like shape which are surrounded by the conglomerate; the grain size of this lithology is variable, from fine sand to very coarse sand grain. Not many channels direction can be measured (just 2-3 measurements with poor confidence), form the measurement they show the channel direction have NE-SW trend. However, this measurement cannot be an exact evidence to argue about paleo-channel direction as they may just part of the bigger depositional environment.

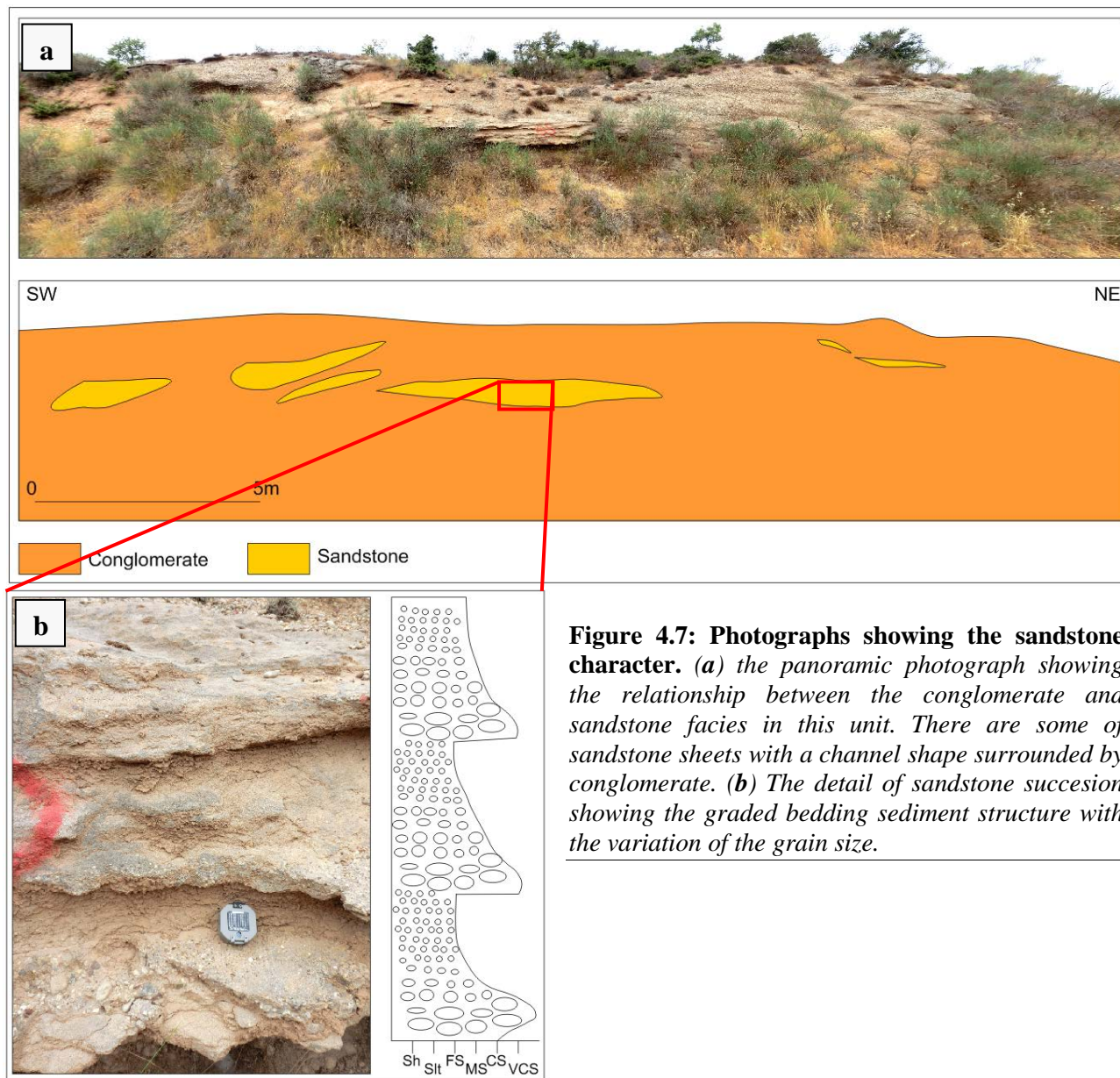


Figure 4.7: Photographs showing the sandstone character. (a) the panoramic photograph showing the relationship between the conglomerate and sandstone facies in this unit. There are some sandstone sheets with a channel shape surrounded by conglomerate. (b) The detail of sandstone succession showing the graded bedding sediment structure with the variation of the grain size.

Sedimentary layers of this unit show the unique trend as shown in Figure 4.8. The dip direction of the layers, in general is N165°E, therefore the trend of the strike is N75°E. This main dip direction is make an angle with Kerpini Fault Block strike for about 45°, whereas the bedding dip directions would expected to be 90° (perpendicular) to the bounding fault. The dip angles of the sediment layers are also have a trend, according to the rose diagram; the dip angle is around 20°.

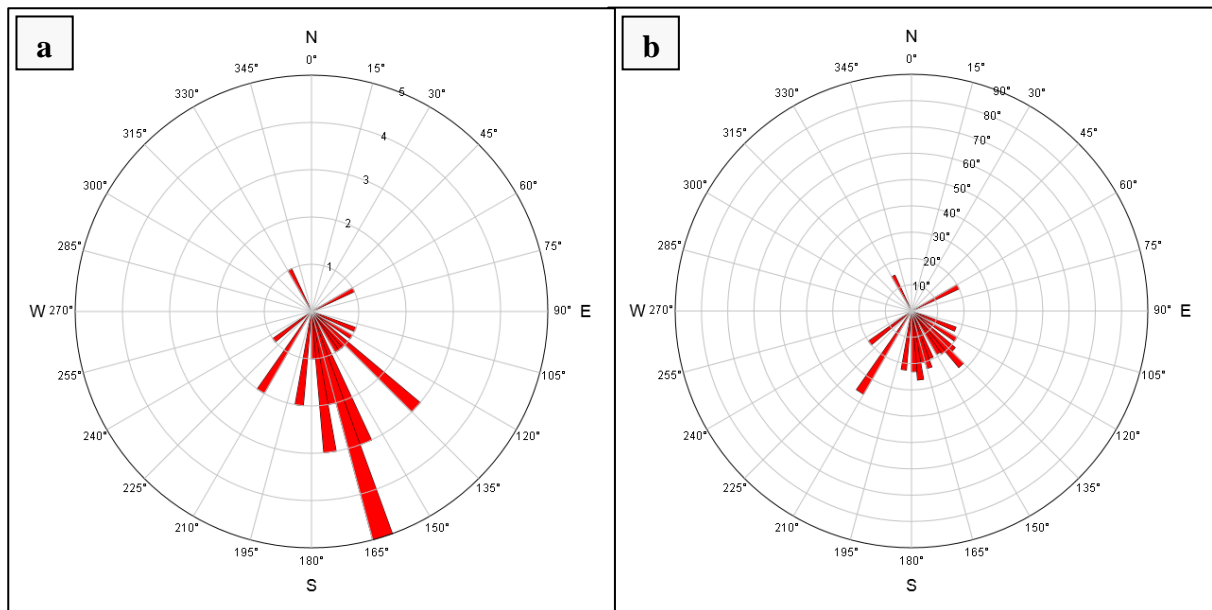


Figure 4.8: Rose Diagram of measured strikes and dips in Early Sandstone-Conglomerate unit. (a) The dip direction of the sedimentary layers showing N165°E trend and **(b)** the dip angles of the sedimentary layers are mostly dipping 20°.

Depositional environment of this unit has been interpreted as the mixing of alluvial and fluvial influence. It is suggested by the chaotic grains organization in the southwestern part of the area and more organized in the central part of the area. The southwestern part is dominated by the debris flow deposit while the central part is influenced by channelized or fluvial system which can be recognized by the finer materials and graded bedding structures. It is maybe part of the big alluvial fan which may have a lateral variation from alluvial and fluvial system dominated.

4.1.4 Late Sandstone-Conglomerate (unit 4)

This unit comprised of sandstones and conglomerates. They are sitting at the northern part of the fault block, close to the foot-wall of the Dhoumena Fault. The lithology has similar characteristics with that of the unit 3, but unit 4 has more well organization of the grains, suggesting more fluvial dominated sedimentation. The sandstones have a channelized shape

whilst the conglomerates form the background sediment of this unit. The sandstones are characterized by medium-very coarse sand grains, grey-brown color, and channelized shape but difficult to decide and measure the channel directions. No sedimentary structures of this lithological unit can be observed but it looks like that this unit has well-organized grain components which might lead to fluvial dominated environment.

The conglomerates are acting as the background of this sediment package. The conglomerate is characterized by the cobble-pebble grain size (10-30 cm, 20cm in average), grey-yellow color, and massive structure with a layering that can be observed only from a distance (Figure 4.9). Clast materials of this unit is comprised of limestones, cherts and some sandstones, they are all bounded together and not well cemented as compared to unit 2 and 3.

As this unit is located at the northern part of the Kerpini Fault Block, close to Dhoumena Fault, there is unconformable contact that can be observed where the conglomerate and sandstone are overlying the Pindos Carbonate Basement (Figure 4.9). There is no good outcrop to measure the strike and dip of the unconformity but it is clear that the unconformity plane has a southward dip. Relationship between this unit to unit 2 and 3 is that this unit seems to be deposited at the latest stage. It may start with deposition of unit 2 and 3, at the same time, as the Kerpini fault was displacing then these units are tilted. Next stage, the Kerpini Fault Block was incised and unit 4 was deposited.

Sedimentary layers of unit 4 also show a common trend. There is an area within this unit which has almost horizontal layers. This unit has an onlapping relationship of the sediment towards the basement which can be observed, particularly at western and eastern part of the fault block (Figure 4.9). The dip direction shows two main dip directions (N355⁰E and N210⁰E) with an average dip angle of around 3⁰-15⁰ although there are layers with dip angle more than 20⁰ (Figure 4.11) it has been interpreted to be not real dip angles since they are have been measured from a distance with +/-10⁰. These flat layers appear in the Roghi Mountain, where dips of the sediments are almost flat and located between two unconformities (Figure 4.10).

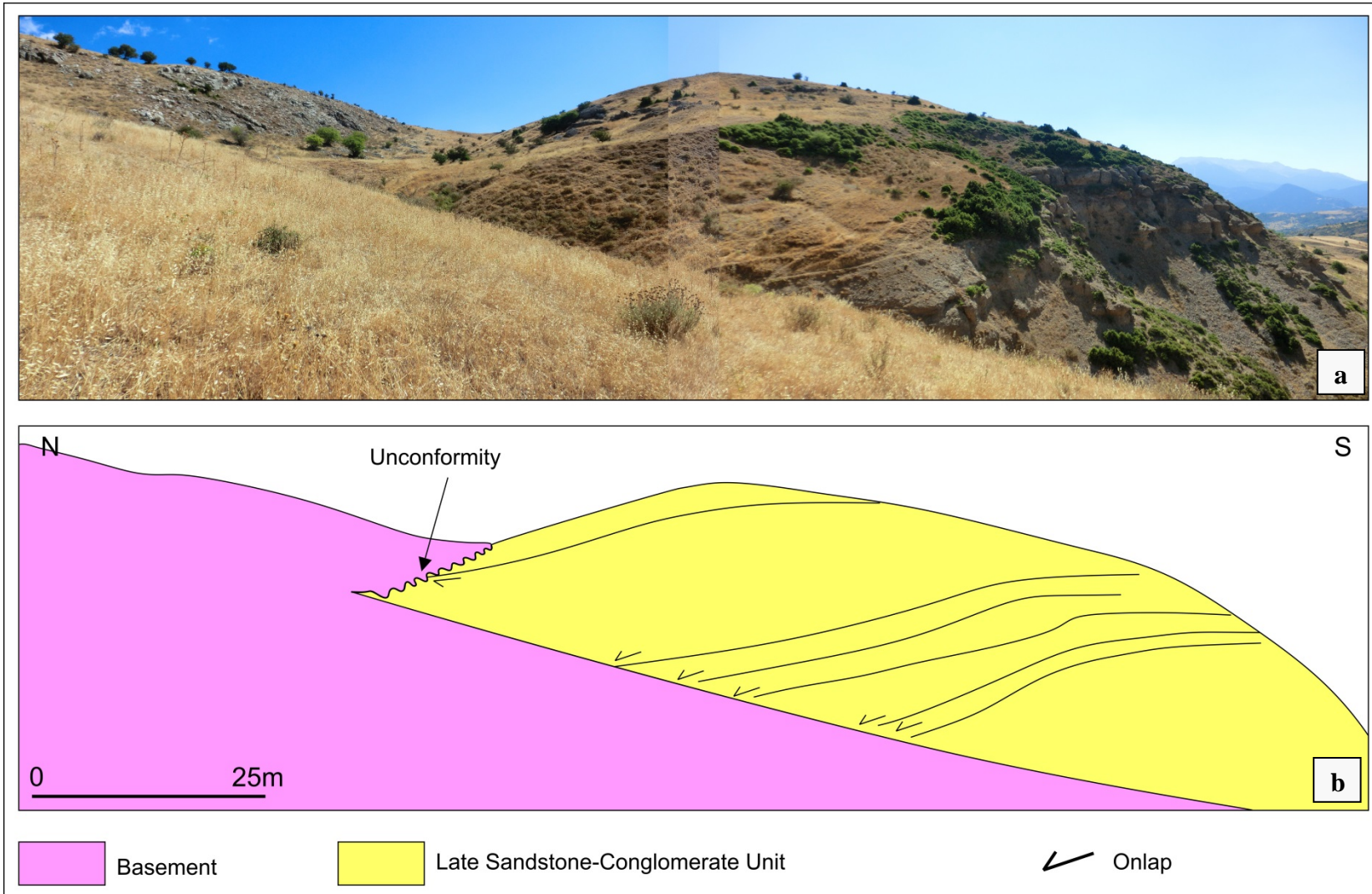


Figure 4.9: Photograph looking east. A photograph shows the sedimentary layers of unit 4 (a) and the interpretation (b). The sedimentary layers are dipping to the north with 5° - 10° of dip angle. There is an onlap relationship between this sediment with the basement, where the conglomerate and sandstone is dying towards the basement, there is also unconformity between them.

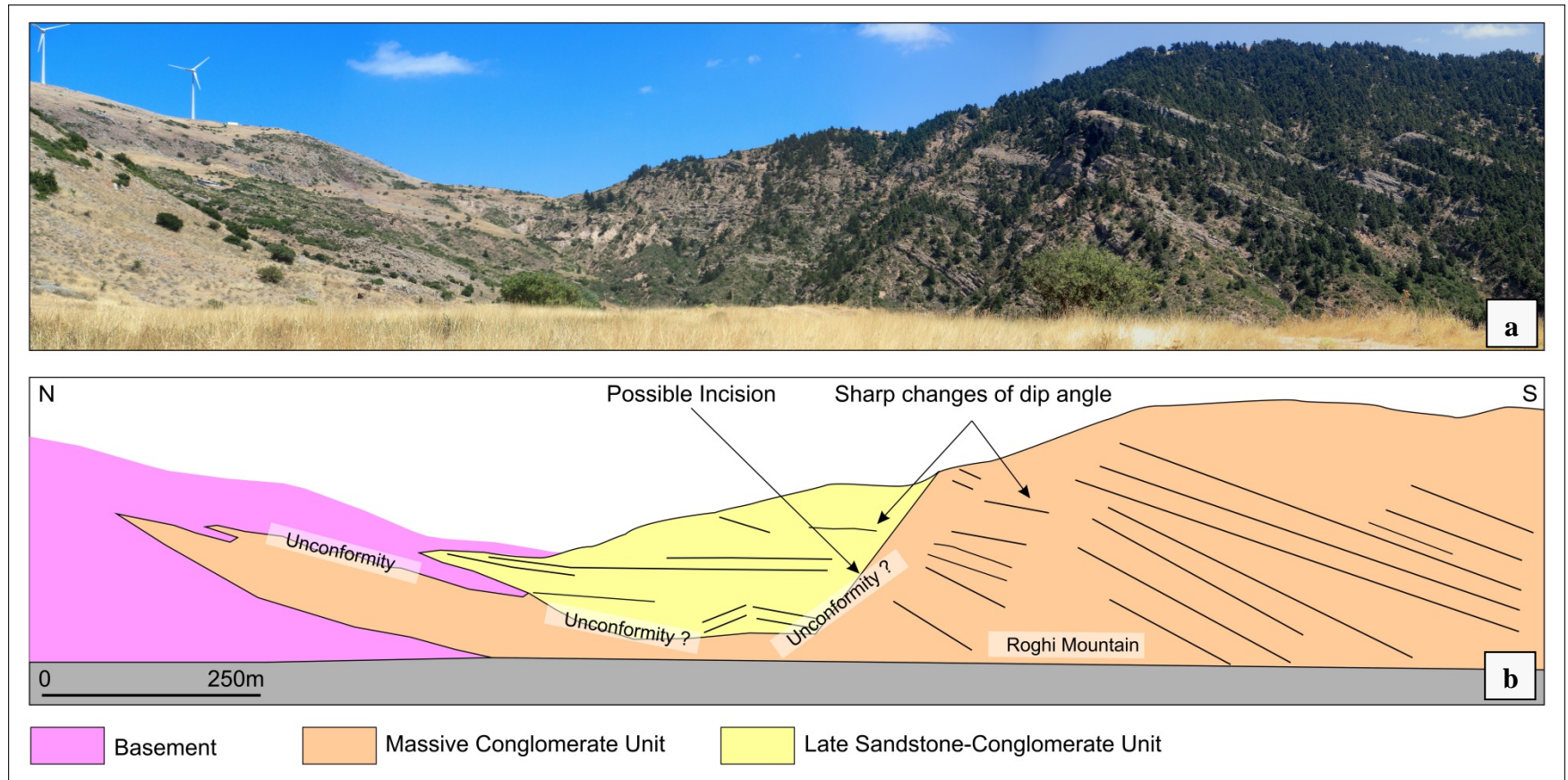


Figure 4.10: A photograph looking east from Roghi to the Roghi Mountain. It shows the relationship between Massive Conglomerate, Late Sandstone-Conglomerate, and Pindos Carbonate. In this picture there are two unconformities, first is the unconformity between Pindos Carbonate and Sediments, and last, is the unconformity between unit 2 and unit 4. It shows also the sedimentary layers, in unit 2 Deposit, the layers seem to have dipping to south, but in the last facies, the layers seem to be flat (it shows a clear dip angle change). This implies that it should be boundary between the unit 2 and 4, it may related to incised fault block and subsequent river channel flow and carry sediments, which might be an unconformity between them.

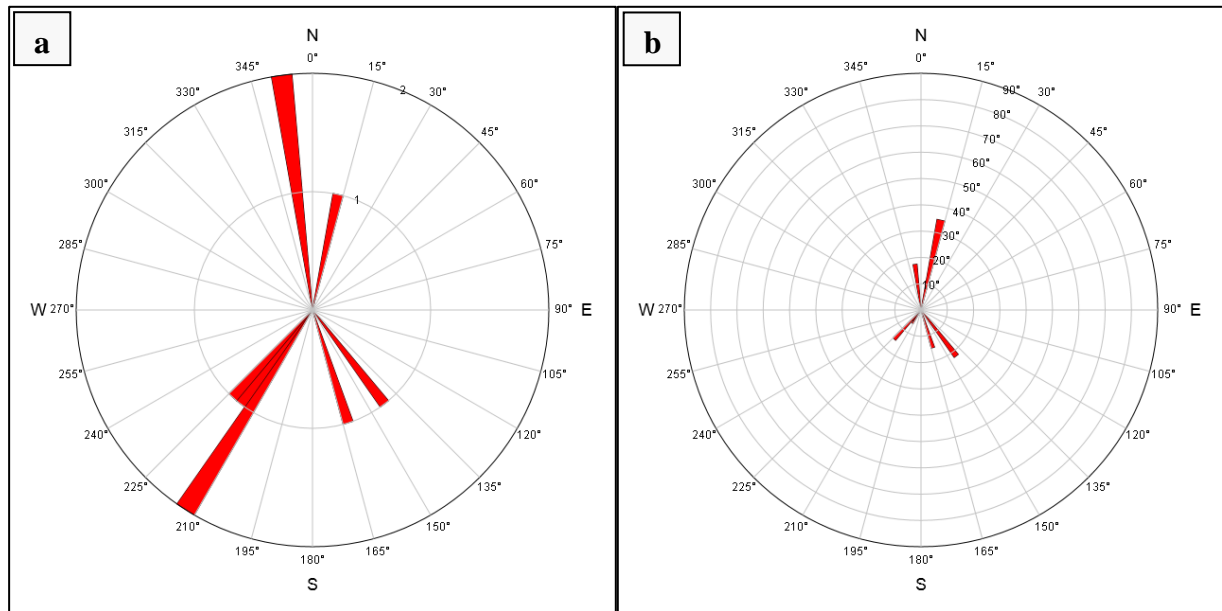


Figure 4.11: Rose diagram of sedimentary layers in Late Sandstone-Conglomerate unit. (a) The rose diagram shows two trends of dip direction (NE-SW and close N-S). (b) North dipping layers have a average of dip angle from 3° - 15° , whilst south dipping layers have a trend 5° and there are also gentle layer sediments with dip angles less than 5° . Those steeper dips have been interpreted as the collapsed layer (not true dips).

4.1.5 Relative Age of Sedimentary Units

There is no absolute dating analysis in this study. Therefore, the analysis about the age will be related to their relative age compared to the events or other sedimentary units. Based on the field observations, the Pindos Carbonate Basement (unit 1) is deposited in the pre-fault phase. When the Kerpini Fault start to move in the early phase of syn-faulting, unit 2 and 3 are deposited almost at the same time. Differences in grain size distribution and clast composition may suggest the 2 sediment sources. In the late phase of syn-fault, the Kerpini Fault movement was slowing down, and the unit 2 and 3 was incised by the channels which bring sediments and deposited as unit 4. Unit 4 has been interpreted as the late phase sedimentation because of their sedimentary layers that gentler compared to unit 2 and 3. It may suggest that unit 4 has no big influenced by the Kerpini Fault. Moreover, the compaction degree of the lithology of the unit 4 is less than the unit 2 and 3.

4.1.5 Grain Size Distribution

Hanging-wall of the Kerpini Fault Block which has been filled by syn-fault deposits is mostly composed by the clastic sediments. They have a variation in term of grain size of the clast

components. Analysis of grain size helps to explain about facies association and transport history. In general, grain sizes vary from 5-40cm.

In Figure 4.12, it shows distribution of grain size of clastic sediments within the Kerpini Fault Block. It seems that the grain size has trends which can be divided into two main trends. First, the trend within the Roghi Mountain, in general grain size in the Roghi Mountain can be observed to have a fining northward, westward, and also coarsening upward. Similar to the grain size trend in the Roghi Mountain, in the Kerpini Area, the grain size analysis is more difficult to be reconstructed due to the topographic expression which makes it harder to reveal a general trend with cross-sections. However, incorporated the data in the Kalavrita Fault Block, the trend of grain size variation in the Kerpini Fault Block has been interpreted to be fining northward as a continuation of sedimentation in the Kalavrita Fault Block, but the vertical trend is difficult to explain.

Cross-sections within the Roghi Mountain show the evidence for the interpretation of trend analysis. P-Q cross-section is showing the grain size distribution from north to south which may support the evidence apparently even it is difficult to differentiate between lateral or vertical variation (Figure 4.13). Bigger grain size close to Inlier Fault has been interpreted to be an effect of faulting which collapsing fault block. Picture A, B, and C are supporting the idea about coarsening upward. In cross-section R-S, there is a reconstruction of lateral variation from east to west. The reconstruction shows that the grain size tend to be smaller to the west and also supported by the pictures A, B, C, and D (Figure 4.14).

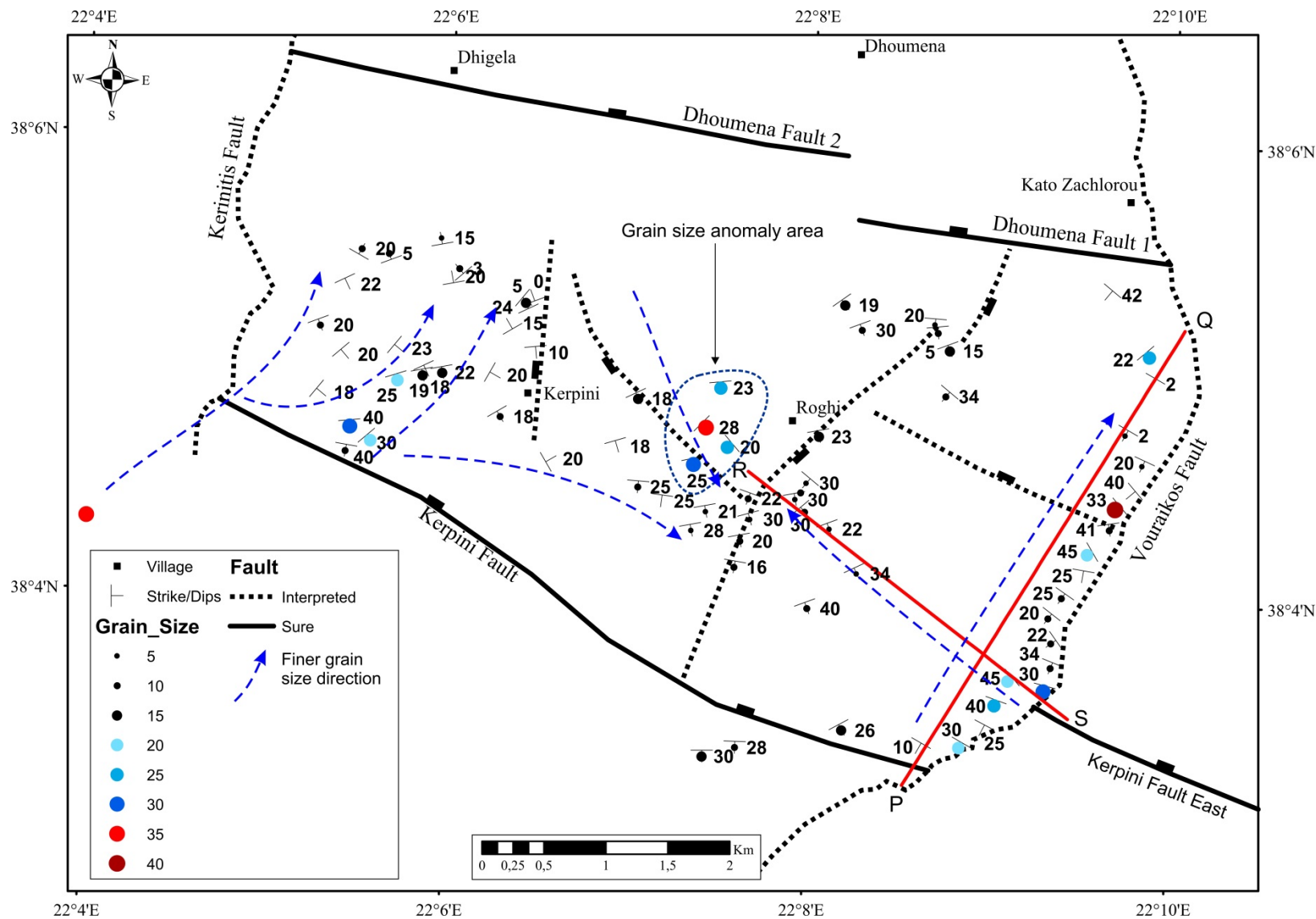


Figure 4.12: Grain size map distribution of sediments within Kerpini Fault Block. The grain size map distribution shows the general trend of fining northward for all of the sediments within the Kerpini Fault Block and coarsening upwards only can be observed in the Roghi Mountain section.

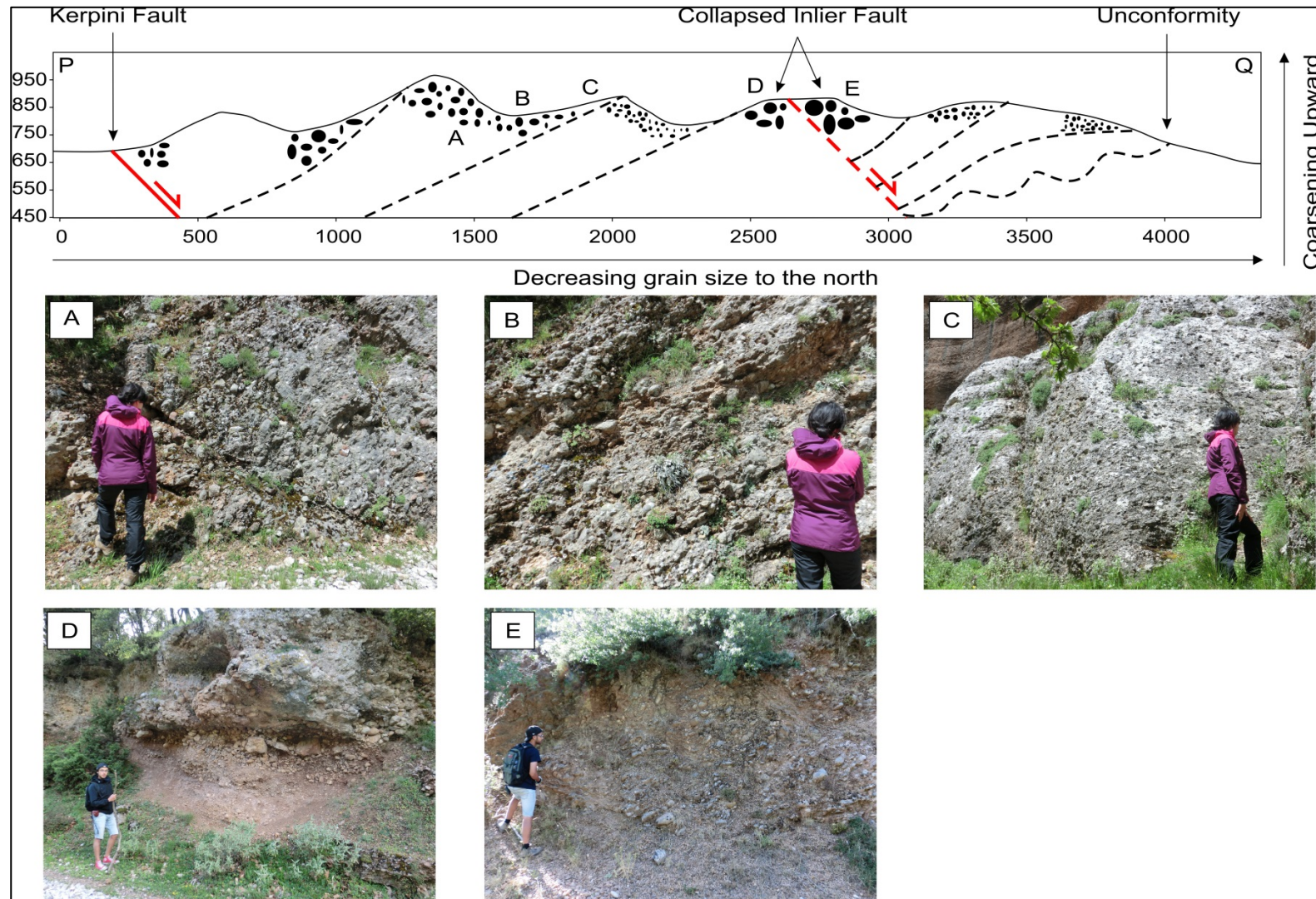


Figure 4.13: Cross-section P-Q shows south to north section. This section is showing that the general trend of grain size within the Kerpini Fault Block is fining northwards and coarsening upward, this interpretation is supported by the filed photo which may represent the real condition in the field.

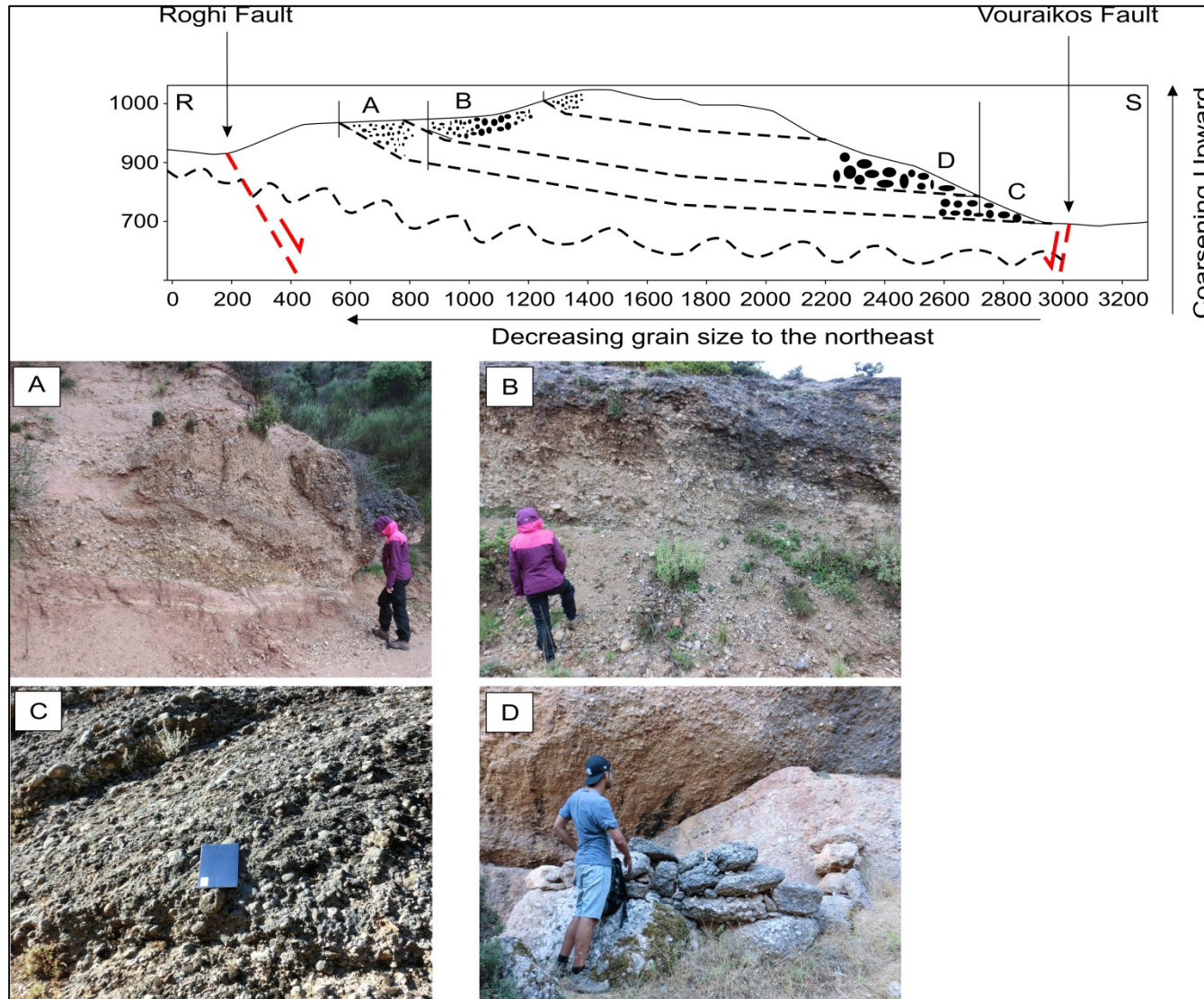


Figure 4.14: Cross-section R-S shows west to east section of Roghi Mountain. This Cross-section is showing the trend analysis for internal Roghi Mountain from west to north, the reconstruction reveals that the grain size of sediments in Roghi Mountain is tend to be smaller to the west and bigger to the east, it may implies to the paleo-drainage or source sediment analysis.

4.2 Geomorphology

Geomorphological investigation in the study area included two steps of analysis. Observations included Digital Elevation Maps (DEM), from which contour maps were produced, and direct field observations.

Fault block morphology, created by a series of normal faults dominates the Gulf of Corinth region. Focus in this study is on one of these faulted blocks, known as the Kerpini Fault Block. It is bounded to the south by the Kerpini Fault, to the north by the Dhoumena Fault, whilst the western and eastern sides are bounded by the Vouraikos and Kerinitis Rivers (Figure 4.15).

4.2.1 Lineament

The lineament pattern analysis was conducted by DEM and contour map observations, as shown in Figure 4.15. Analysis was conducted by marking all of the lineaments in the study area. The lineaments are dominated by a N280°E – N300°E striking trend, matching that of the regional faults (Gulf of Corinth).

Field observations revealed that the lineaments are related to geological features such as faults (scarp), rivers, and valleys. This observation was incorporated in the construction of the geological map.

4.2.2 Drainage Patterns

The drainage patterns created by the rivers are considered to be dendritic and parallel in nature. This can be seen by the irregular shape of the rivers which are generally coupled with parallel drainage systems. The dendritic pattern reflects similar lithology type whilst the parallel pattern is likely a direct effect of local and regional faulting.

The dendritic rivers pattern can be observed in the central part of the fault block where there is an accumulation of conglomerates and sandstones (Figure 4.15). In addition to that, the parallel drainage patterns can be observed at the eastern part of the fault block (West Vouraikos Valley).

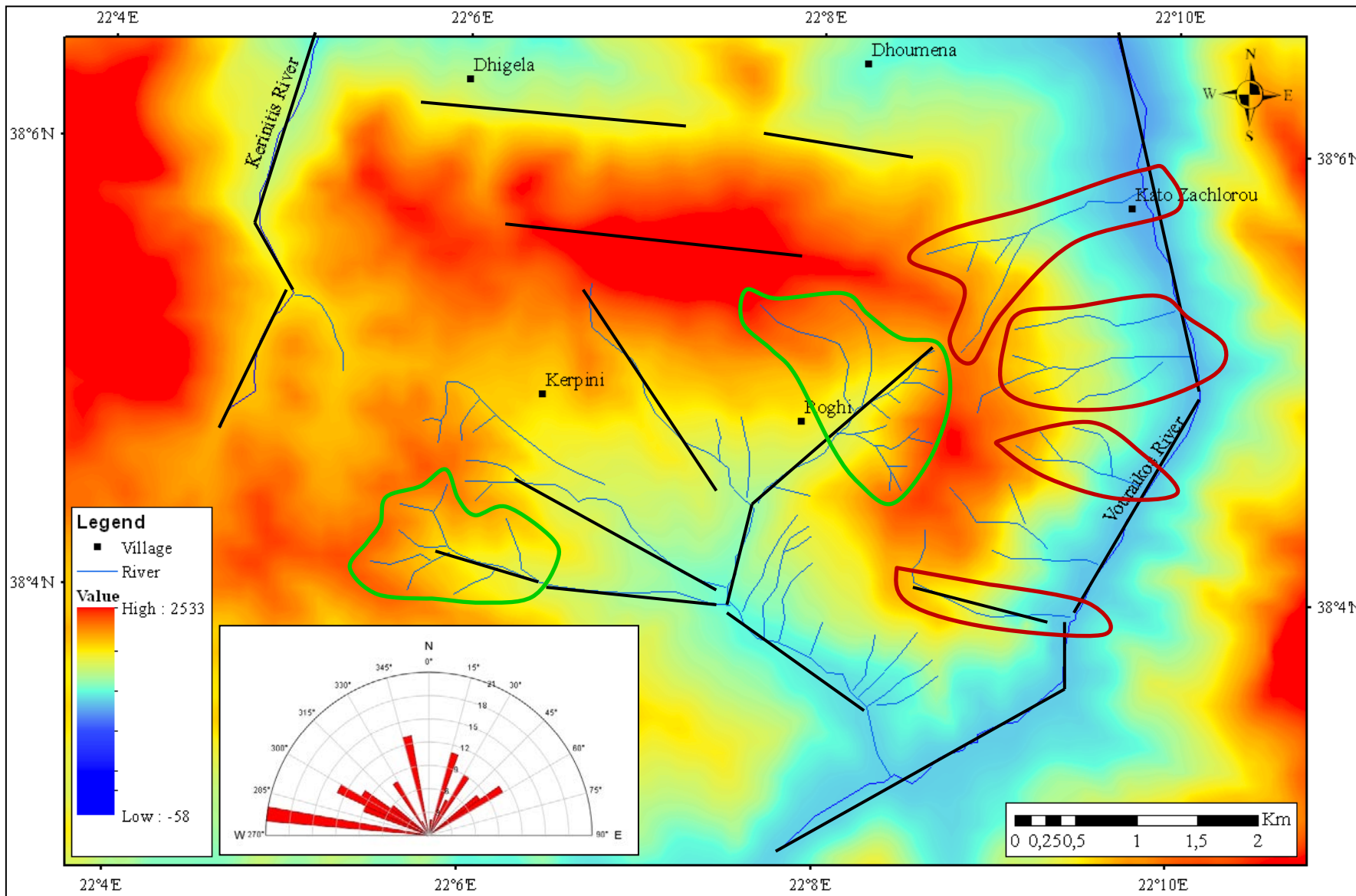


Figure 4.15: Digital Elevation Map (DEM) of the Kerpini Fault Block. *The map shows the elevation map of Kerpini Fault Block where it is bounded by the Kerpini and Dhoumena Fault at south and north, the Vouraikos and Kerinitis Rivers/Valleys at east and west parts. The rose diagram has been produced to show the lineament analysis using this map which tells the trend of lineament is striking $N280^{\circ} - 300^{\circ}E$ (the black lines represent lineaments). Green polygons represent dendritic river pattern while red polygons represent parallel river pattern.*

4.3 Structural Observation

4.3.1 Faults

Structures in Kalavrita-Helike consist mainly of faults, most of which are normal faults with a northeast dip of $40^{\circ} - 45^{\circ}$. These faults result from the Miocene to Recent Gulf of Corinth Rifting event. The faults have been recognized by the DEM, lineament, and field data including the abrupt changes of the lithology and topographic expression. The foot-wall of the faults is dominated by the Pindos Carbonate Basement whilst the hanging-wall consists of the sedimentary rocks known as the syn-fault succession, composed of conglomerates and sandstones.

Three major faults, two inferred faults and five intra block faults are present in the study region (Figure 4.16). The Kerpini and Dhoumena Faults mark the southern and northern boundaries of the Kerpini Fault Block respectively. These faults have ENE-WSW trend and dipping to NNE.

Moreover, intra block faults have also been identified from field observations, changes in lithology and topographic expression. Typically they follow the trend of the rivers within the Kerpini Fault Block.

Furthermore, the western and eastern boundaries of Kerpini Fault Block are marked by large river valleys, the Vouraikos (eastern) and Kerinitis (western) Rivers (Figure 4.16), which have an N-S trend. The Kerpini and Dhoumena faults seem to be truncated towards these valleys as do several other faults which are challenging to correlate across the valleys. However, there are some faults which appear to be continuous across the valley. Therefore, it is debatable whether or not there are significant N-S structures in the valleys.

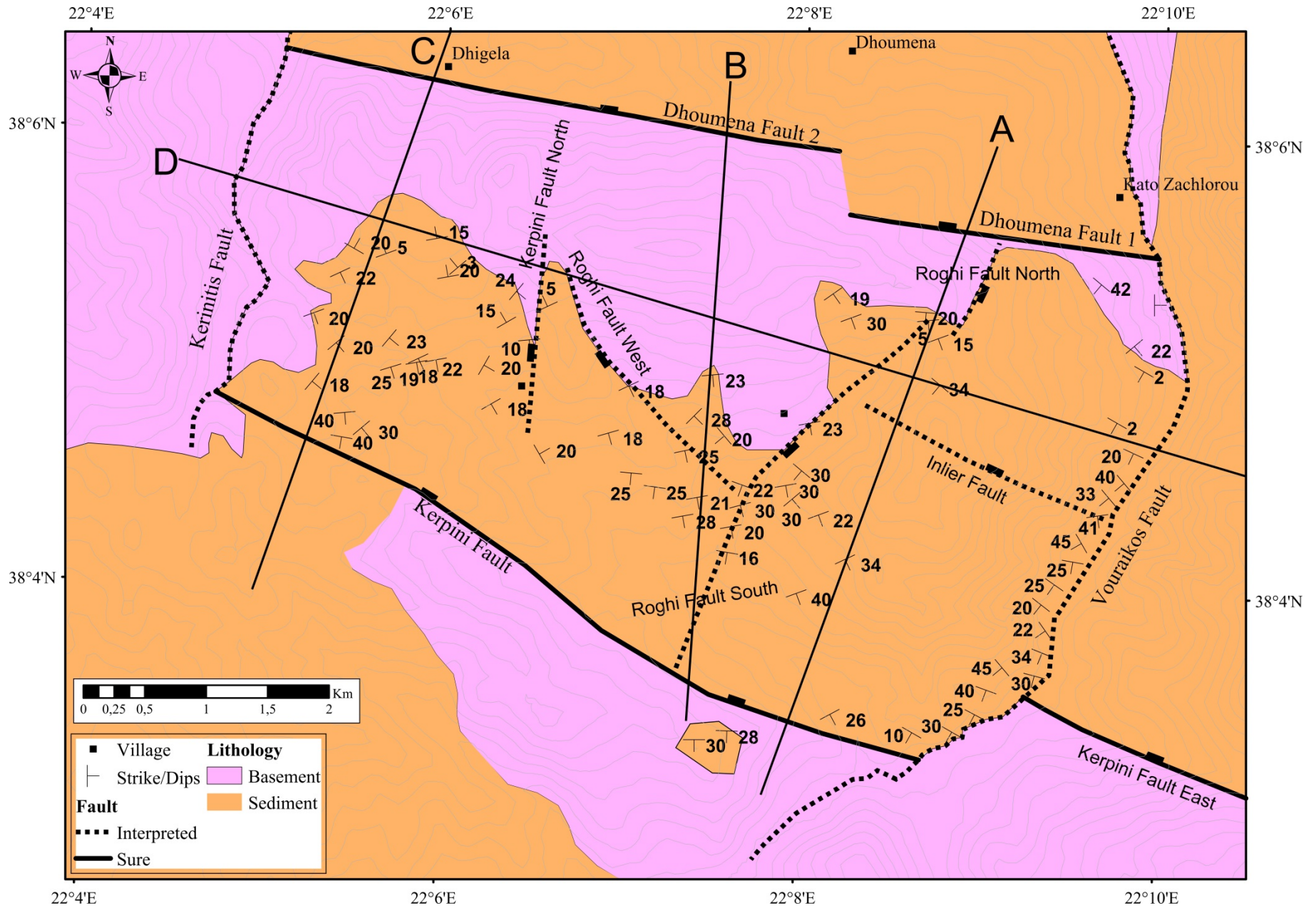


Figure 4.16: Structural map of the Kerpini Fault Block. *The geological map shows the distribution of basement (pre-fault deposit) and sedimentary rocks (syn-fault deposit) in the Kerpini Fault Block. Hanging-wall of the Kerpini Fault is consisted of mostly sedimentary rocks while the foot-wall is consisted of the basement. The basement exposure in foot-wall is the result of the foot-wall uplift erosion. In this fault block, there are 2 certain main faults and 4 interpreted faults. In addition to that, there are valleys at the eastern and western part that could be fault.*

4.3.1.1 Kerpini Fault

The Kerpini Fault marks the southern boundary of Kerpini Fault Block. The name is taken from the closest village. Although the fault plane is not well exposed, DEM analysis, abrupt changes in the lithology from the basement to conglomerate, and the dramatic changes in elevation (+/- 300m) topography suggest the presence of the Kerpini Fault.

The Kerpini Fault is a normal fault, dipping to the northeast with a N120°E strike. The dip angle cannot be measured directly since the fault plane is not exposed. Instead, a dip angle similar to that of the regional fault's dip of 40°- 45° will be assumed. The length of the Kerpini Fault is 6.4km based on the field map with an estimated maximum throw of +/- 1200-1500m which measured from sediment thickness and uncnformity in the Kerpini Fault Block (Figure 4.17). The minimum throw occurs at the western part close to the Kerinitis-Kerpini Fault intersection where the throw is more or less 50-100m. It is not clear if the Kerpini fault is truncated on Kerinitis River, but two options for that are Kerpini Fault is truncated on the Kerinitis River or it is just a fault tip.

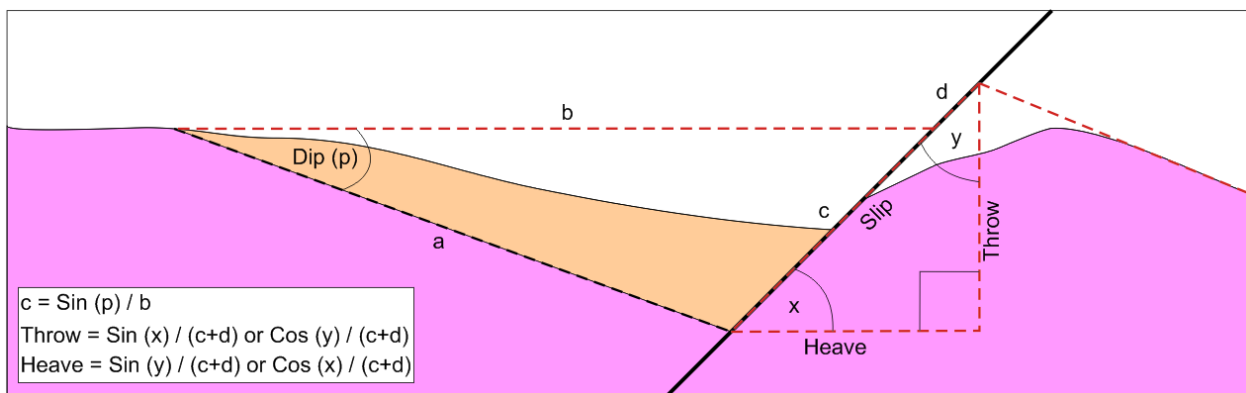


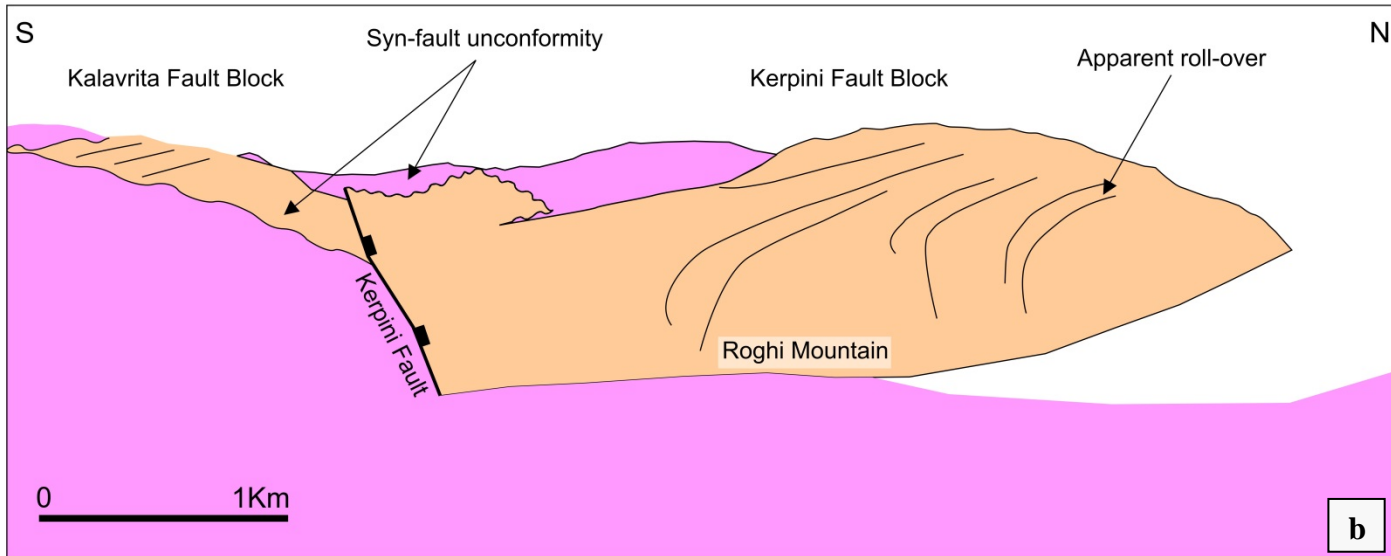
Figure 4.17: Schematic figure to calculate throw of the fault. *Throw is calculated using the projected minimum surface of foot-wall uplift and sediments.*

In order to support the opinion about displacement distribution of the Kerpini Fault, it can be proven by look at the relationship of the foot-wall and hanging-wall of the Kerpini Fault Block.

Close to the Vouraikos River, it has been found basement in the foot-wall and conglomerates in the hanging-wall but move farther to NE follow the trend of this fault, close to Kerinitis River, it has been found that in the hanging-wall and foot-wall of Kerpini Fault are comprised of conglomerates. It may indicate that the maximum throw in the eastern part was causing more erosional sediments.

The foot-wall of Kerpini Fault is part of the Kalavrita Fault Block. The foot-wall is composed of the Pindos Carbonate Basement with unconformably overlying inter-bedded sedimentary rocks (conglomerates and sandstones) at the western area which might have similar properties with unit 3 in Kerpini Fault Block. In the hanging-wall, there are conglomerates and sandstones deposit covered the area which has been described as unit 2, 3 and 4 (Figure 4.18).

As shown in Figure 4.18, unconformities occur in both fault blocks. The unconformity is marked by the Pindos Carbonate Basement lying beneath the sedimentary rocks. The unconformities are usually exposed in the immediate foot-wall of the faults due to its uplift and subsequent erosion. There are apparent roll-over layers which might look like structural properties, but actually they are just the apparent features because of the point of view (Figure 4.18).



Basement Sedimentary Rocks (Syn-fault Deposit)

Figure 4.18: Photograph looking west of the Kerpini Fault Block. (a) A panoramic photograph looking west of Kerpini Fault (taken from Souvardho Village). (b) Illustration of the interpretation from the photo, foot-wall of the Kerpini Fault is mostly composed of Pindos Carbonate Basement whilst the hanging-wall is composed of syn-fault succession (conglomerates and sandstones) with Pindos Carbonate Basement in the immediate foot-wall of Dhoumena Fault. There is an unconformity in this fault block which is related to the erosion of foot-wall uplift.

4.3.1.2 Dhoumena Fault

The Dhoumena Fault forms the northern boundary of the Kerpini Fault Block. The name of this fault is taken from the Dhoumena Village which is situated close to this fault. The fault plane is well exposed as scarp morphology, therefore, the strike and dip of the fault can be measured directly at the fault plane.

Based on the direct measurement, the Dhoumena Fault is a normal fault striking N110⁰E and dipping 44⁰NE. The strike and dip of this fault is consistent with the regional faults configuration. The Dhoumena Fault has been divided into two parts suggested by the sediment bypass deposit at its hanging-wall. Dhoumena Fault 1 is located at the eastern side with 2.5km in length while Dhoumena Fault 2 is located at the western side with 4.5km in length.

In Figure 4.19, the foot-wall of the Dhoumena is comprised of mostly Pindos Carbonate Basement, resulting from erosion of the uplifted foot-wall. The hanging-wall of this fault is composed of sedimentary rocks (syn-fault succession with mostly contain conglomerate, overlying marls, and calcareous sandstones) sitting on top of the basement with unconformable relationship.

This fault has similar displacement distribution as Kerpini Fault. At the centre of the fault, which marked by Dhoumena Village, this is the area where the maximum displacement is. Move to the west, where Dhigela and Plataniotisa Villages located, the displacement of Dhoumena Fault is decreasing gradually towards this direction. Displacement at this point is not zero, but then when this fault reaches the Kerinitis River, suddenly the fault is truncated and died. There is an abrupt change of displacement of this fault, from couple hundred meters at Dhigela and Plataniotisa Villages to 0 meter at Kerinitis River which located more or less 1km from the villages.

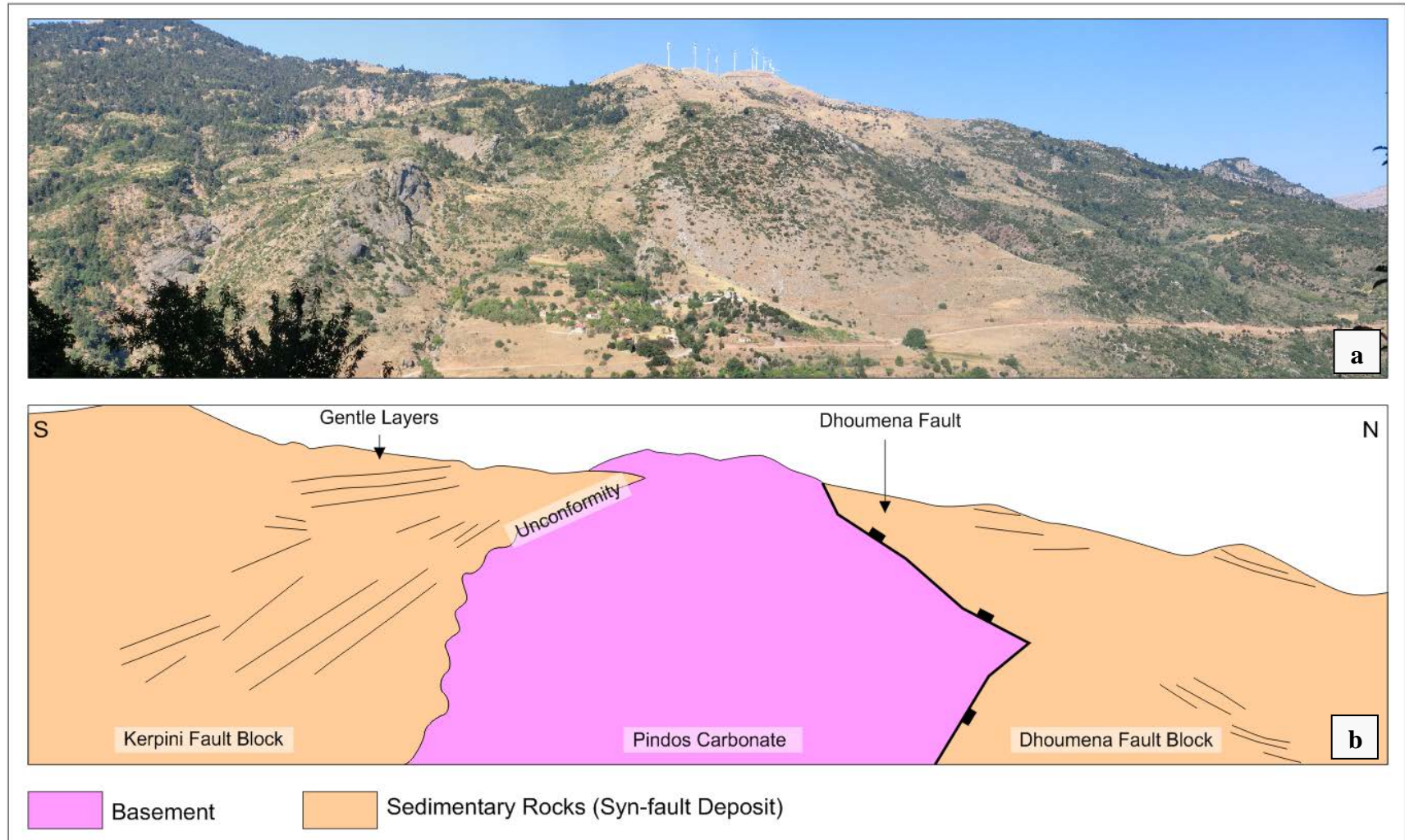


Figure 4.19: Photograph looking west of the Dhoumena Fault. (a) A panoramic photograph looking west of Kerpini Fault (taken from Monestary). (b) Illustration of the interpretation based on the photograph, Dhoumena Fault is striking NW-SW and dipping to NE. In the immediate footwall of Dhoumena Fault which is part of Kerpini Fault Block, there is an unconformity which marked by the syn-fault deposit on the top of Pindos Carbonate Basement. Moreover, the sediments are dipping to SW for except for the gentle layers of sediment at the top of syn-fault succession. Opposite to that, the sediments in Dhoumena Fault Block show the different dip direction, they are mostly dipping to NE.

4.3.1.3 Vouraikos Fault

The Kerpini Fault Block is bounded to the east by the inferred Vouraikos Fault which aligns with the N-S morphology of the rivers (Figure 4.16). The trend of this fault is following the trend of the Vouraikos Rivers (N-S), whilst the dips are unknown, due to non-exposure of the fault plane, therefore, the vertical fault plane is assumed.

The Vouraikos Fault is inferred the lithology and also the major faults. On either side of the valley it is clear that Kerpini Fault cannot be traced to the east across this river. It should have a very sharp bend to connect this fault to Kerpini Fault East which located across the river. The sedimentary rocks in Kerpini Fault Block discontinue as they reach the rivers, in this case, these rocks will face the basement rocks on the other side.

Looking at the regional scale, from Kalavrita to Helike area, normal faults in this area are always truncated or died at Vouraikos Valley. Some of the faults which might be correlated as the same fault usually need to be sharply bended to connect them. Evidence is also, there are faults that stepping to the right and there are faults that stepping to the left. This fact is suggesting the existence of Vouraikos Fault. However, by looking at its displacement which applied to almost all of the normal faults in this area, a best suggestion is to interpret this fault as a transfer fault or transfer zone which might separate structures on both sides.

4.3.1.4 Kerinitis Fault

The Kerpini Fault Block is bounded to the west by another inferred fault, the Kerinitis Fault which aligns with the N-S morphology of the rivers (Figure 4.16). The trend of this fault is following the trend of the Kerinitis River (N-S), whilst the dips are unknown, due to poor exposure of the fault plane, therefore, the vertical fault plane is assumed.

The Kerinitis Fault is supported by the abrupt lithology changes evidence. Conglomerate at the western part of Kerpini Fault Block cannot be traced to the west across the river; it seems that the conglomerate stop at the river. There are no faults close to the Kerpini Fault Block located at the across river, therefore, there is no evidence to support this fault in term of the fault connectivity, but they have an evidence at far north close to the coast where there are couple of faults that

cannot be traced across the Kerinitis Fault. In addition, Dhoumena fault which has hundred meter displacement in Dhigela (+/- 500m) seems to have no significant fault displacement can be observed 1km to west (Kerinitis River). In conclusion, the evidence to support existence of this fault is not as strong as Vouraikos Fault.

4.3.1.5 Kerpini Fault East

This fault has been interpreted to have a similar fault configuration as the Kerpini Fault. The Kerpini Fault East is dipping northeast with a N120^oE strike. This fault is located on the east side of Vouraikos River, on the other side of Roghi Mountain. This fault can be observed by the abrupt changes of lithology. Moving from south to north, there is a change from basement to conglomerate. It has an offset to the Kerpini Fault, which may suggest the existence of the Vouraikos Fault.

4.2.1.6 Intra Block faults

Aside from the major faults, there are four intra block faults within the Kerpini Fault Block (Figure 4.16). These faults can commonly be observed by looking at the topography and discontinuity of the lithology. Some of them clearly follow the rivers. Most of them are N-S striking fault except for one fault which has been interpreted as NW-SE fault (similar with regional structure in this area). The N-S faults have been interpreted to have similar geometry with the Vouraikos and Kerinitis Faults. Most of the faults are difficult to calculate their displacement. Explanations about these faults are given below.

a. Kerpini Fault North

This fault is located very close to Kerpini Village. It has been interpreted as normal fault striking N350^oE with an unknown dip angle, due to poor exposure of the fault plane. The dip of the fault is therefore assumed to be almost vertical with a SE dip direction. The sedimentary facies close to the fault and topographic expression surround this fault suggest the existence of the Kerpini Fault North. The offset of this fault is difficult to predict.

b. Roghi Fault South

This fault is going through Roghi Village. It has been interpreted as a normal fault striking N30^oE again with an unknown dip angle due to poor exposure of the fault

plane. The dip of this fault is assumed to be almost vertical with a SE dip direction. This fault can be identified in a river valley within the Kerpini Fault Block and is distinguished by different lithological facies in the interpreted foot-wall (Roghi Mountain) and hanging-wall (Kerpini Village) of the fault, moreover, the increasing sediment thickness at Roghi Mountain which might indicate deeper unconformity level compared to what exist at the Kerpini Area is also become an evidence to support the existence of the fault. It is difficult to calculate the displacement, but based on the unconformities level in the hanging-wall and foot-wall of this fault, this fault has been interpreted to have a displacement about 100-200m.

c. Roghi Fault North

This is the smallest fault compared to the other minor fault. This fault is located close to Profitis Illias. This fault has been interpreted as a normal fault striking $N20^{\circ}E$ but the dip of the fault cannot be observed. Same as the other minor fault, the dip of fault is assumed to be almost vertical downthrown to SE. This fault has an offset relative to the Roghi Fault South. It is difficult to calculate the displacement of this fault.

d. Roghi Fault West

This fault has been interpreted after the analysis of unconformity distribution where the foot-wall of this fault is mostly composed by limestone and the hanging-wall is composed by conglomerates. It must have a big jump of unconformity surface to make a continuous unconformity. Actually, there are two options to explain this feature. 1) This feature may relate to the inherited topographic expression of basement depression or 2) there is a fault in between. After the observation and analysis, the option number 2 has been chosen to explain this feature. This fault has been interpreted as a normal fault striking $N120^{\circ}E$ and unknown dip angle, but interpreted SW dip direction.

e. Inlier Fault

This is the only NW-SE fault in this minor fault. This fault is located in the middle of Kerpini Fault Block at eastern part. This fault can be observed by looking at the presence of Pindos Carbonate Basement. The outcrop is well exposed close to the Vouraikos Valley. This fault has been interpreted as a normal fault striking $N110^{\circ}E$ and dipping 40° - $45^{\circ}NE$. The conglomerates are sitting on top of the basement striking $N82^{\circ}E$ and dipping $41^{\circ}SE$.

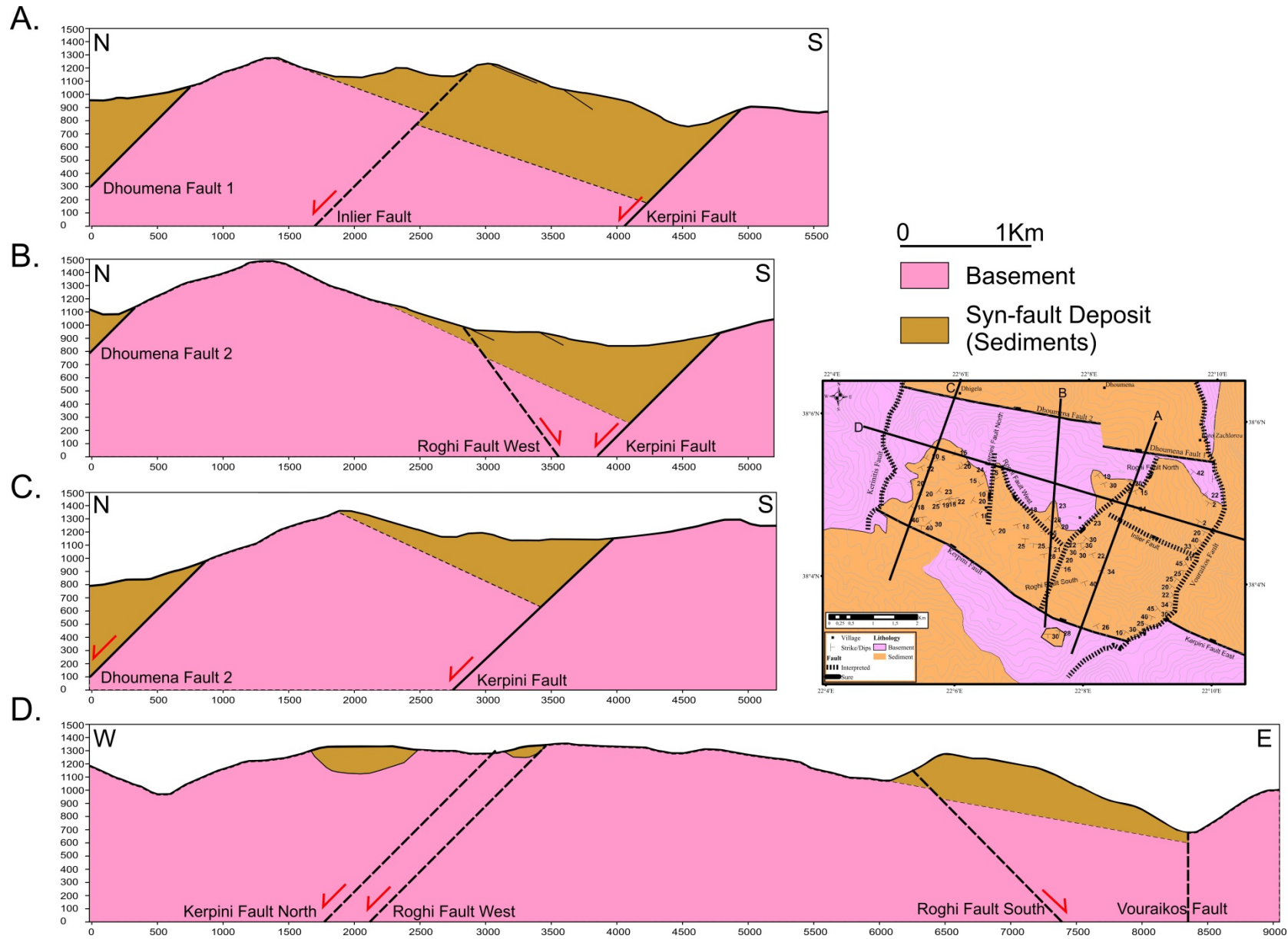


Figure 4.20: Cross sections through the Kerpini Fault Block. *Cross sections are showing the structural configuration within Kerpini Fault Block and their relationship between faults, basements, and sediments.*

4.4 Kerpini Fault Block Sedimentary Layers

Strike and dip measurements of sedimentary layers across the whole fault block have been conducted in the field work. Most of the measurements were taken by direct measurements and in some cases, particularly in the massive conglomerates usually difficult to be taken; some of the measurements are mostly have done from a distance.

Observations show that the mean dip direction is towards the southeast with an NE-SW strike (Figure 4.21). The dip directions appear to be not directly into the fault, but slightly oriented towards the maximum throw of the Kerpini Fault. The dip angle of the sedimentary layers has a 20° - 25° trend towards the fault (Figure 4.21). This oblique angle between the bed dip and fault dip is consistent with the eastward increase in fault displacement along the Kerpini Fault.

There is one unit of sediments that has a different dip angle and direction. This sediment package is located far north away from Kerpini Fault and close to Dhoumena Fault which is called as unit 4. This unit has gentler dips with a variable of dip direction. Some of them are oriented towards the fault with shallow angle, and some of them towards the basement with steeper angle. The shallower dips of this unit led to the conclusion that this unit should have been deposited as the younger aged sediments after the ca. 20° - 25° southwards tilting of the older units.

At the foot-wall of the Dhoumena Fault there is a good exposure of an unconformity where the conglomerate is lying above the basement. The direct measurement was found that the unconformity plane is striking $N130^{\circ}E$ and dipping $42^{\circ}SW$. In addition to that, the sediments in Kerpini Fault Block (foot-wall of the Dhoumena Fault) are dipping to the SW, except, the gentle layers at the top of the syn-fault succession (Figure 4.19). The dip direction of the sediments in the hanging-wall of Dhoumena Fault seem to have a different direction, they are dipping to the NE.

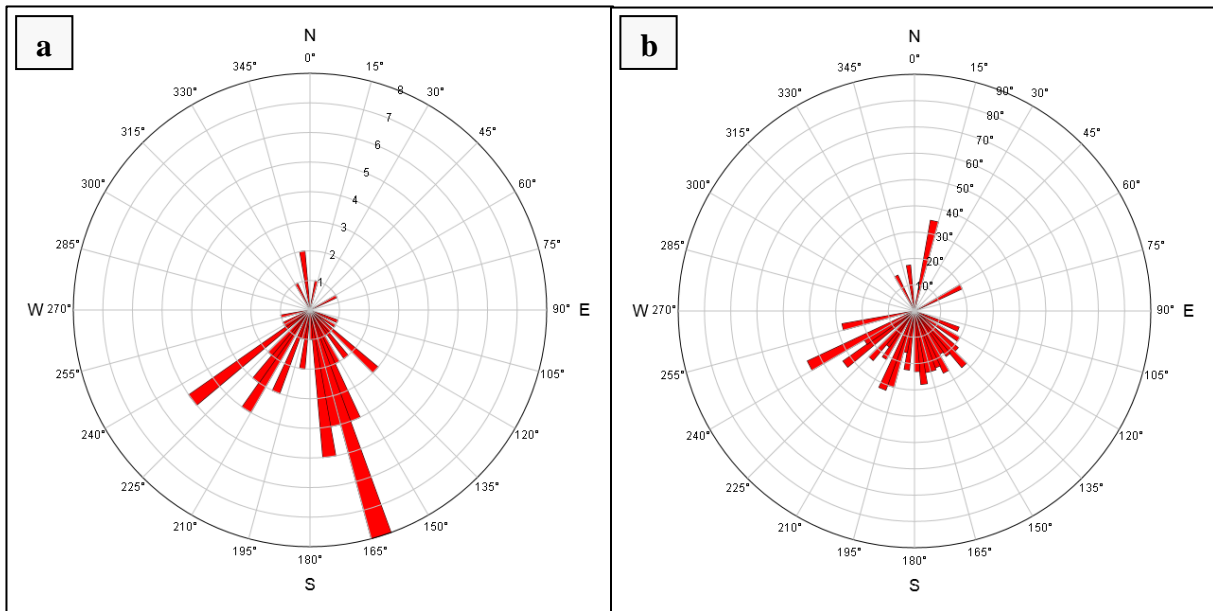


Figure 4.21: Rose diagram of the measured strikes and dips in the Kerpini Fault Block. (a) Rose diagram shows the distribution of dips direction in the kerpini Fault Block, it can be seen that most of the sediments are dipping to the SE. (b) Rose diagram shows the distribution of dips angle, most of the sediments have a dip angle around 20° - 25° .

4.5 New Discoveries

Field work observations have been done in the Greece. Based on the observations and analyses, there are several new findings within the Kerpini Fault Block. The findings could be as a structural elements, lithological variation, etc. and here are the new findings based on the field observations as a summary of the field observations chapter (Table 4.2):

Type	Name	Notes
Faults	Kerpini Fault	Regional Fault
	Kerpini Fault East	Regional Fault
	Dhoumena Fault 1	Regional Fault
	Dhoumena Fault 2	Regional Fault
	Vouraikos Fault	Inferred Transfer Fault
	Kerinitis Fault	Inferred Transfer Fault
	Inlier Fault	Interpreted Intra Block Faults
	Roghi Fault south	
	Roghi Fault North	
	Roghi Fault West	
Kerpini Fault North		
Stratigraphy	Basement (Unit 1)	Regional Basement (Limestone)
	Massive Conglomerate (Unit 2)	Three main units for syn-fault deposits
	Early Sandstone-Conglomerate (Unit 3)	
	Late Sandstone-Conglomerate (Unit 4)	
Sedimentary Layers	Unit 2	Oriented towards N230 ⁰ E with an average dip angle of 20 ⁰ -25 ⁰
	Unit 3	Oriented towards N165 ⁰ E with an average dip angle of 20 ⁰
	Unit 4	They seem to be flat with an average dip angle of 3 ⁰ -15 ⁰ and dip direction to be south and north equally.

Table 4.2: New important findings in the field work compiled together with the initial knowledge.

Chapter 5 : MODEL CONSTRUCTION

The aim of geological models is to explain the things geological field observations, in particular, the lack of increasing of dip angle with age of the sediments of the Kerpini Fault Block. This chapter explains the geological models which have been generated to present the relationship between the evolving faults and sedimentation pattern in syn-fault deposits.

5.1 RMS 2013

RMS 2013 is an up to date geological modelling software program, developed by ROXAR. This software has been utilized for the modelling part of the thesis. There are a number of new modules, tools and methods that are provided in this new version. Moreover, the models were constructed using “Fault displacement estimation” tool which is part of the big fault uncertainty module. It accommodates several new options, for example, RMS 2013 provides an option to work with reverse drag. It is called correction range in horizon modelling tab where certain value should be specified as a maximum distance of zero displacement points to the fault in a perpendicular direction (Appendix-1).

The purpose of this modelling project is to build a forward model and observe the development of sedimentary layers in syn-fault deposits. However, the software officially fault uncertainty and fault displacement estimation are not designed to model a syn-rift novel approach; therefore, problems are to be expected. There are three different models and one final structural model of the Kerpini Fault Block in this chapter that explain the power of the method.

5.1.1 Fault Uncertainty

Geological interpretation and the model itself will always carry uncertainty. In terms of the fault or structural model, the uncertainties are related to its position and displacement. Fault uncertainty is one of the tools in RMS 2013 which has been designed to apply the uncertainty analysis into the structural model. In RMS 2013 the fault uncertainty tool has several options to improve the structural model. This tool allows the geo-modeller to manipulate the fault model by using position, dip, strike, and throw changes. The throw of the fault could be changed by input a value into the software and set the modification to be scale, add, or add by scaling based on the input value (Figure 5.1).

This tool is very useful for geological model assessment. It can take into account all the uncertainties that may be present in the geological model. For example, seismic processing, which affects the geological interpretation, and the seismic interpretation itself. Therefore, the Fault uncertainty tool helps to generate several possible geological scenarios for the geological model.

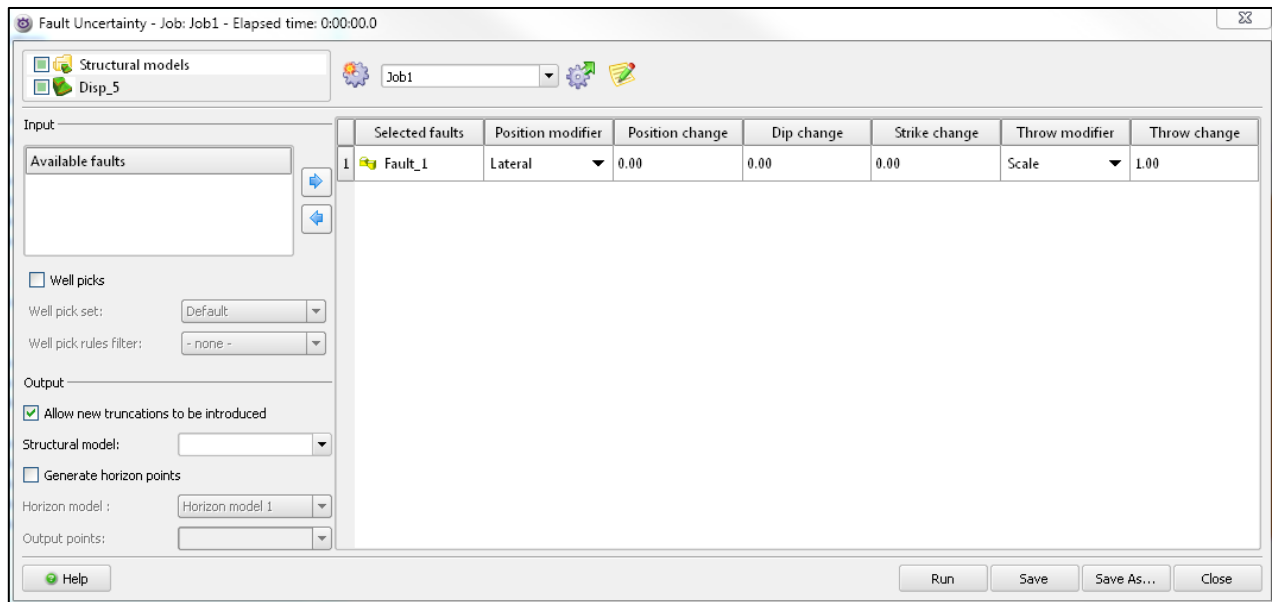


Figure 5.1: Fault uncertainty tab in RMS 2013. The figure shows the interface of fault uncertainty module in RMS 2013, in this window, geo-modellers could change the position, dip, strike, throw of the faults.

5.1.2 Fault Displacement Estimation

This method is a new method for structural modelling and is an extension of Havana (structural geology software) that was integrated in the new RMS version. Fault displacement estimation method has been designed to create a high quality structural model, especially regarding its displacement. The unique use of it is that the geo-modeller could have better controls on their structural model. The controls include their fault displacement distribution along the fault, specific displacement at some points and many more.

There are 3 way of using the fault displacement estimation and these are classified by the input source. First, horizon as an input source, here the geo-modeller can choose a reference horizon in the structural model and the fault displacement would be the same as the horizon's displacement.

Second, maximum throw as an input source, this option allows the geo modeller to put a specific value as a maximum throw of the fault and the displacement would be gradually decreased towards the fault tip. Third, attribute as an input source, this attribute allows the geo-modeller to build displacement points along the fault based on their interpretation. It can be done by creating a table containing X, Y, Z position and displacement values for each location along the fault (Appendix-1).

5.2 Preparation and Parameters

In order to generate the models, there are several assumptions that have been applied in data preparation and parameters. The assumptions included faults, horizons, reverse drag and displacement points sets (Figure 5.2).

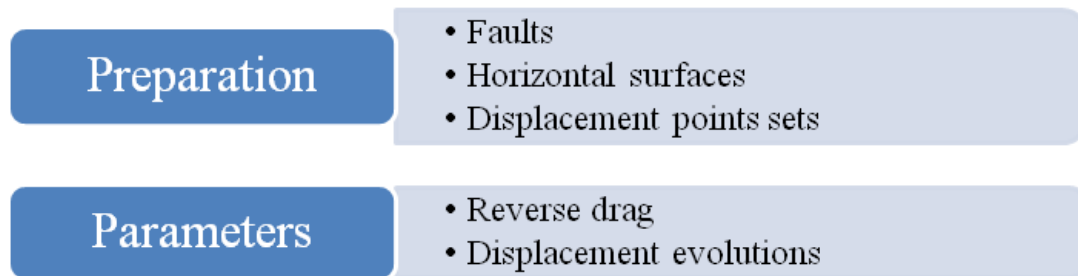


Figure 5.2: Schematic modelling preparation and parameters steps, figure shows the things that have done in preparation phase and all the parameters which used for the modeling.

Various scenario models were expected to improve the understanding of fault influence in sediment layers in three-dimensional point of view. The models have been constructed using modelling box (Table 5.1).

Modelling Box (in meters)			
X center	0	X length	15000
Y center	0	Y length	15000
Z center	0	Z length	7500

Table 5.1: Modelling box for models construction, Table shows the modeling box that which used for the models construction in this chapter.

5.2.1 Faults

Faults in models have been setup to simplify the real conditions. In this case, there are 2 kinds of faults which incorporated in this model. First, east-west normal fault, this fault has been setup striking N90°E with a dip of 45° to the north represents the Kerpini Fault. Second, the north-south boundary structure which is representing the Vouraikos Fault. It has been setup striking to the north with a vertical plane. All of the faults that used for this modelling are linear faults.

5.2.2 Horizons

Horizons in models have been simplified. Initially, the horizons are flat horizons with a 0m elevation. There are several flat horizons have been generated as the preparation of modelling.

5.2.3 Reverse Drag

Reverse drag is one of the parameters in the modelling process. In RMS 2013, reverse drag can be applied by using a number as an input for “Correction range” tab in the horizon modeling process. In general, there are three values that have been used; they are 2500m, 5000m, and 8000m normal to the faults.

5.2.4 Displacement Points Sets

The modelling process used “Fault displacement estimation” tool in RMS 2013. It controls the displacement for each horizon. The displacement point sets have been created as a table considering desired scenarios. In simply words, the displacement points are the amount of displacement in each position of the fault. The displacement number in this case refers to throw of the fault. In addition to that, the displacements have been setup to be equally distributed for the hanging-wall and foot-wall.

5.3 Workflow

The objective of generate this model is to look at how fault controlled sedimentation in a fault block. Therefore, forward modelling is needed. Here is the workflow (Figure 5.3):

- The models are started by displacing the initial flat horizon by the first displacement of the fault (creates a topography high in foot-wall, low in hanging-wall).
- A new sequence is added with 0m elevation representing the syn-rift – then on the second displacement, surface 1 and 2 are displaced.

- And those two main steps are repeated.

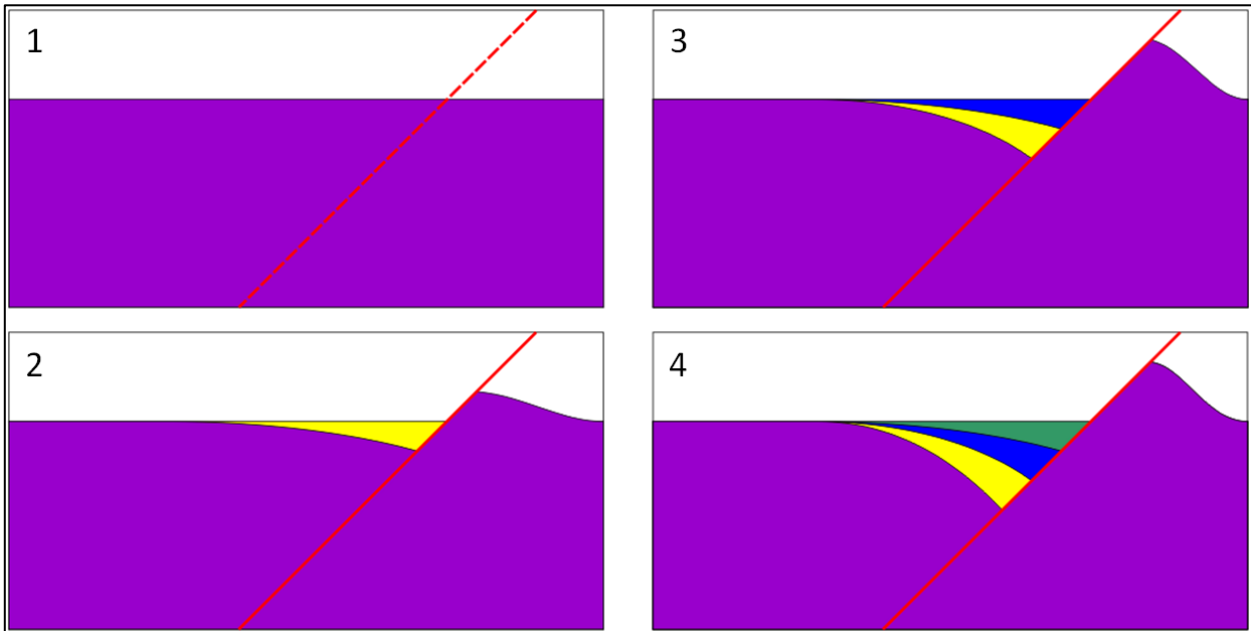


Figure 5.3: Modelling workflow illustration, this illustrations shows how the modeling was conducted, it starts with figure 1) initial geological condition with horizontal surface and no fault is involved, move to number 2) fault was stars to move and create a depocentre and filled by the sediments, next to number 3) second phase of fault movement and sediments infill the space, last is number 4) fault was keep move and the space was filled by the sediments.

5.3.1 Problem and Solution

As the RMS 2013 is not designed to model the syn-rift novel approach, the main problem of this modelling is the faulted horizons cannot be displaced by the same fault with different amount of displacement.

Instead, the solution for this kind problem has been discovered. In order to generate the desired forward modelling, every single horizon must be stored in the different structural models. They are displaced in different structural models using same faults but different displacement point sets. The displacement point sets have been setup for each horizon depending on the scenarios and it has been setup as the final condition of horizons after the fault evolutions. A minus point for this solution is that, the step by step pictures cannot be obtained since the models are jumping into the final result. The only one control for this solution is to setup reliable displacement point sets for each scenario.

5.4 Models

There are several scenarios models that have been generated in modelling process. In this case, the scenarios are differentiated by the distance of reverse drag and fault displacement evolution. Each case has its parameters which are unique compared to the others (Table 5.2). Apart from the differences between them, there is one common assumption for all of the models, sedimentation rate is assumed to be constant and always fill the gap in the hanging-wall.

It should be clarified at beginning that the RMS 2013 has different visualization configuration compared to the other geological modelling softwares. The positive values in the structural map show the deeper or lower part of the structure, and minus values mean higher positions.

There are three different setup models to explain the relationship between fault and sedimentary layers. Each model is using three segment 'class' where different reverse drag values are used (Table 5.2).

Model	Fault length (km)	Maximum displacement (m)	Fault tip evolution	Models classification	
				Class	Reverse drag distance (meters)
1	10	2000	Constant	Class 1	2500
2	8	2000	Propagate to both directions	Class 2	5000
3	8	2000	Propagate to one direction	Class 3	8000

Table 5.2: Classification of the models based on the fault evolution and reverse drag distance. *The table shows the classification of model according to their reverse drag distance.*

5.4.1 Constant Fault Tip (Model 1)

The First geological model, constant fault tip model, is the simplest geological model by using one fault. This model assumes that the fault has static fault tip position; therefore, displacement points have been setup to have the same position of fault tip as the fault develops.

Displacement point set has been plotted as length (in X-axis) versus displacement (Figure 5.4). The plot shows that the both fault tip are static in same positions. Horizon 1 (assumed as pre-faulting deposit) was displaced for 400m in each step until reach maximum displacement of 2000m. The following horizons are the syn-fault deposits which fill the accommodation space

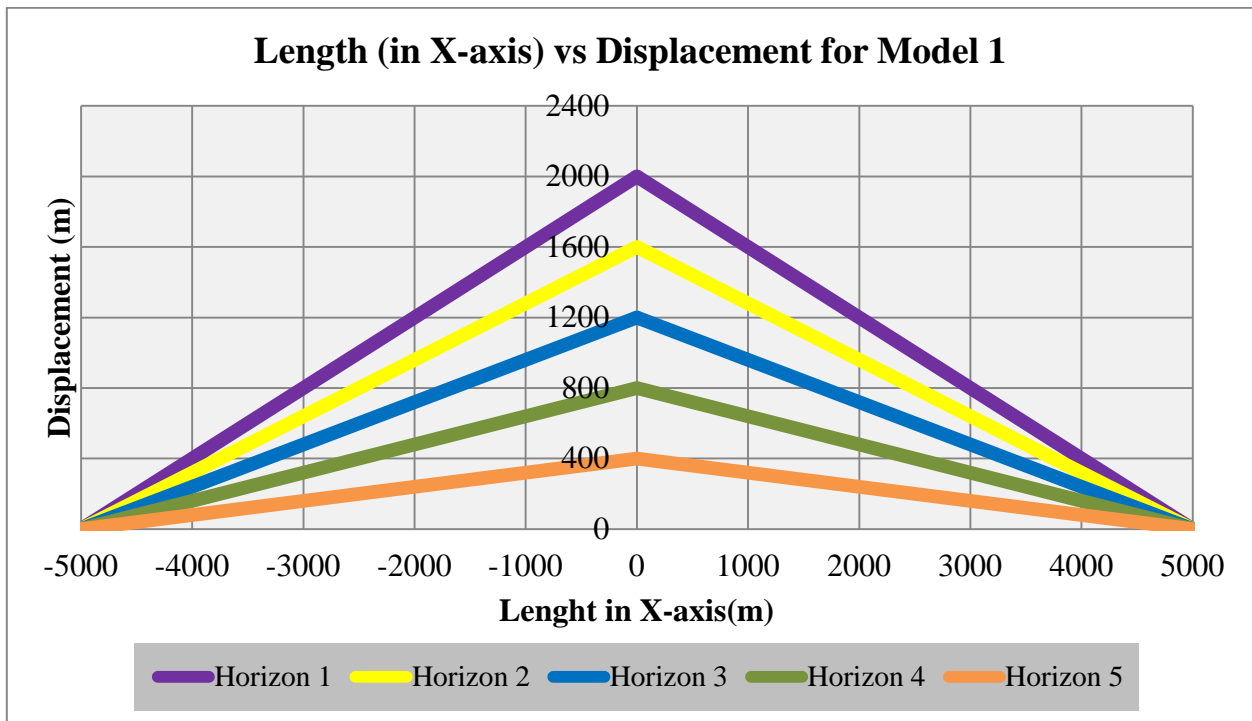


Figure 5.4: Length Vs displacement plot of model 1. The plot shows relationship between length and displacement for each horizon in model 1, it shows that the fault tip is constant.

Class 1, structural map of horizon 1 shows the fault is 10000m in length (Figure 5.5). The fault has maximum throw in the centre of the fault and gradually decreases towards the fault tip. Based on the displacement points set which has been applied, maximum elevation in the foot-wall shows -1000m and minimum elevation in the hanging-wall is 1000m, it happens as the respect of the hanging-wall and foot-wall displacement fraction set which has been applied to be equally distributed (0.5). As this class used 2500m away from the fault as the reverse drag parameter, there is a narrow depocentre in hanging-wall and uplifted foot-wall which created by the fault movement (Figure 5.5).

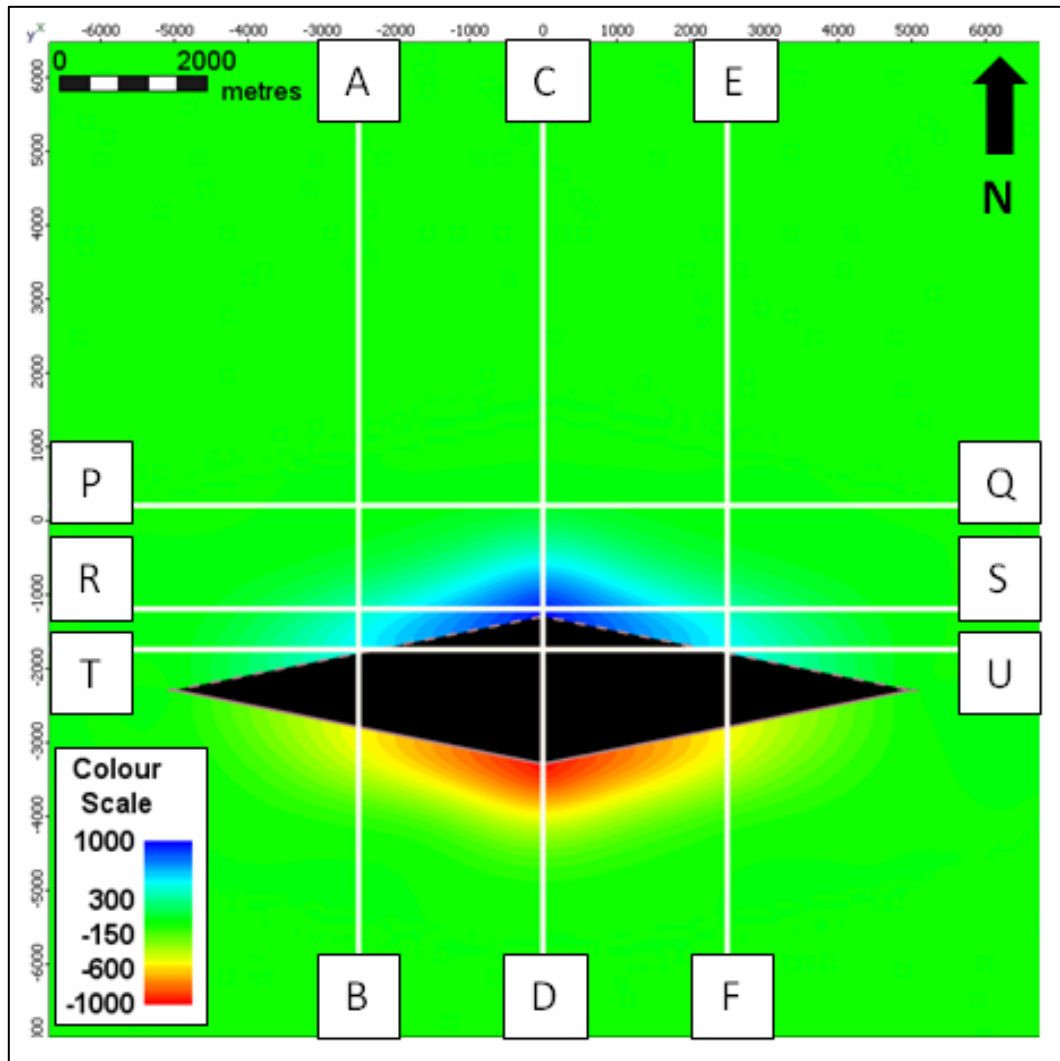


Figure 5.5: Structural map of horizon 1 (model 1 - class 1). *The structural map shows the structural configuration in the final evolution of model, the fault has 10000m in length with maximum throw (2000m) at the centre of the fault and gradually decreases towards the fault tip.*

Group of cross-sections shows the variation of structural configuration in different areas within the fault block (Figure 5.6). Cross-section C-D has shown steeper dips of sedimentary layers which is located in the center of the fault, while the cross-section A-B and E-F show the same thing as they have same distance from the center (gentler dip angle). Strike-sections also provide an idea about the accommodation space which controlled by the reverse drag, move further away to the north, smaller accommodation space is discovered which affect the thickness of sediments (cross-section P-Q). In the strike-sections also it can be seen that the syn-fault sediment packages are pinching out towards the fault tip represent a boundary for sediments to be deposited (Figure 5.6).

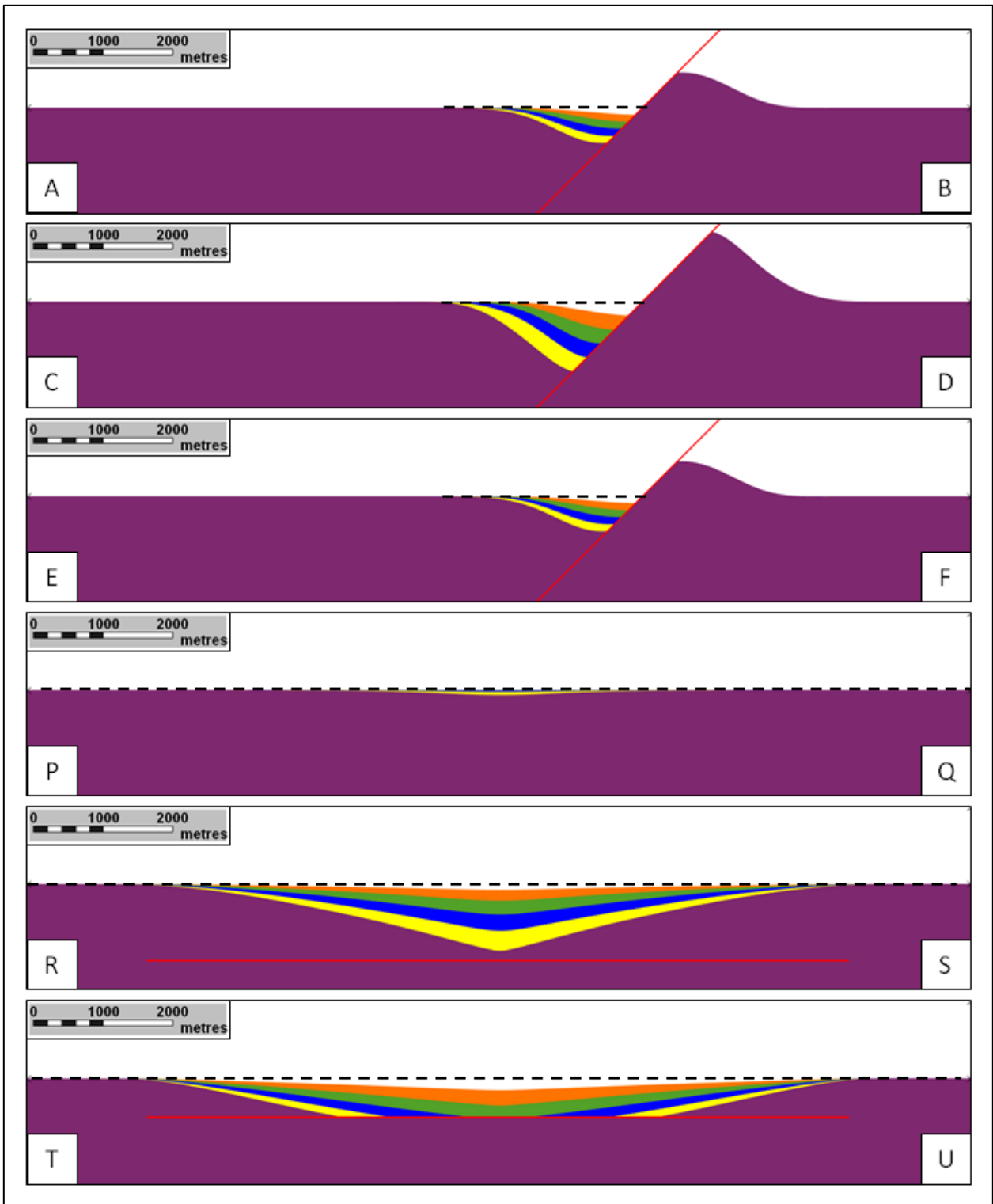


Figure 5.6: Group of cross-sections of model 1 - class 1. This group of cross-sections shows variation in structural of sedimentary layers across the fault block. Cross-sections (perpendicular to the fault) bring an idea about the dip of sediment while the strike-sections show the sediments distribution. (VE= 1:1)

Class 2, structural map of horizon 1 shows the fault has 10000m in length (Figure 5.7). The fault has maximum throw in the centre of the fault and gradually decreased towards the fault tip. Based on the displacement points set which has been applied, maximum elevation in the foot-wall shows -1000m and minimum elevation in the hanging-wall is 1000m. As this class used 5000m away from the fault as the distance of reverse drag, there is a bigger depocentre in hanging-wall and uplifted foot-wall than the depocentre in class 1, which created by the fault movement (Figure 5.7). The different between classes can be observed by looking at the cross-sections.

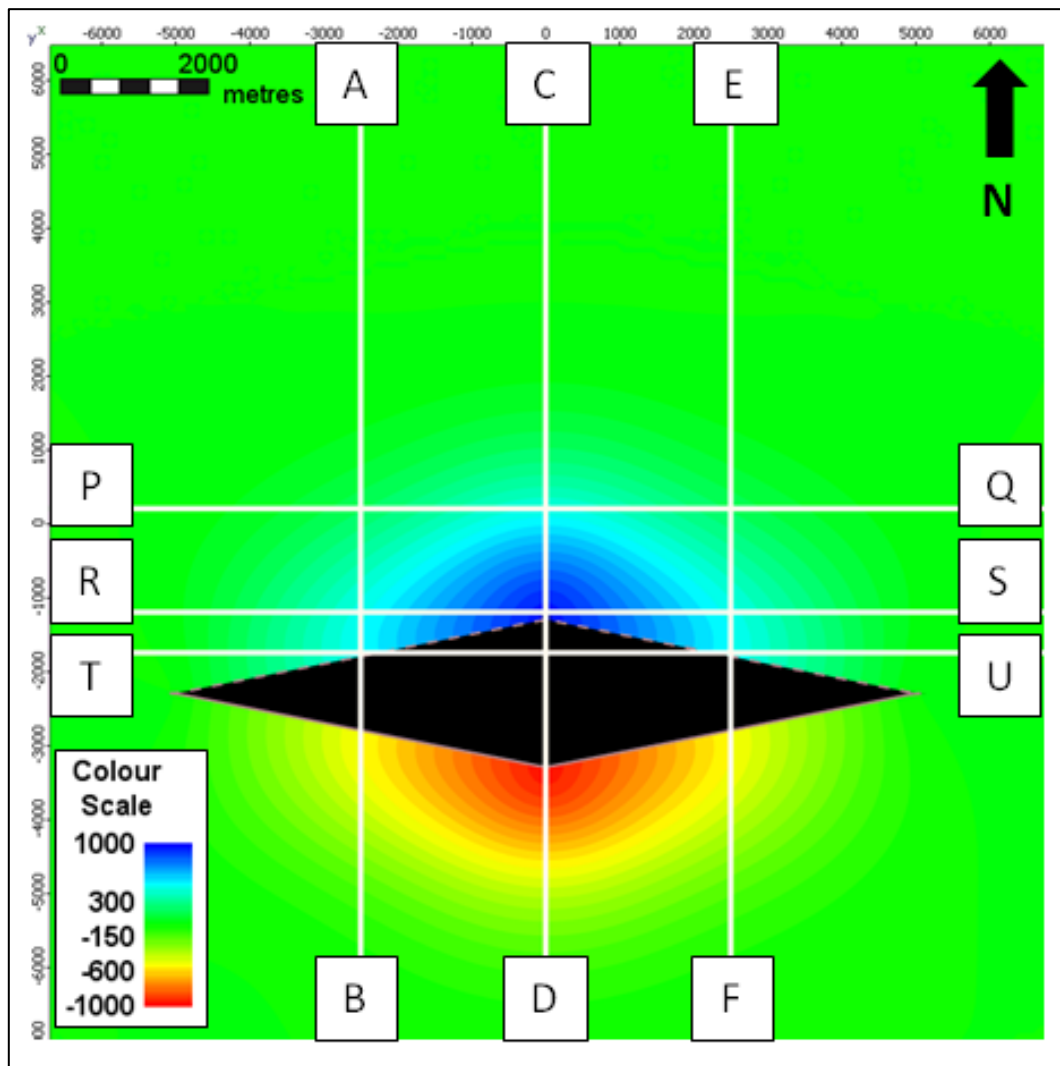


Figure 5.7: Structural map of horizon 1 (model 1 - class 2). *The structural map of horizon 1 shows the structural configuration of class 2, where the reverse drag distance was setup for 5000m, the fundamental difference compared to the class 1 is just the dimension of accommodation space and foot-wall uplift.*

Group of cross-sections shows the variation of structural configuration in different areas within the fault block. Cross-sections (perpendicular to the faults) show the dips angles of sediments are different compared to the class 1 (Figure 5.8). It shows that the dip angle of oldest sediment is gentler as compared to the class 1. It also shows that the difference of dip angles between the oldest and youngest sediments are less than the difference of dip angles in class 1.

Strike-sections show the influence of reverse drag distance. It is clearly showed in cross-section P-Q, there is a clear difference that the amount of sediments in this class are more than the amount of sediments in class 1 (Figure 5.8). It can be proved by such cross-sections at the same location produce different features. Similar to the class 1, as the model is using the assumption that both fault tips are constant or stay at the same position through the time, all the syn-fault sediment packages are pinching out towards the fault tip where there is no displacement of the fault.

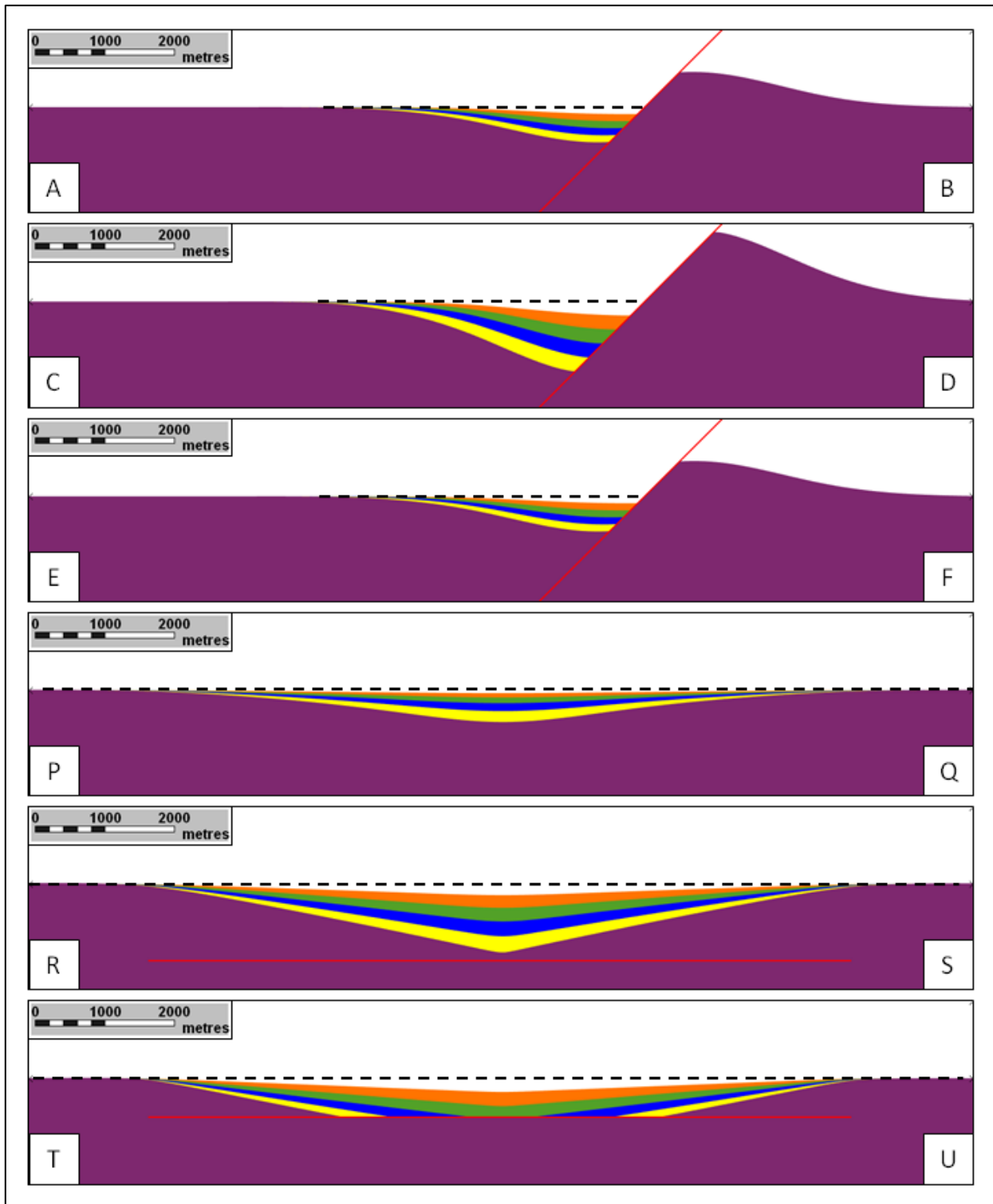


Figure 5.8: Group of cross-sections of model 1 - class 2. This group of cross-sections shows variation in structural of sedimentary layers across the fault block. Cross-sections (perpendicular to the fault) bring an idea about the dip of sediment while the strike-sections show the sediments distribution. It shows the longer reverse drag distance will produce a bigger space for sediments and less decreasing dip angle towards the younger sediments. (VE= 1:1)

Class 3, this class was generated using the displacement point set for model 1 but reverse drag distance of 8000m in the fault which has 10000m in length. Horizon 1 structural map shows almost similar result compared to the class 1 and class 2 – only the distance of reverse drag is different. As this class using the longer distance for reverse drag, the only difference between them is about the accommodation space that shows a bigger depression which may be filled by the sediments (Figure 5.9). The difference between them can be observed by looking at cross-sections as it is difficult to see the difference in this structural map.

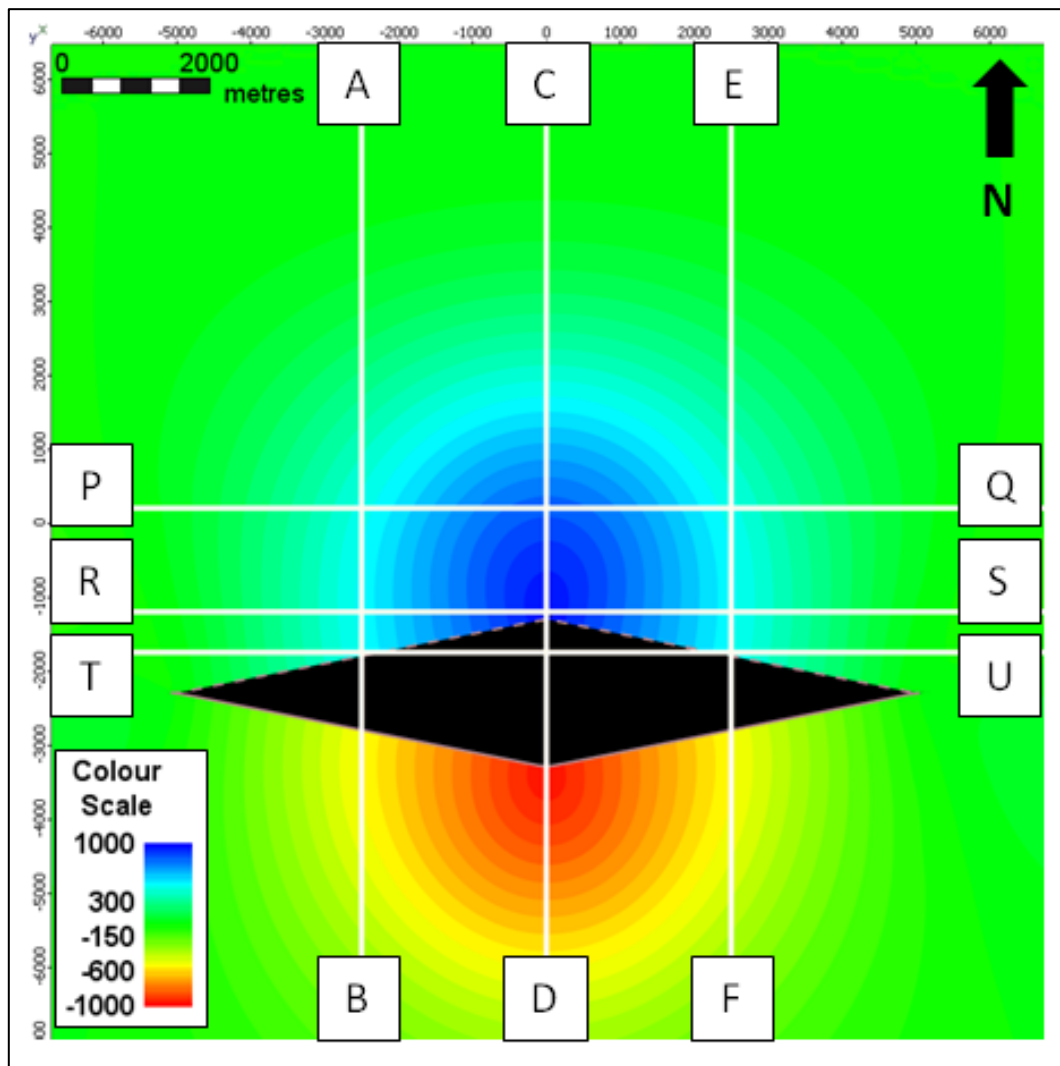


Figure 5.9: Structural map of horizon 1 (model 1 - class 3). The structural map of horizon 1 shows the structural configuration of class 3, where the reverse drag distance was setup for 8000m, the fundamental difference compared to the class 1 and 2 is just the dimension of accommodation space and foot-wall uplift which can be observed from the structure maps.

Group of cross-sections shows the variation of structural configuration in different areas within the fault block. Cross-sections (perpendicular to the faults) shows the dips angle of sediments are different compared to the class 1 and 2 (Figure 5.10). It shows that the dip angle of oldest sediment is gentler as compared to the class 1 and 2. It also shows that the difference of dip angle between the oldest and youngest sediments are less than the difference of dip angle in class 1 and 2.

Strike-sections show the influence of reverse drag distance. It is clearly showed in cross-section P-Q, there are very clear difference that the amounts of sediments in this class are more than the amount of sediments in class 1 and 2 (Figure 5.10). It can be proved by such cross-sections at the same location produce different features; the sediments volume in class 3 is more than the sediments volume in class 1 and class 2. It is caused by the distance of reverse drag is longer than the other classes which created bigger accommodation space for sediments. It is also showed that the sediments are pinching out towards the fault tip as well as shown in class 1 and 2. This configuration can be concluded as the result of static fault tip.

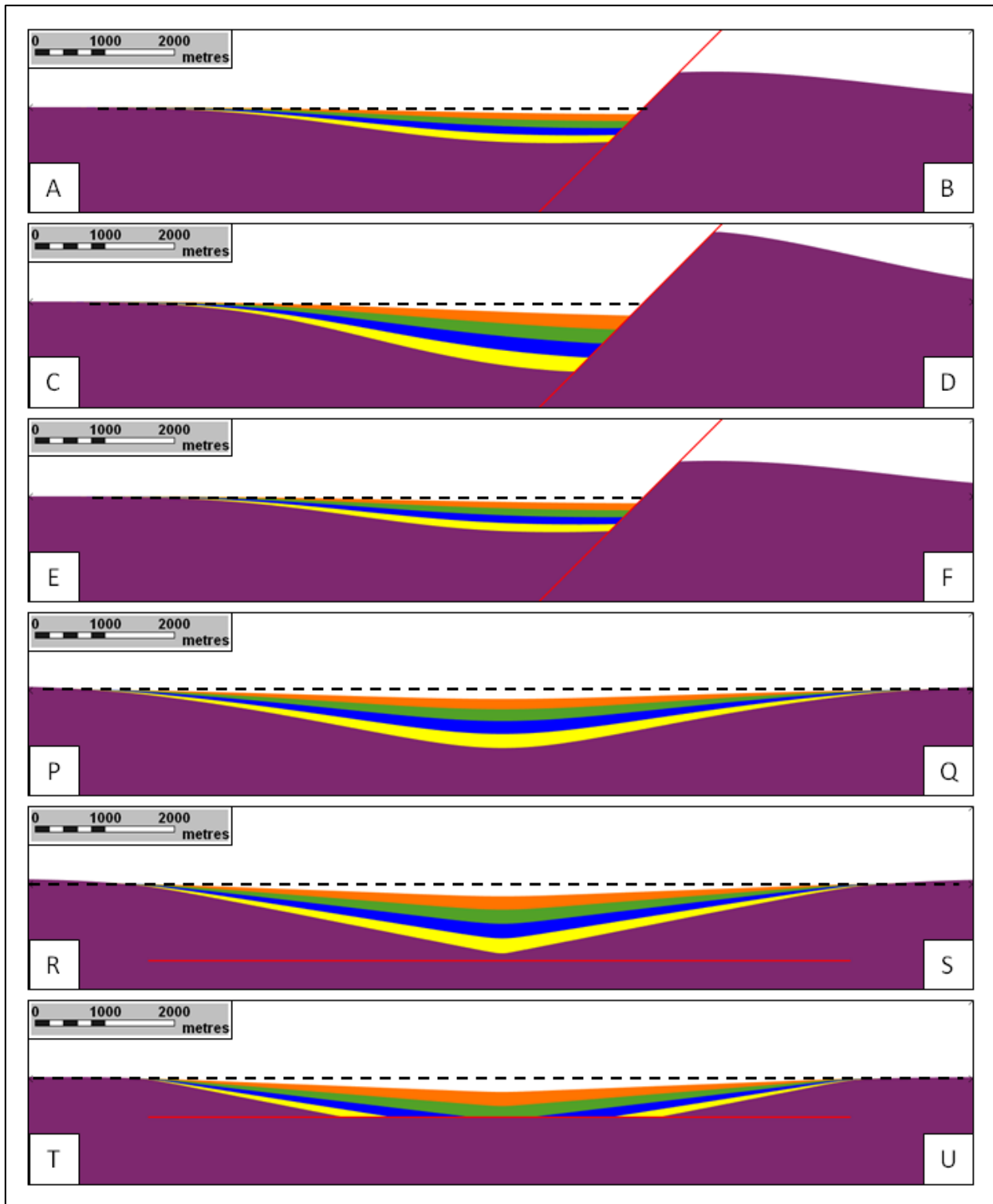


Figure 5.10: Group of cross-sections of model 1 - class 3. This group of cross-sections shows variation in structural of sedimentary layers across the fault block. Cross-sections (perpendicular to the fault) bring an idea about the dip of sediment while the strike-sections show the sediments distribution. Comparing class 1, 2, and 3, it seems that the longer reverse drag distance will produce a bigger space for sediments and less decreasing dip angle towards the younger sediments. (VE= 1:1)

5.4.2 Propagate Fault Tip (Model 2)

Second geological model, propagate fault tip model, is using an assumption that the both fault tip propagate in the same propagation rate. In early stage, the fault was 2000m in length. It was gradually propagating until the fault reach 8000m in length at final stage. Total amount of propagation for each step is 2000m which equally distribute to the east and west.

Displacement point set has been plotted as length (in X-axis) versus displacement. The plot shows that the both fault tip are propagating in both directions with the same propagation rate (Figure 5.11). Horizon 1 (assumed as pre-faulting deposit) was displaced for 400m in each step until reach maximum displacement of 2000m. It shows that from the pre-faulting period until the fault was stop (horizon 5 deposited) the propagation rate is constant.

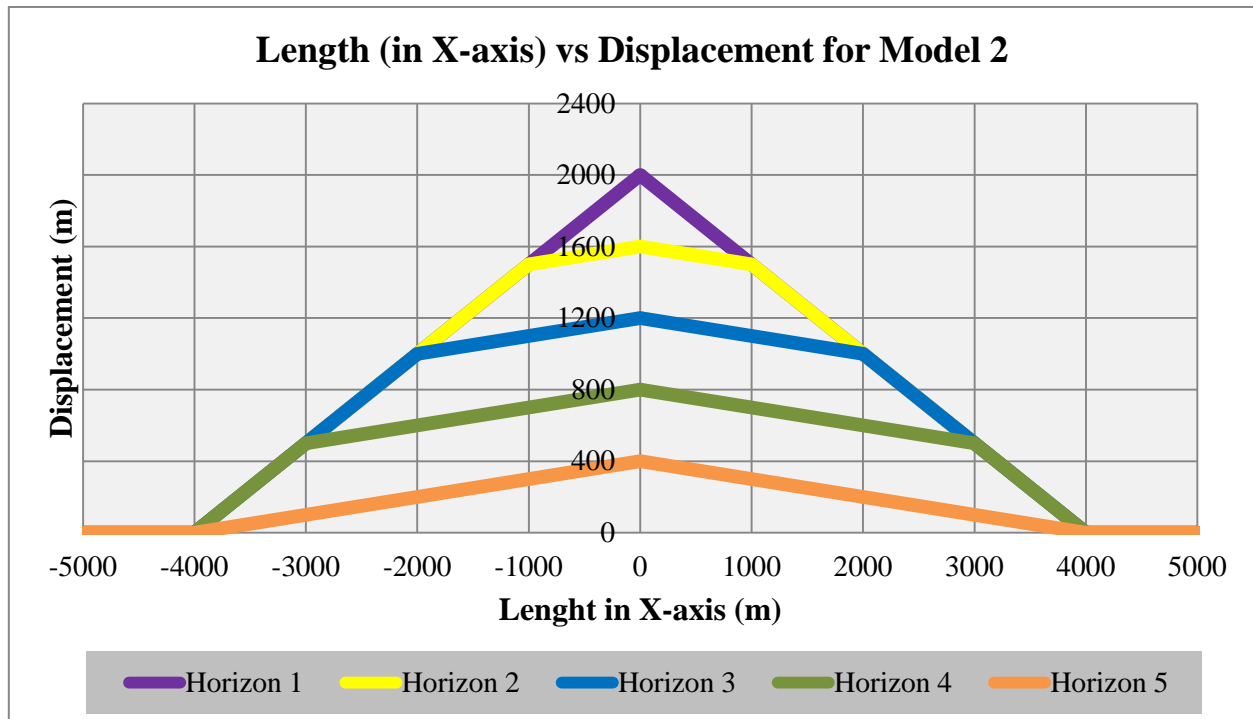


Figure 5.11: Length (in X-axis) Vs displacement plot of model 2. The plot shows relationship between length and displacement for each horizon in model 2, it shows that the fault tip are propagate to the west and east at the same propagation rate, and it is also constant in term of the fault development, there is no acceleration or slowness for the propagation rate when the fault starts to move and stops.

Class 1, structural map of horizon 1 shows the fault has 8000m in length (Figure 5.12). The fault has maximum throw in the centre of the fault and gradually decreased towards the fault tip. Based on the displacement points set which has been applied, maximum elevation in the foot-wall

shows -1000m and minimum elevation in the hanging-wall is 1000m, it happens as the respect of the hanging-wall and foot-wall displacement fraction set which has been applied to be equally distribute (0.5). As this class used 2500m away from the fault as the reverse drag parameter, there is a narrow depocentre in hanging-wall and uplifted foot-wall which created by the fault movement (Figure 5.12). It is difficult to see the difference between model 1 and model 2 by looking at the structural maps. The difference between them can be observed by looking at the cross-sections and the other classes in model 2 in this Chapter.

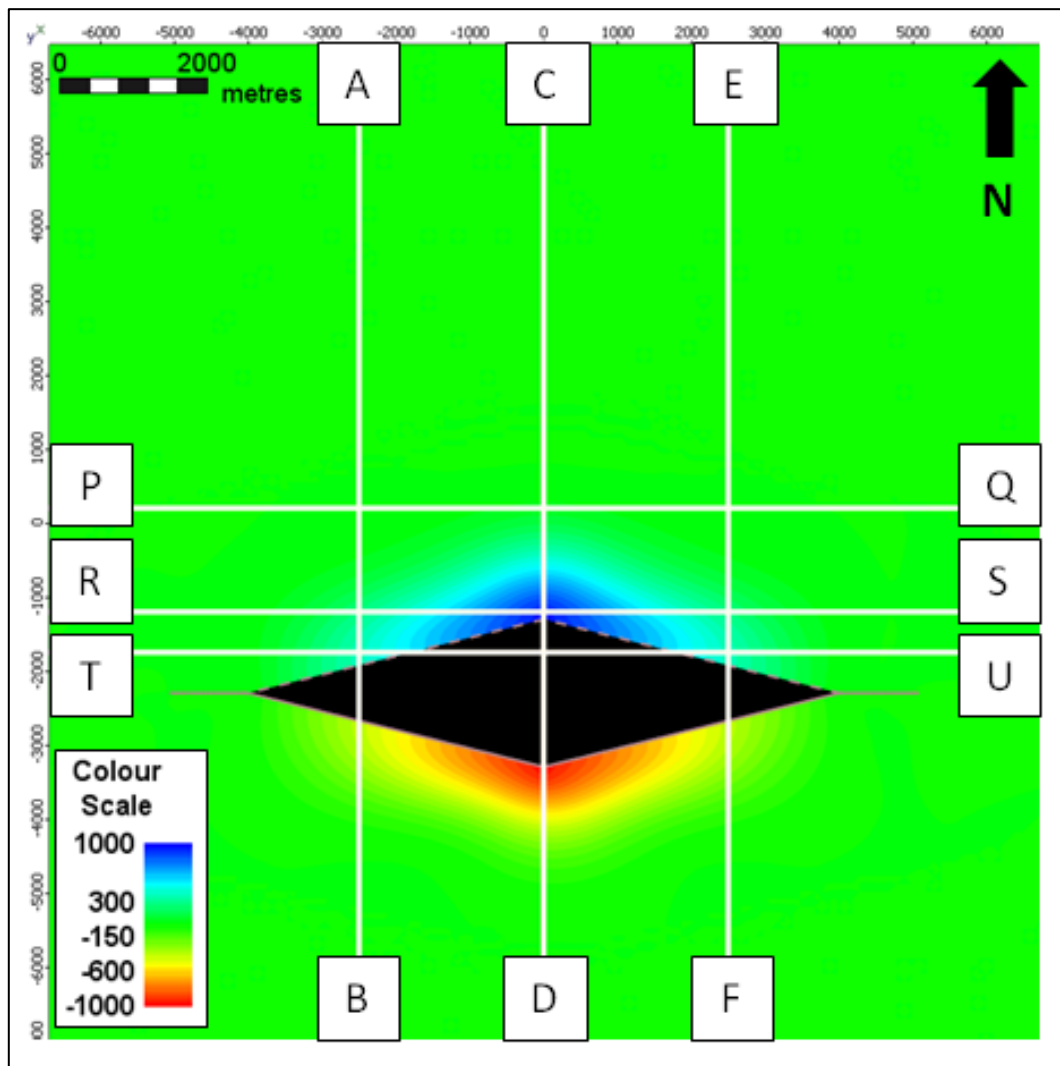


Figure 5.12: Structural map of horizon 1 (model 2 - class 1). *The structural map shows the structural configuration in the final evolution of class 1, the fault has 8000m in length with maximum throw (2000m) at the centre of the fault and gradually decreases towards the fault tip.*

Group of cross-sections shows the variation of structural configuration in different areas within the fault block (Figure 5.13). This model shows unique results as the fault were propagating. The

evolution of the fault which propagated to the east and west are resulting the different sedimentation dispersal and distribution of model 1 and model 2. Cross-section C-D shows the same thing as the model 1, the difference between them can be seen in cross-section A-B and E-F (Figure 5.13), model 2 only shows horizon 4 and 5 as the model 1 shows all the horizons in these lines. It happened because the accommodation spaces at those locations were not created yet when the horizon 2 and 3 were deposited. Therefore, there are no sediment packages 2 and 3 at such locations.

Strike-sections also show unique results. In model 2, the sediments are not pinching out towards the fault tip as can be seen in model 1 (Figure 5.13). Not only show the effect of reverse drag which has been observed in model 1, but also shows the effect of fault evolution. As the fault propagates, the depocenter or accommodation space is also evolved. It can be seen that fault was started by the short length fault (approximately 2000m) and grew. Shorter fault length will produce smaller accommodation space, in cross-section R-S, the oldest sediments (package 2 which is represented by yellow color) is pinching out towards the basement. The Distance of the pinch out at the west and east area of package 2 is approximately 2000m which represents the fault length at the time package 2 was deposited. It is also applied for the younger sediments.

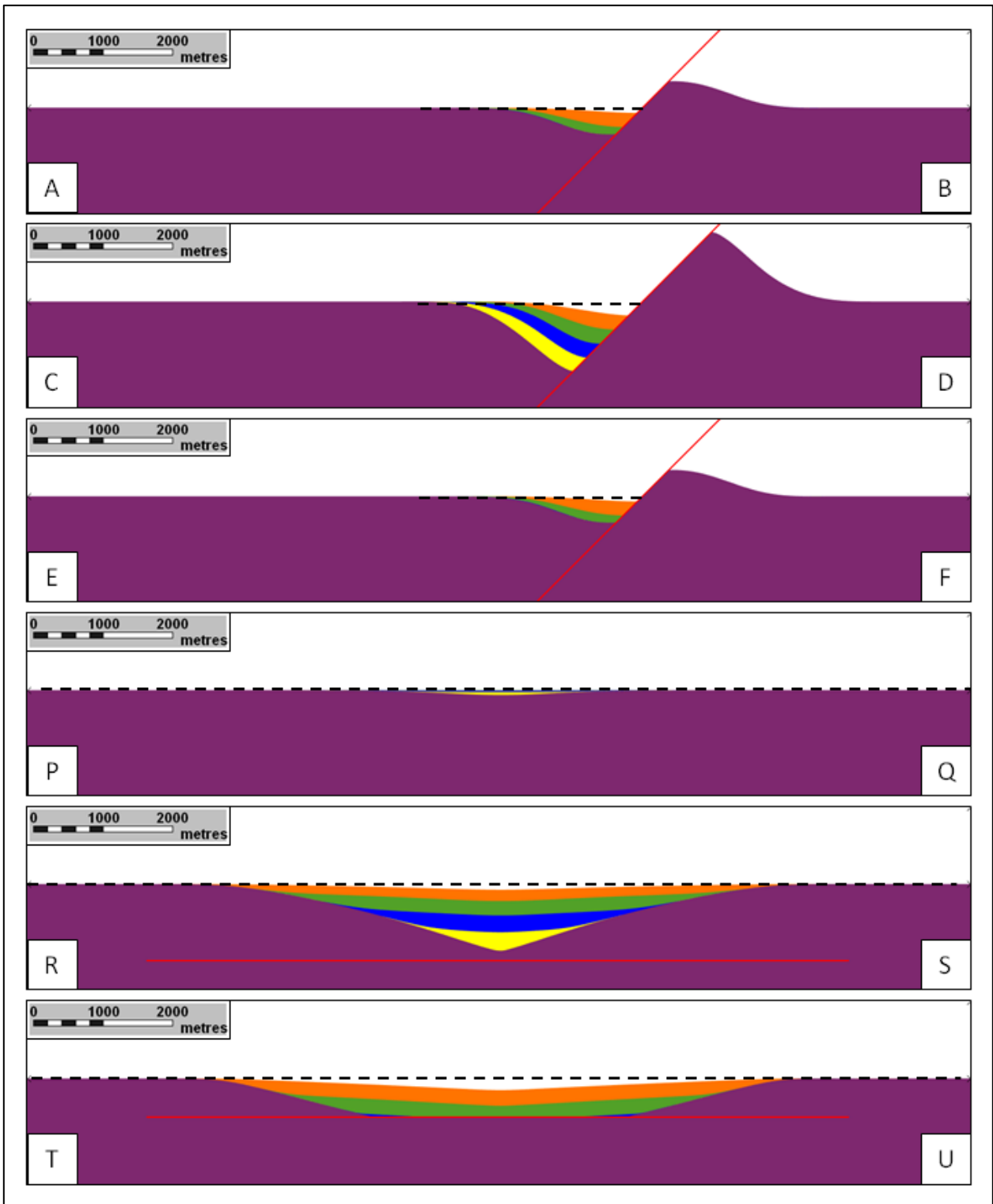


Figure 5.13: Group of cross-sections of model 2 - class 1. This group of cross-sections shows variation in structural of sedimentary layers across the fault block. Cross-sections (perpendicular to the fault) bring an idea about the dips of sediments while the strike-sections show the sediments distribution. It shows unique results that not all the sediment packages can be found all over the area as the fault were propagating. (VE= 1:1)

Class 2, as stated before, this class was generated using the displacement point set for model 2 but using 5000m as the distance for reverse drag in the 8000m length of fault. The structural map of Horizon 1 shows almost similar result compared to the class 1, but as this class using the longer distance for reverse drag, the accommodation space shows a bigger depression which may be filled by the sediments (Figure 5.14). The maximum and minimum elevation which are represented by foot-wall and hanging-wall elevation are -1000m and 1000m respectively.

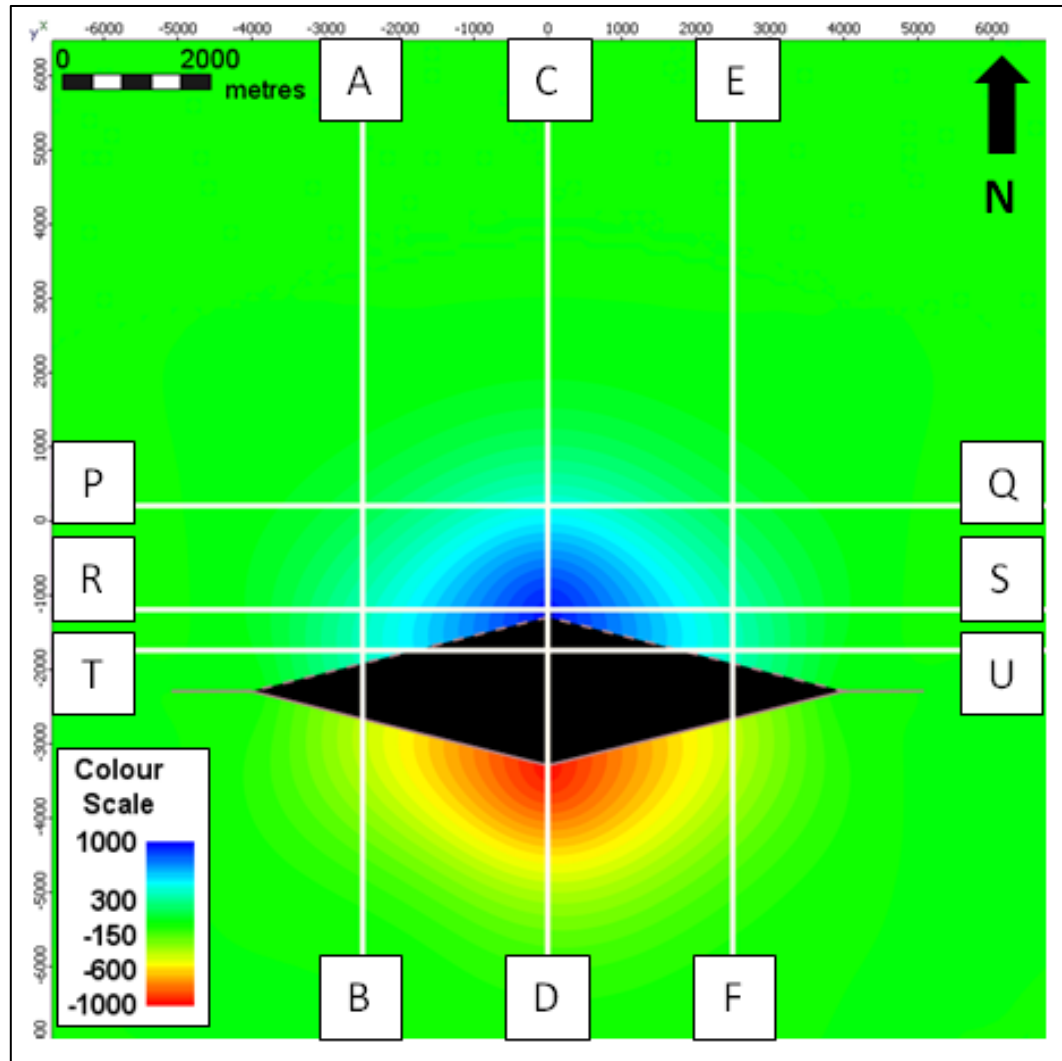


Figure 5.14: Structural map of horizon 1 (model 2 - class 2). The structural map shows the structural configuration in the final evolution of class 2, the fault has 8000m in length with maximum throw (2000m) at the center of the fault and gradually decreases towards the fault tip. It seems similar with class 1.

Group of cross-sections shows the variation of structural configuration of the whole modelled area (Figure 5.15). Similar to the results of class 1, the unique configuration also appears in this class. Propagation fault tip have an influence for the sedimentation dispersal. As shown in the

figure, cross-section A-B and E-F shows only at least two horizons. It is because of the development of the fault where the fault was not that extensive to create an accommodation space at the areas which those cross-sections are located when the horizon 2 and 3 were deposited. Cross-section C-D also brings an idea about the effect of reverse drag distance; it seems that dips of sediments are gentler than the dip of sediments in class 1.

Strike-sections for this model are showing the similar result with class 1 (Figure 5.15). There is no big different between them except the extensive sedimentation dispersal as can be proved by looking at cross-section P-Q and compare it with the same cross-sections in class 1. The difference between them is about the amount of sediments that have been deposited, the longer distance of reverse drag the bigger amount of sediment which may fill the depocentre.

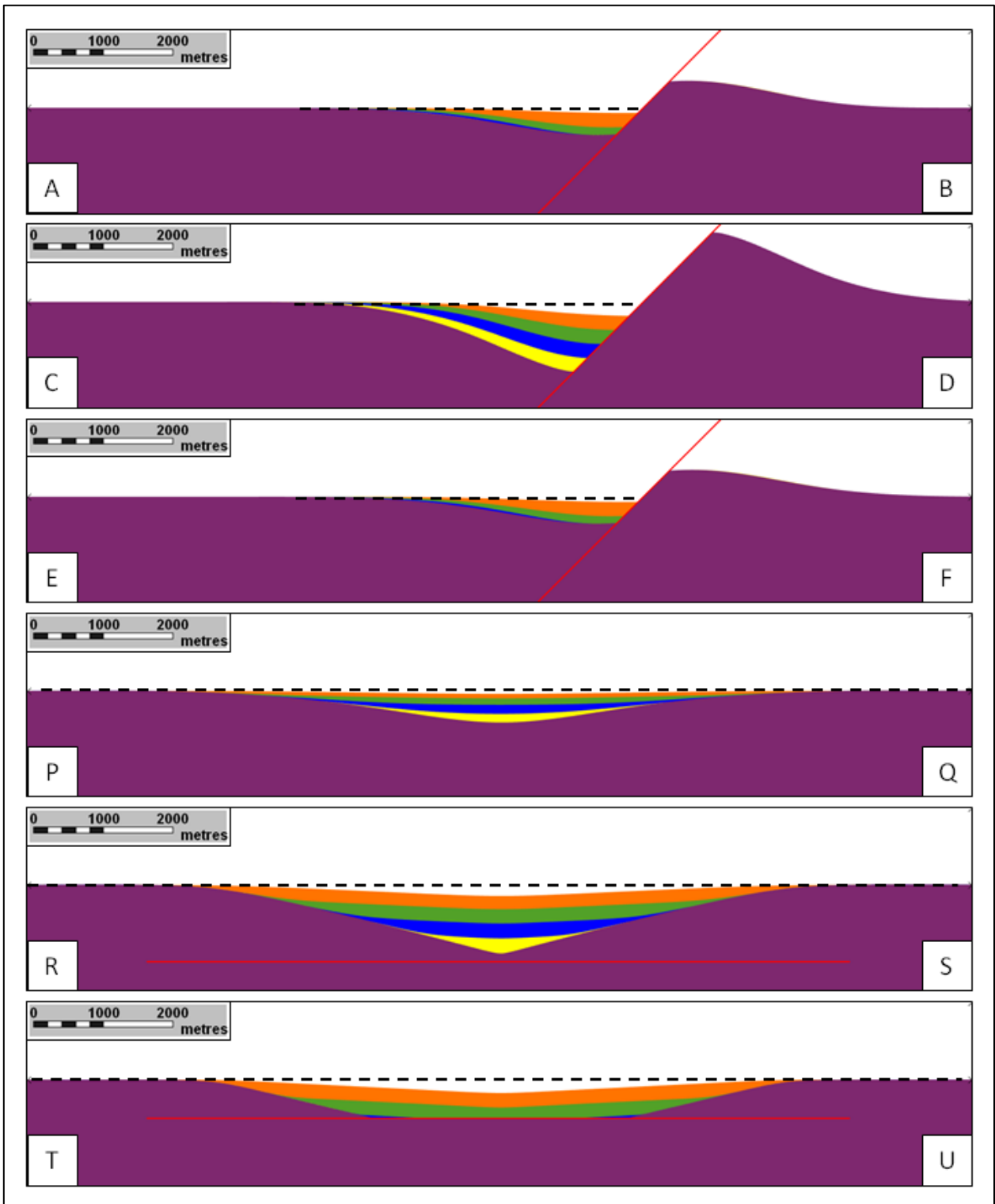


Figure 5.15: Group of cross-sections of model 2 - class 2. This group of cross-sections shows variation in structural of sedimentary layers across the fault block. Cross-sections (perpendicular to the fault) bring an idea about the dip of sediment while the strike-sections show the sediments distribution. It shows unique results were not all the sediment packages can be found all over the area as the fault were propagating. It also showing bigger accommodation space compared to class 1. (VE= 1:1)

Class 3, this class was generated using the displacement point set for model 2 but set the distance of reverse drag for 8000m. Horizon 1 structural map shows almost similar result compared to the class 1 and class 2 – only the distance of reverse drag is different (Figure 5.16). As this class using the longer distance for reverse drag, the accommodation space shows a bigger depression which may be filled by the sediments. Honoring the displacement points set data, the maximum foot-wall and hanging-wall elevations are -1000m and 1000m respectively.

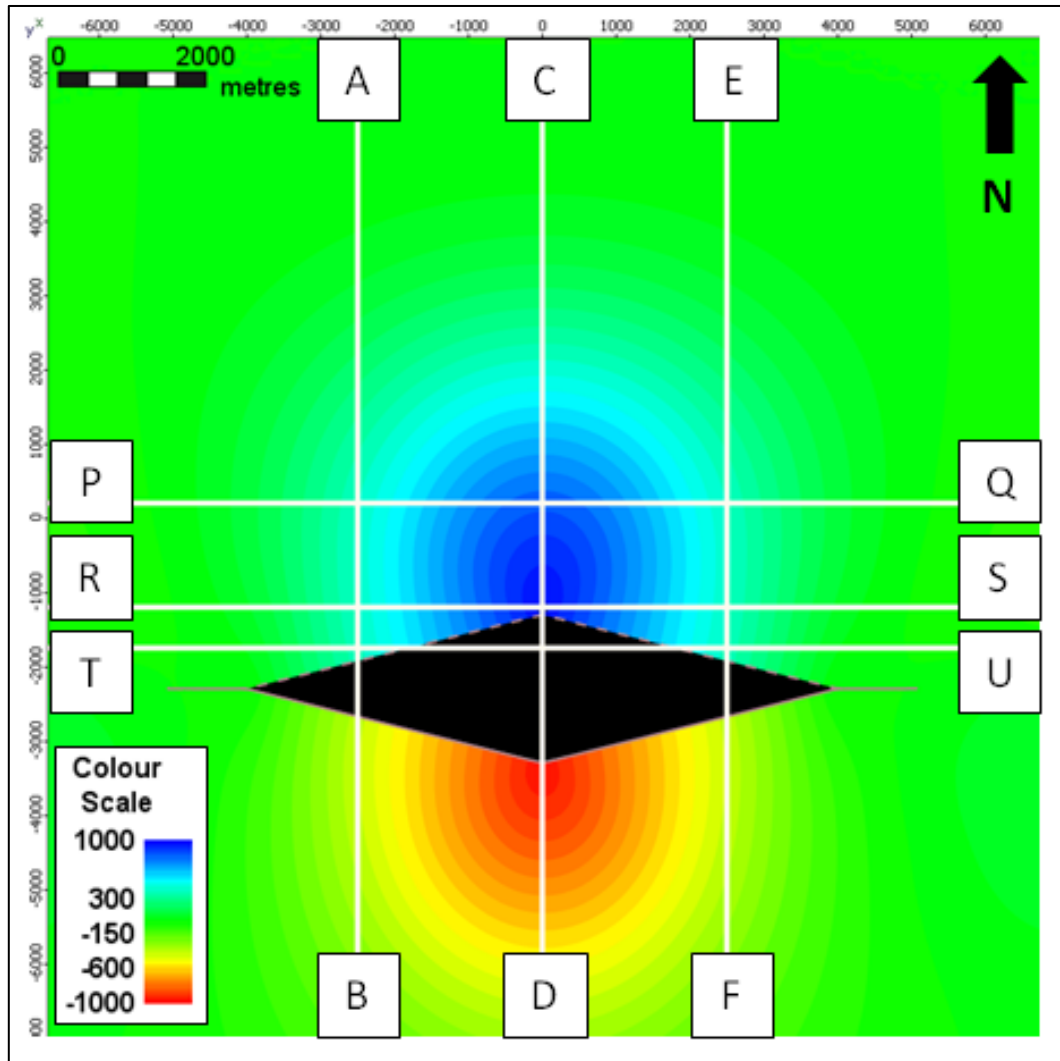


Figure 5.16: Structural map of horizon 1 (model 2 - class 3). *The structural map shows the structural configuration in the final evolution of class 3, the fault has 8000m in length with maximum throw (2000m) at the centre of the fault and gradually decreases towards the fault tip. It seems similar with class 1 and 2 except the size of accommodation space and foot-wall uplift.*

Group of cross-sections shows the variation of structural configuration of the whole modelled area (Figure 5.17). Similar to the results of class 1 and 2, the unique configuration also appears in this class. Propagation fault tip have an influence for the sedimentation dispersal. As shown in the figure, cross-section A-B and E-F shows only at least two clear horizons (4 and 5) and just small part of horizon 2 and 3. It is because of the development of the fault where the fault was not that extensive to create an accommodation space at those areas which those cross-sections are located when the horizon 2 and 3 were deposited. Cross-section C-D brings an idea about the effect of reverse drag distance; it seems that dips of sediments are gentler than the dip of sediments in class 1 and 2; this class is showing the shallowest sedimentary layers dip angles configuration for this model 2.

Strike-sections for this model are showing the similar result with class 1 and 2 (Figure 5.17). There is no big different between them except the extensive sedimentation dispersal as can be proved by looking at strike-sections P-Q and compare it with the same cross-sections in class 1 and 2. The difference between them is about the amount of sediments that have been deposited, the longer distance of reverse drag the bigger amount of sediment which may fill the depocentre.

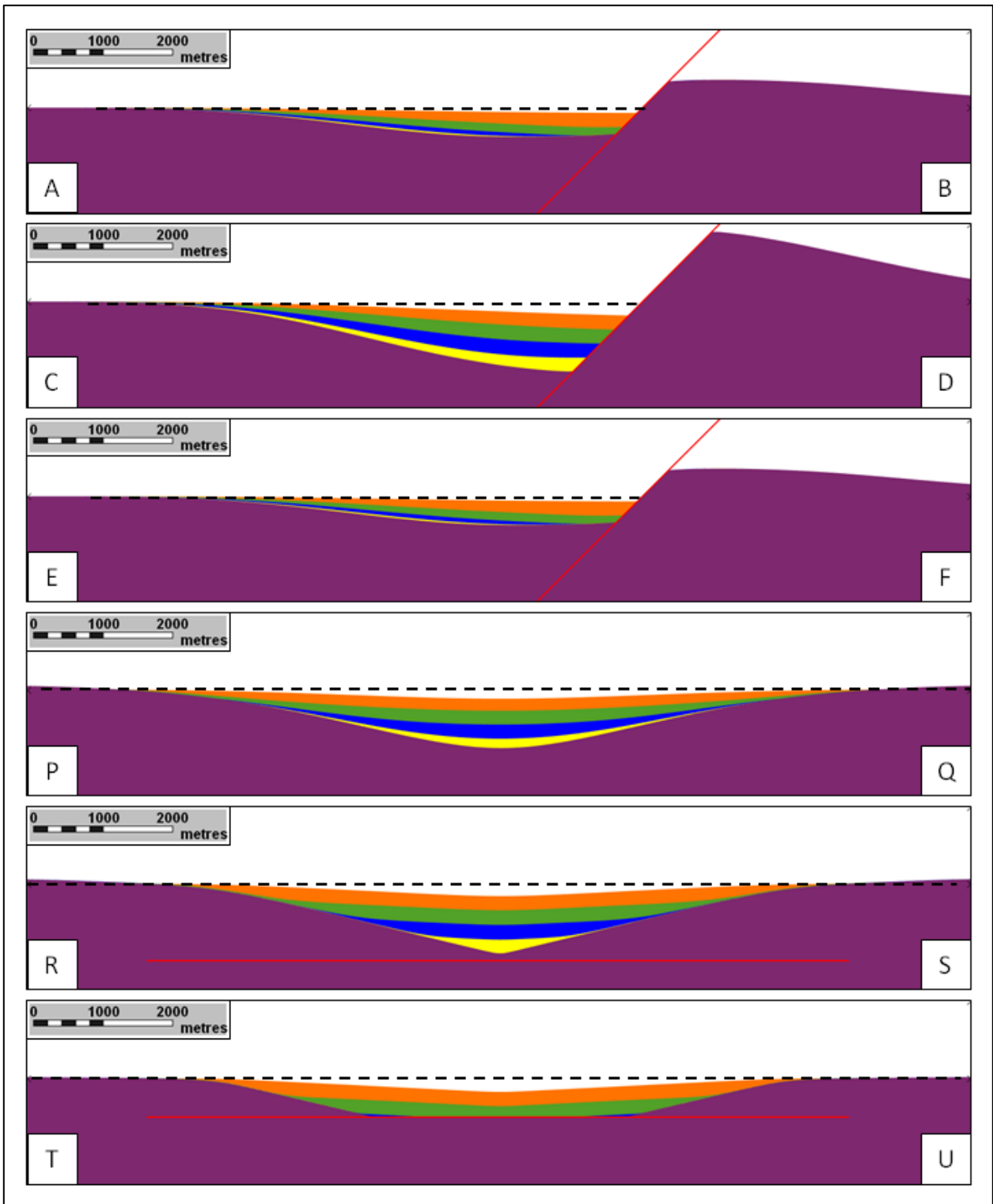


Figure 5.17: Group of cross-sections of model 2 - class 3. This group of cross-sections shows variation in structural of sedimentary layers across the fault block. Cross-sections (perpendicular to the fault) bring an idea about the dip of sediment while the strike sections show the sediments distribution. It shows unique results that not all the sediment packages can be found all over the area as the fault were propagating (growth). It shows that this class has shallowest dip angles in model 2. (VE= 1:1)

5.4.3 Propagate Fault Tip in One Direction (Model 3)

Third geological model, propagate fault tip in one direction model, is the model that using an assumption that only one of the fault tip is propagating to the east. In early stage, the fault was 2000m in length. It was propagating gradually 2000m per movement to the east until the fault reach 8000m in length in final stage (Figure 5.18). The total amount of propagation is the same as model 2, but in this model all the propagation rate was moving one fault tip to the east whilst in model 1 and 2, fault stays at the initial condition or propagates to both tip directions. There is no bounding structure for this model, therefore, it seems that both tips are propagating but actually location western tip is not moving.

Displacement point set has been plotted as length (in X-axis) versus displacement (Figure 5.18). The plot shows that the both fault tip are propagating to the east direction. Horizon 1 (assumed as pre-faulting deposit) was displaced for 400m in each step until reach maximum displacement of 2000m.

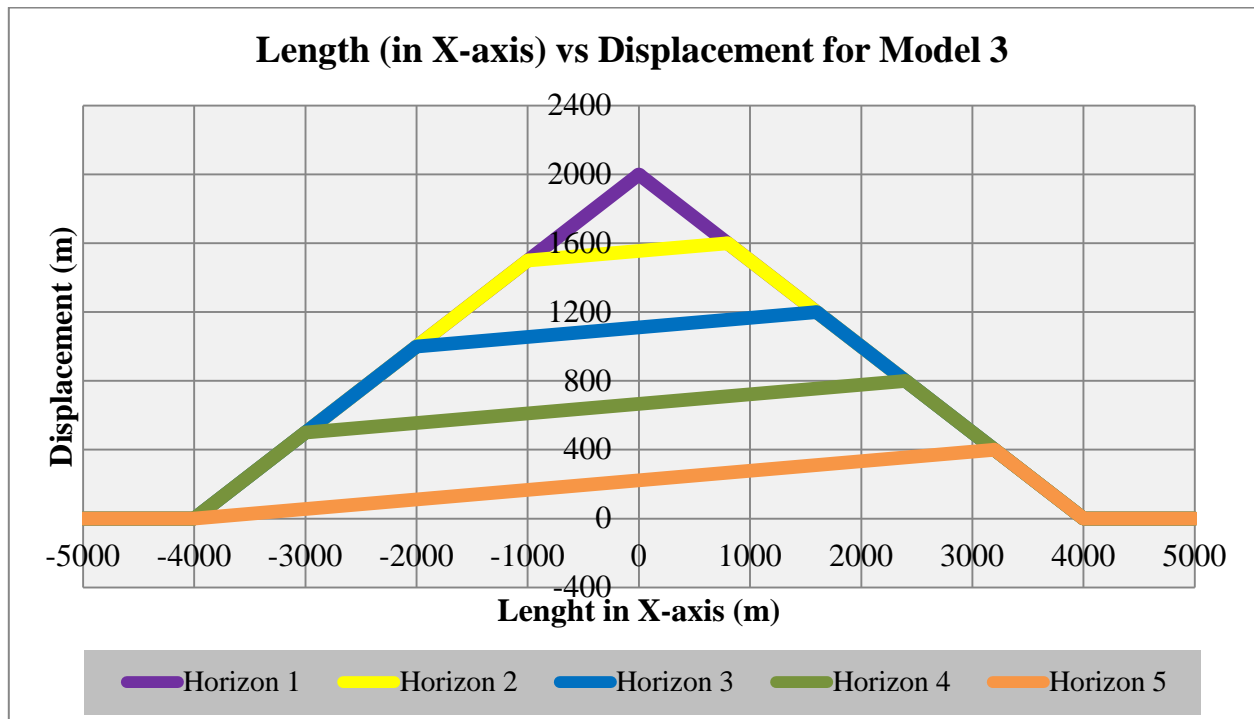


Figure 5.18: Length (in X-axis) Vs displacement plot of model 3. The plot shows relationship between length and displacement for each horizon in model 3, it shows that the fault tip is propagating only to the east. The total propagation rate is the same as model 2.

Class 1, structural map of horizon 1 shows the fault has 8000m in length (Figure 5.19). The fault has maximum throw in the centre of the fault and zero at the fault tip. Based on the displacement points set which has been applied, maximum elevation in the foot-wall shows -1000m and minimum elevation in the hanging-wall is 1000m. As this class used 2500m away from the fault as the reverse drag parameter, there is a narrow depocentre in hanging-wall and uplifted foot-wall which is created by the fault movement (Figure 5.19). It is difficult to see the difference between model 1, model 2, and model 3 by looking at the structural maps of horizon 1. The difference between them can be observed by looking at the cross-sections.

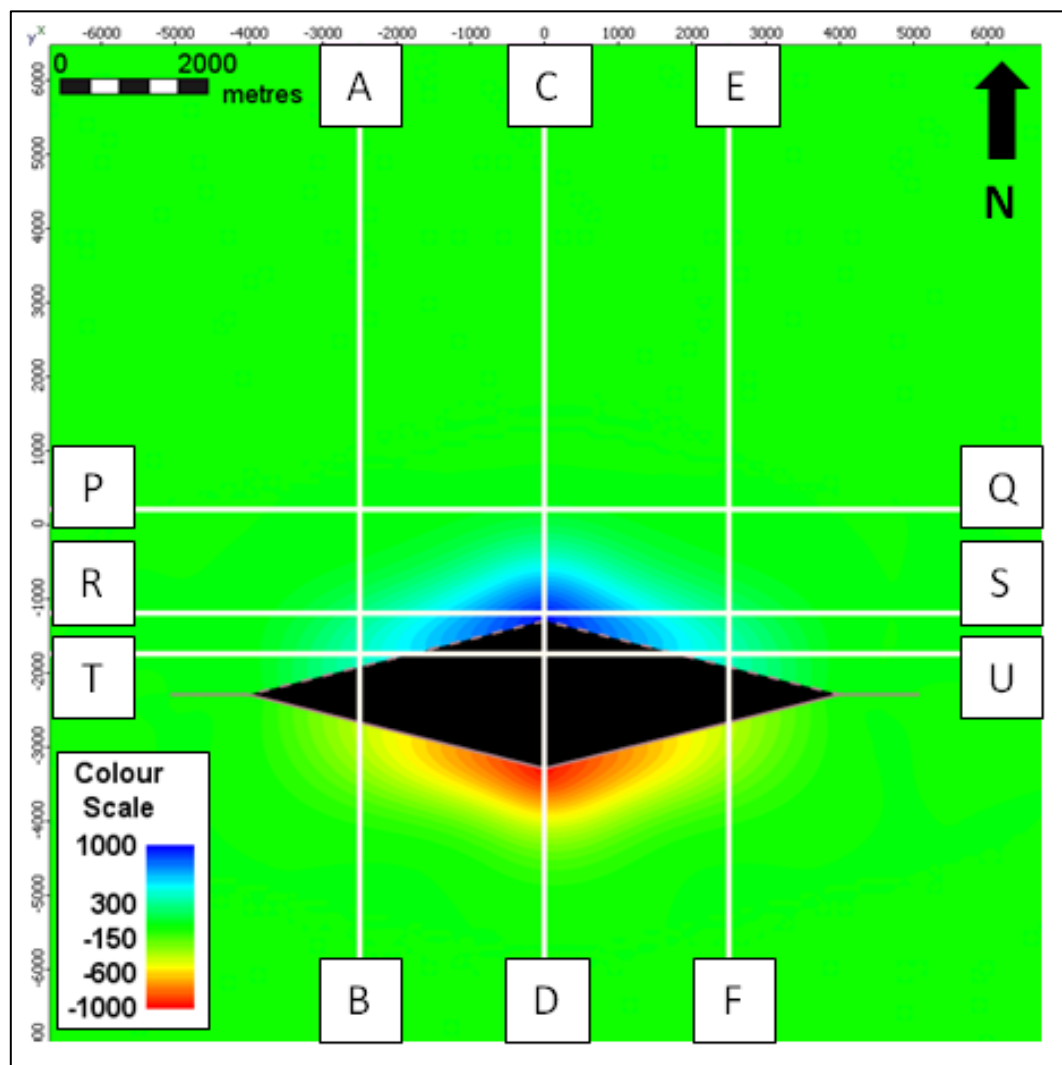


Figure 5.19: Structural map of horizon 1 (model 3 - class 1). *The structural map shows the structural configuration in the final evolution of class 1, the fault has 8000m in length with maximum throw (2000m) at the centre of the fault and gradually decreases towards the fault tip.*

Group of cross-sections shows the variation of structural configuration of the whole modelled area (Figure 5.20). The unique configuration also appears in this class. Propagation fault tip in one direction while the other fault tip seems to be constant has an influence for the sedimentation dispersal. As shown in the figure, cross-section A-B and E-F shows different configuration compared to the previous models. In the cross-sections A-B, there are two horizons (horizon 4 and 5) which deposited at the area while in cross-sections E-F just horizon 5 was deposited. It is related to the development of the fault that has bigger accommodation space at western part of the area as the fault propagates to the east (Figure 5.20).

Strike-sections for this model are different as model 1 and 2 (Figure 5.20). The propagation towards one direction brings a unique effect to the sedimentary layers structures. In strike-sections, the different between them can be addressed by looking at pinching out pattern. In this model, the pinching out strata is not leveled, this is because of the amount of displacement along the fault was not equal (slightly dipping to the east). The eastern part has a bigger displacement field than the western part. That is the reason that the sediments are apparently dipping towards the east.

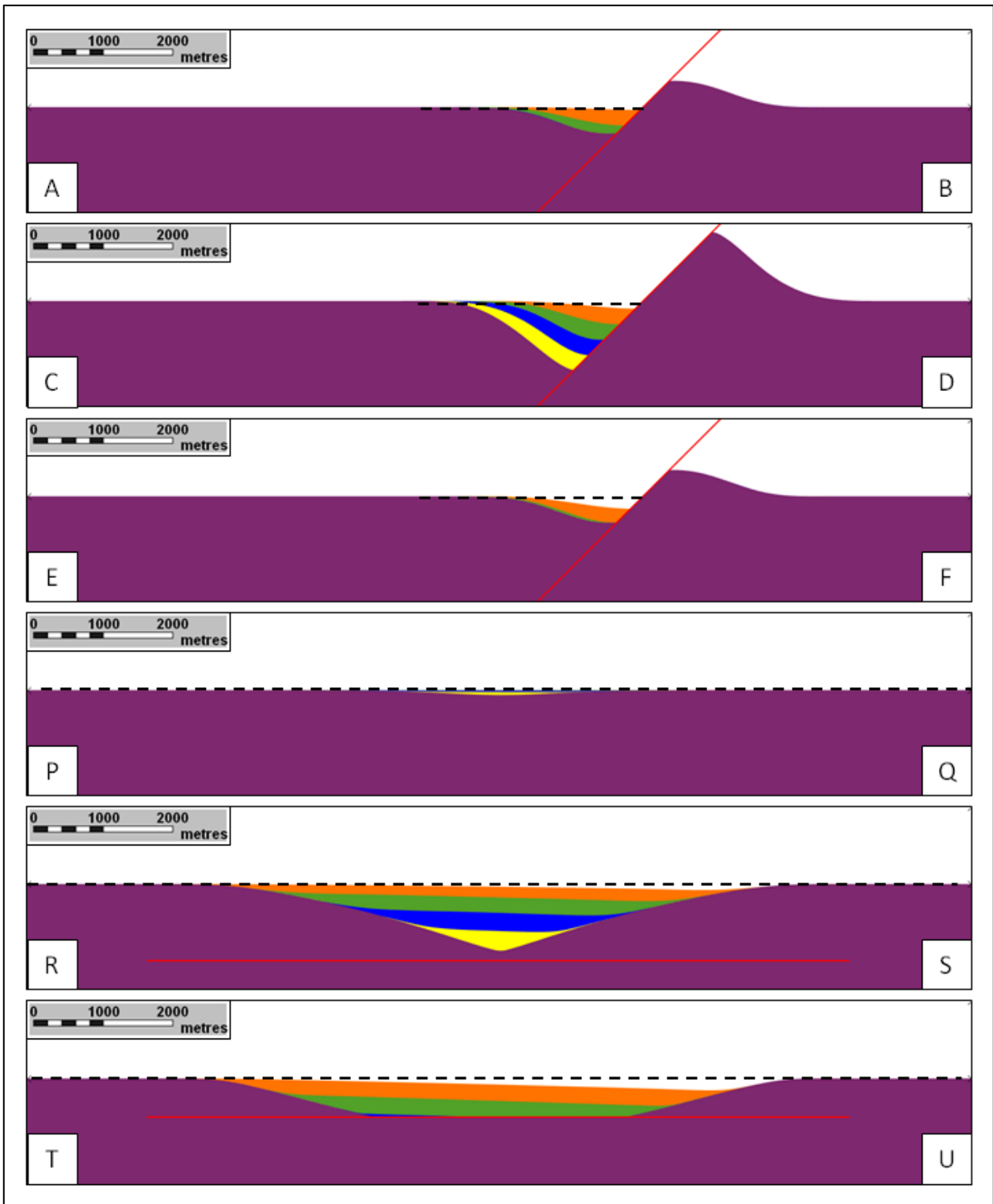


Figure 5.20: Group of cross-sections of model 3 - class 1. This group of cross-sections shows variation in structural of sedimentary layers across the fault block. Cross-sections (perpendicular to the fault) bring an idea about the dip of sediment while the strike-sections show the sediments distribution. It shows unique results of sedimentary distribution and sedimentary layers dipping slightly dipping to the east. (VE= 1:1)

Class 2, structural map of horizon 1 shows the fault has 8000m in length (Figure 5.21). The fault has maximum throw in the centre of the fault and gradually decreased towards the fault tip. Based on the displacement points set which has been applied, maximum elevation in the foot-wall shows -1000m and minimum elevation in the hanging-wall is 1000m. As this class used 5000m away from the fault as the reverse drag parameter, there are narrow depocentre in hanging-wall and uplifted foot-wall which created by the fault movement (Figure 5.21). It is difficult to see the difference between model 1, model 2, and model 3 by looking at the structural maps of horizon 1. The difference between them can be observed by looking at the cross-sections.

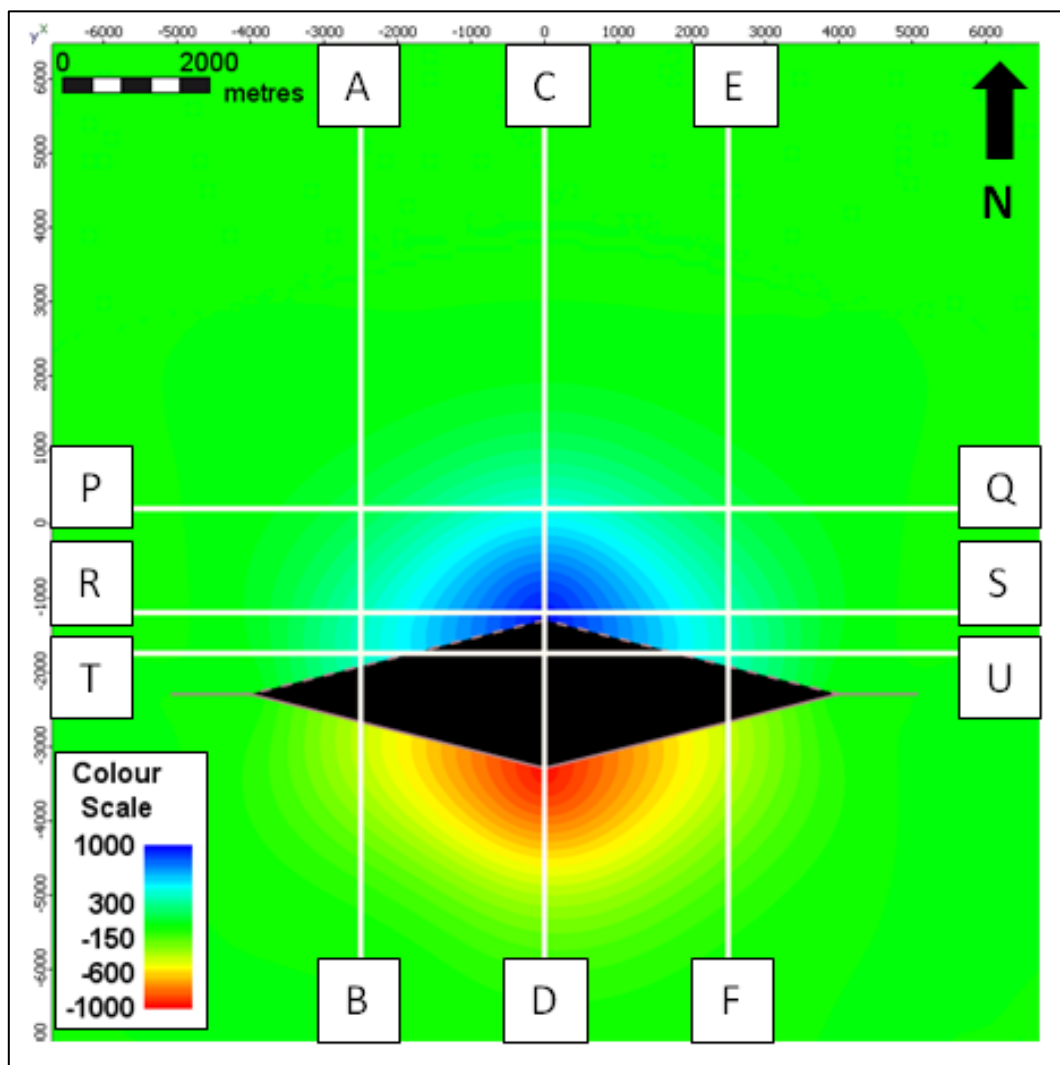


Figure 5.21: Structural map of horizon 1 (model 3 - class 2). *The structural map shows the structural configuration in the final evolution of class 2, the fault has 8000m in length with maximum throw (2000m) at the centre of the fault and gradually decreases towards the fault tip. It seems similar as model 3-class 1, while the basement structural configuration shows the structural high (foot-wall uplift) hanging-wall depocentre. Bigger accommodation space should be expected due to the longer reverse drag.*

Group of cross-sections shows the variation of structural configuration of the whole modelled area (Figure 5.22). The unique configuration also appears in this class. Propagation fault tip in one direction while the other fault tip seems to be constant has an influence for the sedimentation dispersal. As shown in the figure, similar to class 1, cross-section A-B and E-F shows different configuration compared to the previous models. In the cross-sections A-B, there are two horizons (horizon 4 and 5) which deposited at the area while in cross-sections E-F just horizon 5 was deposited. It is related to the development of the fault that has bigger accommodation space at western part (Figure 5.22). the same thing happen while the distance of reverse drag was setup to be longer, the dip of the sediments seem to be gentler than the shorter distance's model.

Strike-sections for this model are showing the similar result with class 1 (Figure 5.22). Besides the fundamental difference about the sedimentary layers dipping in strike-sections, in this class which used longer distance for reverse drag, as can be observed from previous models that it created a bigger an accommodation space which can be represented by cross-section P-Q where numbers of sediments were deposited on that area (Figure 5.22).

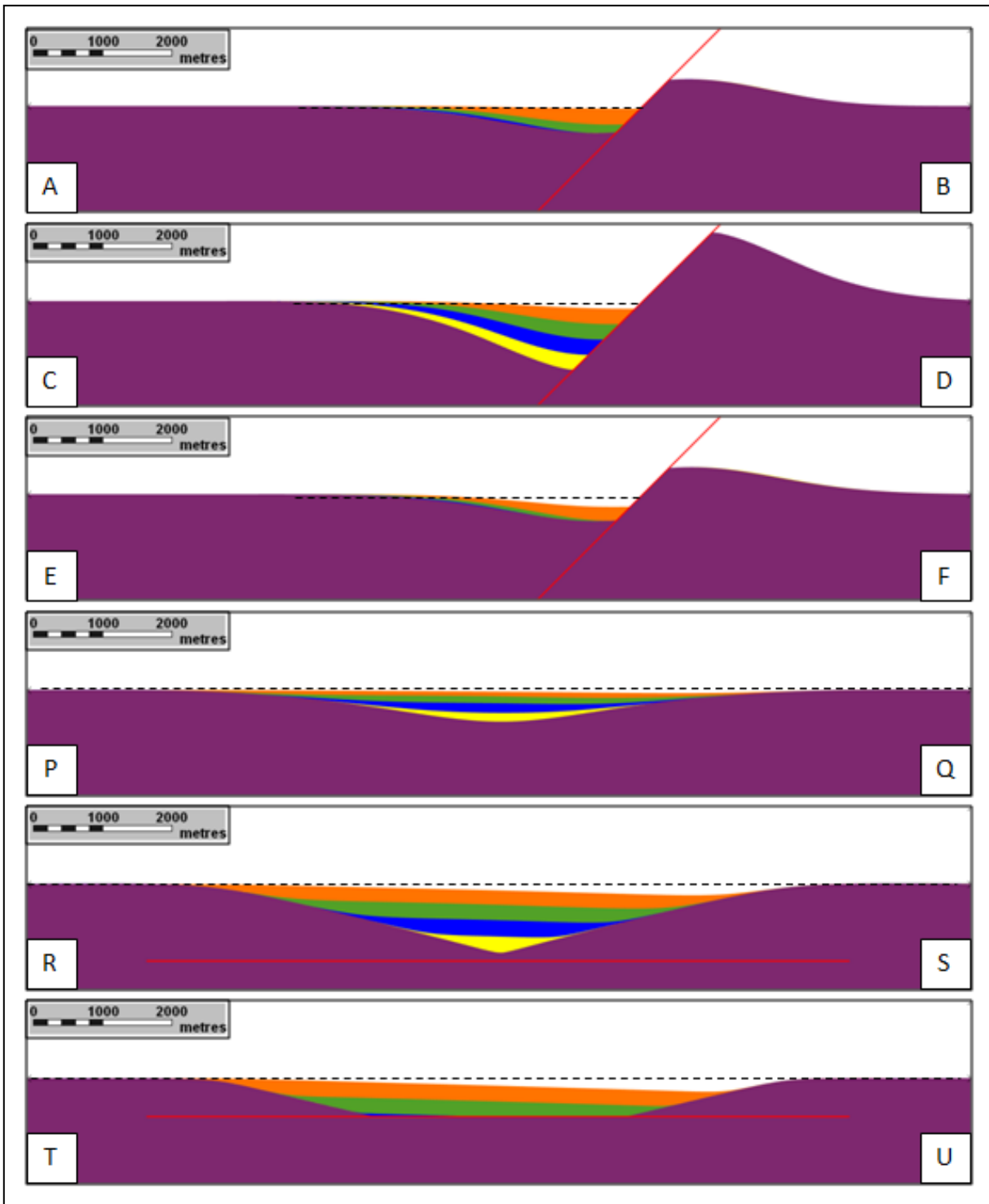


Figure 5.22: Group of cross-sections of model 3 - class 2. This group of cross-sections shows variation in structural of sedimentary layers in the fault block. Cross-sections (perpendicular to the fault) show that the dip angles of the sediment is gentler than dip angles of sediments in class 1. It shows the different size of accommodation space which is created by different reverse drag distance represented by cross-sections P-Q. (VE= 1:1)

Class 3, this class was generated using the displacement point set for model 1 but set the distance of reverse drag for 8000m in the 8000m in length fault set (Figure 5.23). Horizon 1 structural map shows almost similar result compared to the class 1 and class 2 – only the distance of reverse drag is different. As this class using the longer distance for reverse drag, the accommodation space shows a bigger depression which may be filled by the sediments (Figure 5.23) and there is no big difference about the configuration and maximum displacement as this fault was using the same displacement point set for this model 3.

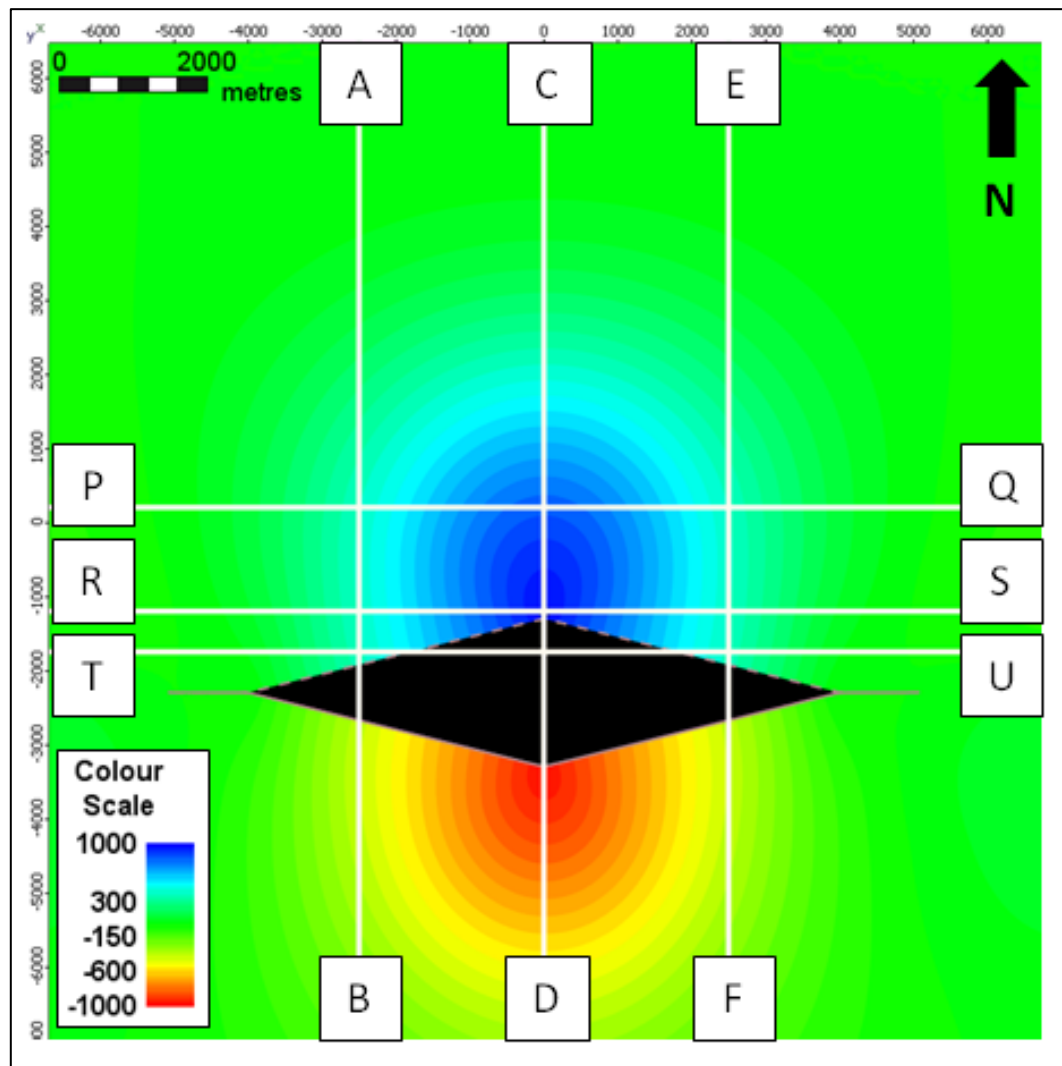


Figure 5.23: Structural map of horizon 1 (model 3 - class 3). *The structural map shows the structural configuration in the final evolution of class 3, the fault has 8000m in length with maximum throw (2000m) at the centre of the fault and gradually decreases towards the fault tip. It seems similar as model 3-class 1 and 2. Bigger accommodation space than the class 1 and 2 should be expected because of the longer reverse drag.*

Group of cross-sections shows the variation of structural configuration of the whole modelled area (Figure 5.24). The unique configuration also appears in this class. Propagation fault tip in one direction while the other fault tip seems to be constant has an influence for the sedimentation dispersal. As shown in the figure, similar to class 1 and class 2, cross-section A-B and E-F shows different configuration compared to the previous models. In the cross-sections A-B, there are two horizons (horizon 4 and 5) which deposited at the area while in cross-sections E-F just horizon 5 was deposited. It is related to the development of the fault that has bigger accommodation space at western part of the area (Figure 5.24). the same thing happen while the distance of reverse drag was setup to be longer, the dip of the sediments seem to be gentler than the shorter distance. This class shows the lowest dip angles of sediments configuration in model 3 which used the longest distance of reverse drag.

Strike-sections for this model are showing the similar result with class 1 and 2 (Figure 5.24). Besides the fundamental difference about the sedimentary layers dipping in strike-sections, in this class which used longer distance for reverse drag, as can be observed from previous models that it created a bigger an accommodation space which can be represented by cross-section P-Q where numbers of sediments were deposited on that area (Figure 5.24). The volume of sediments of this class is the biggest in model 3 which is related to the longest reverse drag distance model.

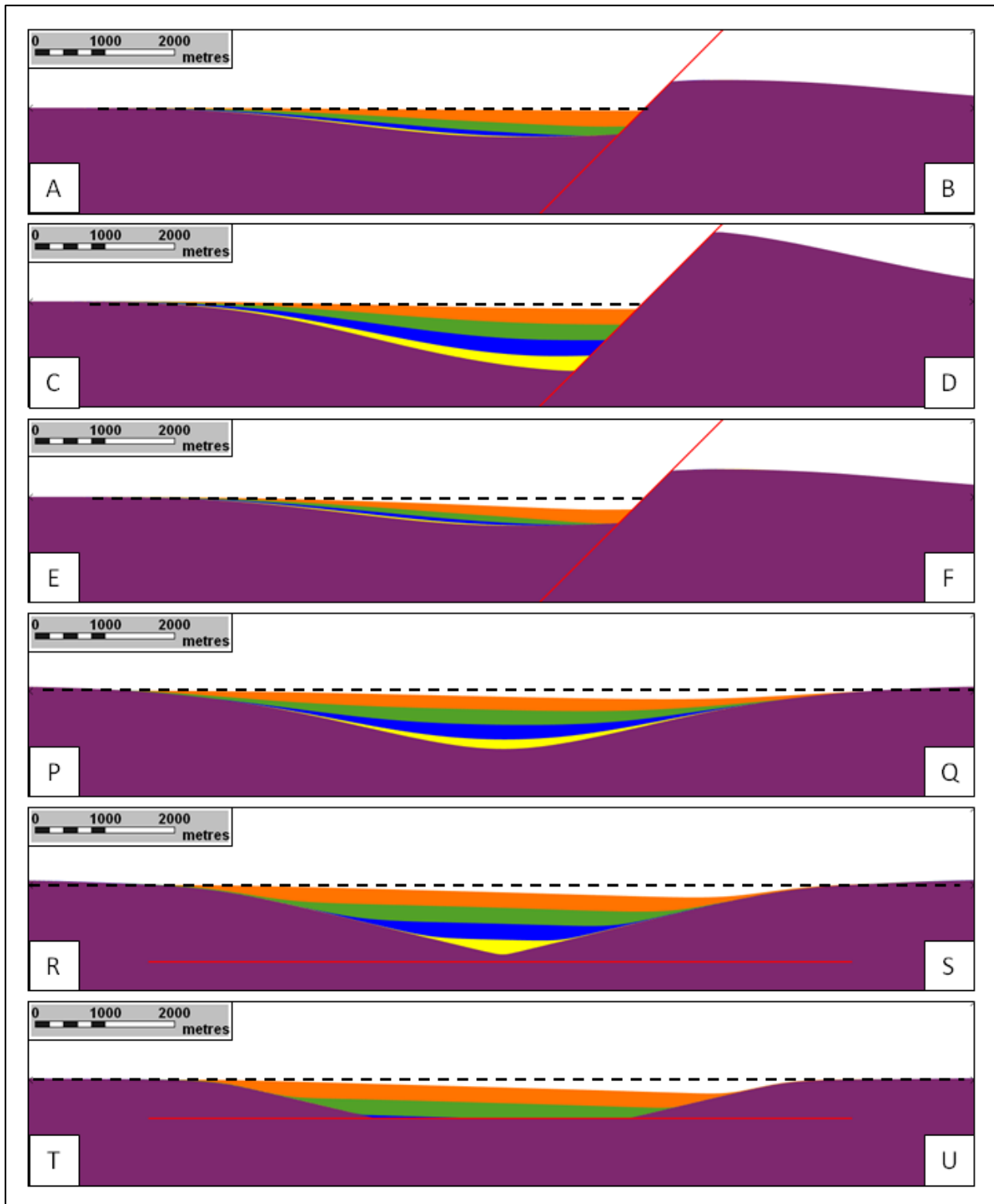


Figure 5.24: Group of cross-sections of model 3 - class 3. This group of cross-sections shows variation in structural of sedimentary layers in the fault block. Cross-sections (perpendicular to the fault) show the most shallow dip angle of model 3 compared to class 1 and 2. It shows the different size of accommodation space which created by different reverse drag distance represented by cross-sections P-Q and also the gentler dip configuration as compared to the other class in model 3. (VE= 1:1)

5.5 Kerpini Fault Block Model

Structural model of Kerpini Fault Block was generated to explain the unique sedimentation layers orientation and structural relationship in the fault block. The model has been generated using all of the field observation data which may lead to produce a best model that similar to the real case. Several assumptions have been applied in the model construction such as sediment thickness variation where the sediments are thicker to the east and also the Kerpini Fault is truncated the Vouraikos and Kerinitis Faults.

The model is also using preliminary hypothesis from previous experiments. The key parameters which may apply in the Kerpini Fault Block model are the influence of reverse drag distance and fault tip evolution. Initial hypothesis for this are longer reverse drag will produce a lack of increased dip from the older to younger deposit and sedimentation dispersal while the fault tip evolution only related to the sedimentation dispersal. The fault displacement distribution can be seen in Figure 5.25.

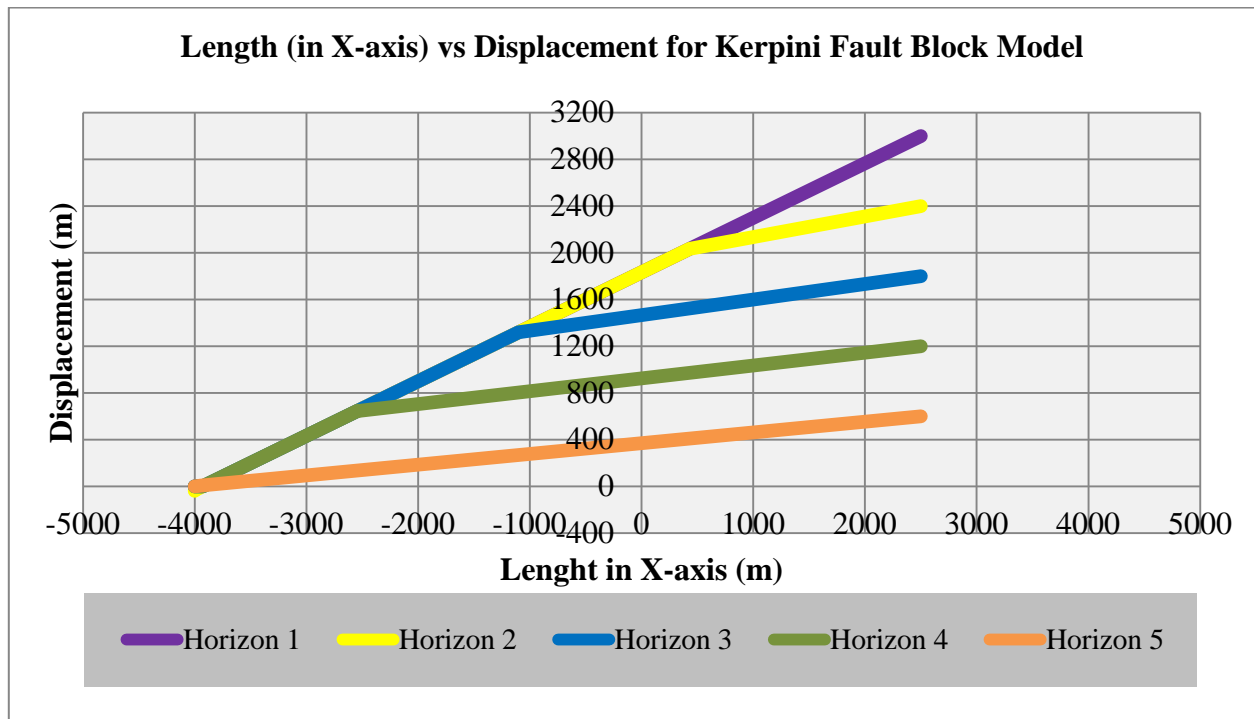


Figure 5.25: Length (in X-axis) Vs Displacement plot for Kerpini Fault Block Model. The plot shows relationship between length and displacement for each horizon in the Kerpini Fault Block model, it shows that the fault tip is propagating only to the west and bounded to the structure to the east.

In early stage, the fault was 2000m in length. It was propagate gradually until the fault reach 6250m in length in final stage (approximated length is similar to the Kerpini Fault). Propagation direction is defined to the west (Figure 5.26). This assumption is driven by the assymetrical fault movement interpretation. Based on the field mapping, the lithology distribution at the foot-wall of the Kerpini Fault suggests this idea. Eastern part of foot-wall of the Kerpini Fault is dominated by the basement in contrast with the western part as this part is contained syn-fault succession by domination of conglomerate. This lithology distribution suggest that the erosion of foot-wall uplift at the eastern part is more than at the western part, therefore, the maximum throw of the fault is approximately located at the eastern part of the area and decreases gradually to the west. Displacement distribution assumption for the model is also supported by the sedimentary layers of the syn-fault deposit. The main general dip direction is oriented to N165⁰E support the idea about the maximum throw of the fault to the southeast.

The existence of the Kerpini Fault East with hundred meters of step from the Kerpini Fault also supports the Vouraikos existence. It is difficult to generate a model of the Kerpini Fault Block without the Vouraikos Fault included. In western part, the existence is not that really convincing, and has not that much influence to the structural model; therefore, the Kerinitis Fault is not included in this model.

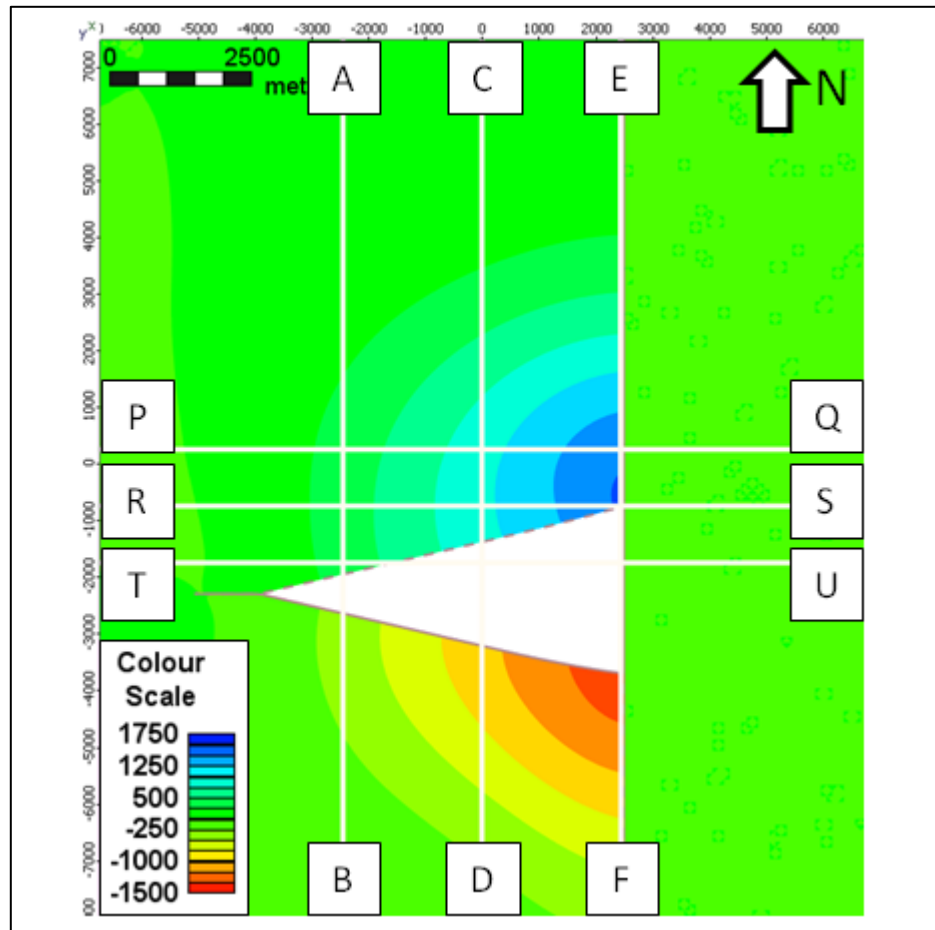


Figure 5.26: Structural map of Kerpini Fault Block (taken from the model). A map showing the structural configuration of the basement in the Kerpini Fault Block, it shows that the maximum displacement is located at the eastern part of the area and decreases gradually to the west, the existence of the North-South Structure (Vouraikos Fault) is essential to build a reliable model of this block. (The model is simplified in term of the direction; it is not following the real field orientation).

Field observation in chapter 4 about sediments distribution includes their sedimentary layers can be explained by look at the group of cross-sections in Figure 5.27. Steeper dip angle at eastern part of the Kerpini Fault Block (Roghi Mountain) is revealed by look at the cross-sections, cross-section E-F is located at the easternmost of the area and shows the steeper dip angle compared to cross-section A-B and C-D which are located at central and western part of the fault block. It is also show that lack of decreasing of dip angle in syn-fault deposits within the Kerpini Fault Block is possibly caused by the distance of reverse drag of this fault is far away from the fault plane (approximately 10km to the north).

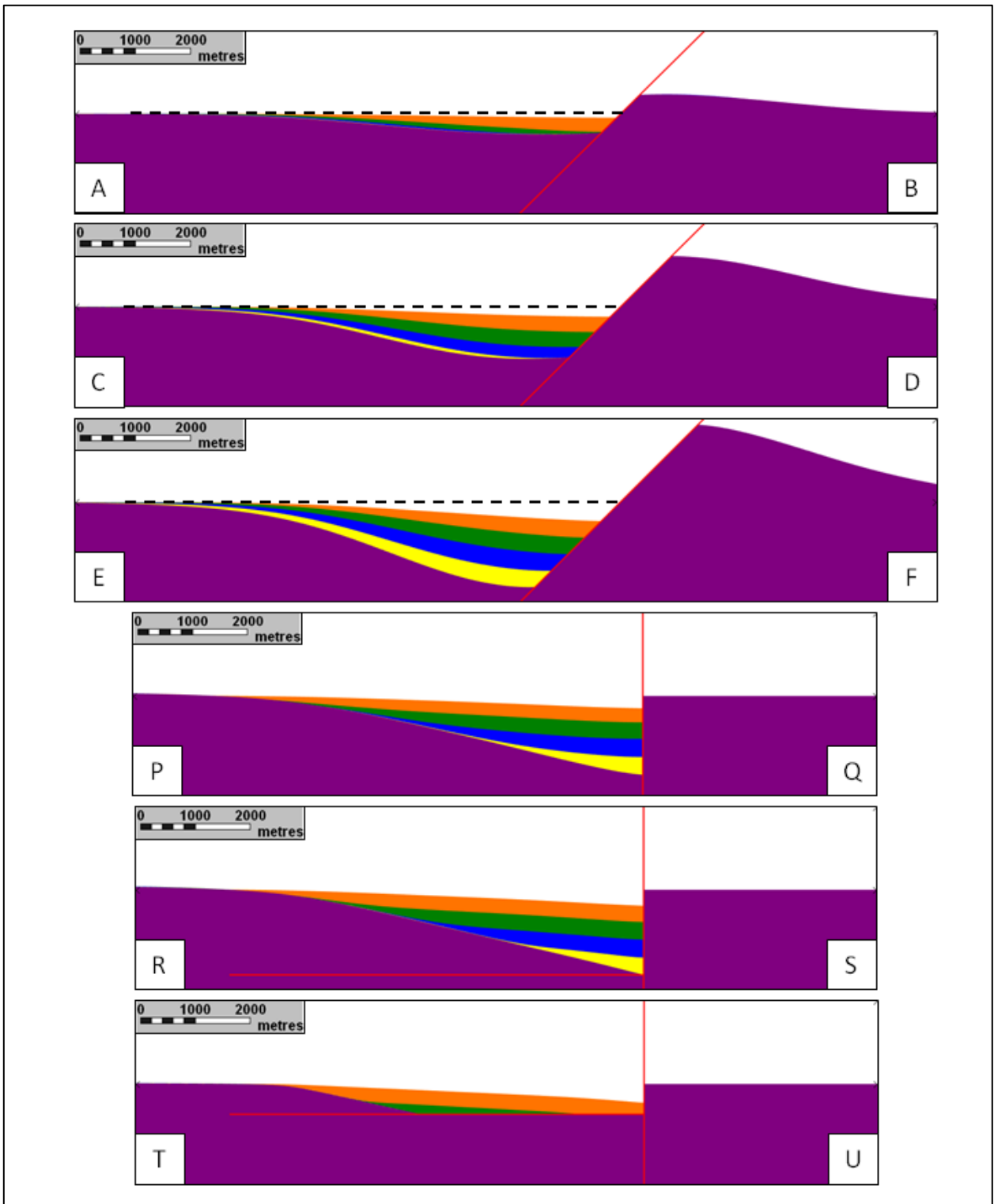


Figure 5.27: Group of cross-sections within the model of the Kerpini Fault Block. *These cross-sections have been constructed to show the syn-fault deposits configuration within the Kerpini Fault Block. (VE= 1:1)*

5.6 Modelling Summary

Based on the models, there are numbers of summary that can be extracted from the model to have a better understanding for the structural modelling prediction. According to the models, reverse drag will have a big influence for the sedimentary layers (dip angle and dip direction variation) and also size of accommodation space. Longer reverse drag point in normal direction to the fault will produce gentler sedimentary dips angle compared to the shorter reverse drag point.

Dip angle estimation by the calculation and deterministic method by the direct measurement from the cross-section can be seen in Figure 5.28. Based on the calculation and comparison between determined and estimated dip angle, shorter reverse drag has a better dip estimation. It proved by the result which longer reverse drag have a close estimation result compared to the deterministic method (Table 5.3). It can be caused by the flexibility of sediment layers, where longer reverse drag provides more space for sediment to bend more than the shorter reverse drag.

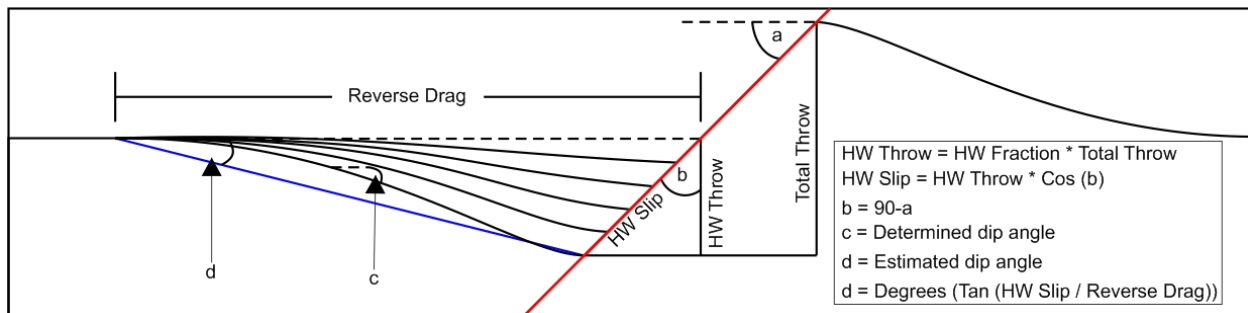


Figure 5.28: Estimation calculation for dip of sediments. *The diagram shows the way to estimate the dip of sediments in faulted block using the simple mathematical and trigonometric equations, given the dip of the fault; reverse drag, total throw, and displacement fraction, the dip of sediments can be estimated.*

Based on the observation in Table 5.3, the dip range of the oldest and youngest strata are getting smaller as the reverse drag is getting longer. It can be a suggestion that longer reverse drag will produce a lack of decreasing dip towards the younger sediment package, while shorter reverse drag will produce the opposite way (obvious decreasing dip of sedimentary layers).

Fault Dip	HW fraction	Total Displacement	HW Displacement	Reverse Drag	Determenistic Dip (Oldest)	Deterministic Dip (Youngest)	Estimated Dip (Oldest)	Estimated Dip (Younger)
45	0,5	2000	1000	2500	36	9	36,38	6,51
45	0,5	2000	1000	5000	22	5	16,65	3,24
45	0,5	2000	1000	8000	13	2	10,24	2,03

Table 5.3: Table of estimated and determined dip observations of model 1 (class 1, 2, and 3). *The observations in the table show that it is possible to estimate the dip angle of the sediments with an uncertainty around 5°. The table also shows that the dip range of the oldest and youngest strata are getting smaller as the reverse drag distance is longer.*

Besides reverse drag, there is another factor that will bring an influenced to the sedimentary layers in syn-fault deposit, it is the fault evolution. In these modelling cases, the fault evolution is determined by the propagation of fault tip which will produce a growth fault. Propagation of fault tip will have a direct effect to sedimentation dispersal.

Chapter 6 : DISCUSSION

The unique configuration of sedimentary layers which are in contrast with classical syn-fault sedimentation rules in the Kerpini Fault Block is the main topic for discussion. The dip angles of sedimentary rocks in syn-fault phase within the Kerpini Fault Block seem to be consistent although it should be decreasing towards the younger sediments according to the classical syn-sedimentary theory. Not only that, but also facies distribution is also another problem to be discussed; the facies analysis within the Kerpini Fault Block and their sedimentation patterns are the main focus, including a paleo-drainage analysis.

The Kerpini Fault Block model has been generated using field observation data. For example, the Kerpini Fault has a maximum displacement at the eastern tip and gradually decreases towards the western tip. This scenario was built in order to approach the real field evidence in the Kerpini Fault Block, where the north-south structure (Vouraikos Fault) bounds the Kerpini Fault and the facies distribution within the Kerpini Fault Block, which was coming from the lithological description in the field work.

6.1 Structural Model of the Kerpini Fault Block

6.1.1 Effect of reverse drag on sedimentary layers

The Kerpini Fault Block model in Chapter 5 has been generated to illustrate the structural features of syn-fault deposits in the Kerpini Fault Block. Having compared all of the models in Chapter 5, the dip angle of syn-fault deposits depends on the reverse drag distance and fault evolution including its total displacement, but in this case, the reverse drag remains to be the main factor. Longer reverse drag distance provides a lack of decreasing of dip angles in syn-fault deposits compared to a shorter reverse drag distance.

6.1.2 Alternative Interpretations

Classic Normal Fault Block System

In the classical normal fault block system, the fault movement is continuous. The sediments come within the same broad time with the fault movement. As the fault growth, the sediments come in and fill the space. Therefore, growth strata and sharp decreasing of dip angles towards the

younger sediments should be expected and it does not fit with the evidences in the Kerpini Fault Block (Figure 6.1).

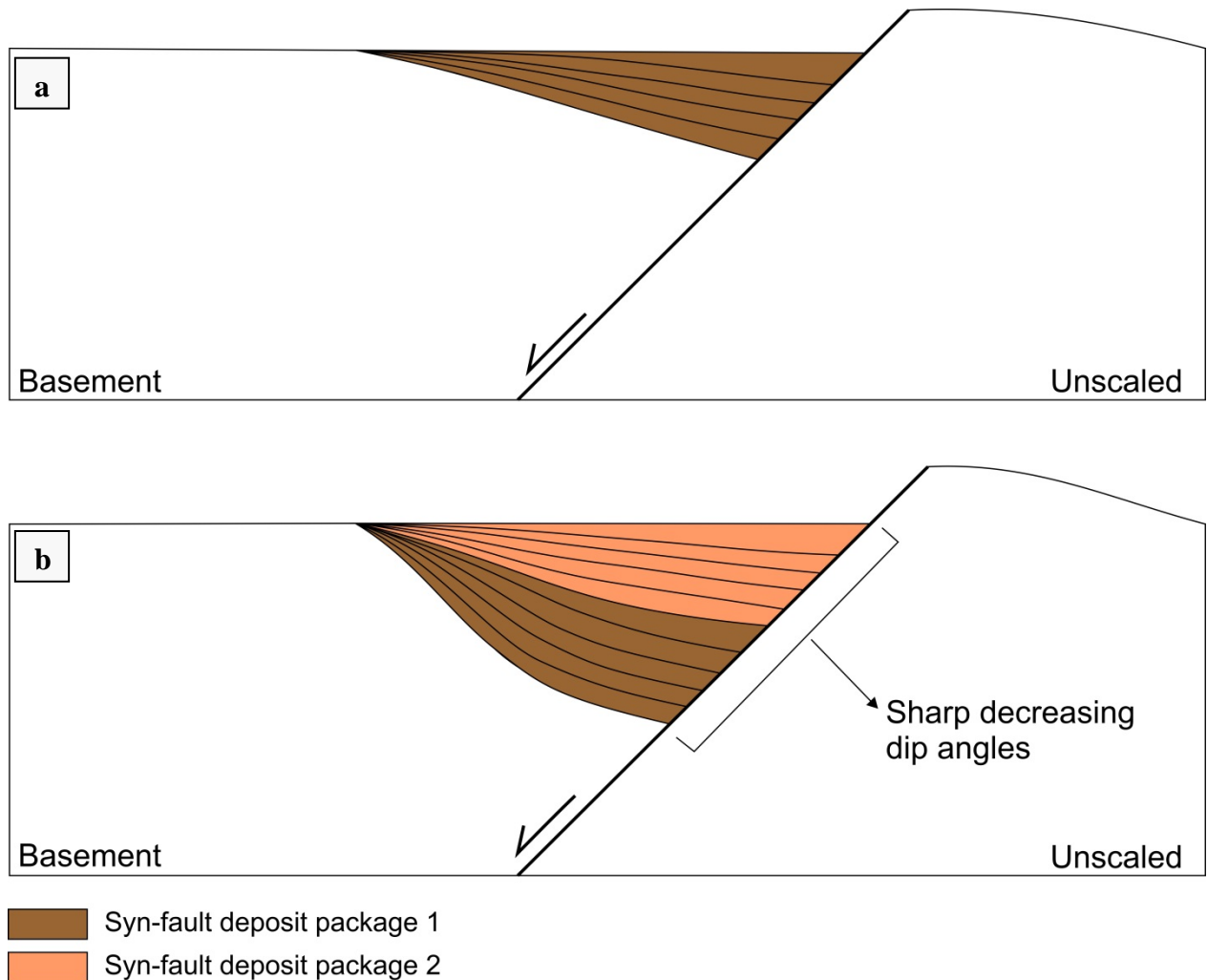


Figure 6.1: A schematic classical syn-faulting configuration. *The model shows the sharp decreasing dip angles of syn-fault deposits. (a) This figure is showing the first step of fault movement while (b) is showing the second step of fault movement.*

Syn-fault configuration with reverse drag control

The controls of reverse drag on the sedimentary layer seem promising to explain the consistent dip angle configuration in the Kerpini Fault Block. However, the longer reverse drag model still has slightly decreasing dip angles that can be observed (Figure 6.2). The Kerpini Fault Block used 10km of reverse drag distance (Chapter 5). The oldest layer has dip angle of 20° - 25° , but the younger layer has a dip angle of 5° - 8° . This differs with the field data which shows consistent dip angles. Therefore, this kind of explanation may not fully answer the question of

structural (sedimentary layers) features of syn-fault deposits in the Kerpini Fault Block. It has been illustrated in the Figure 6.2.

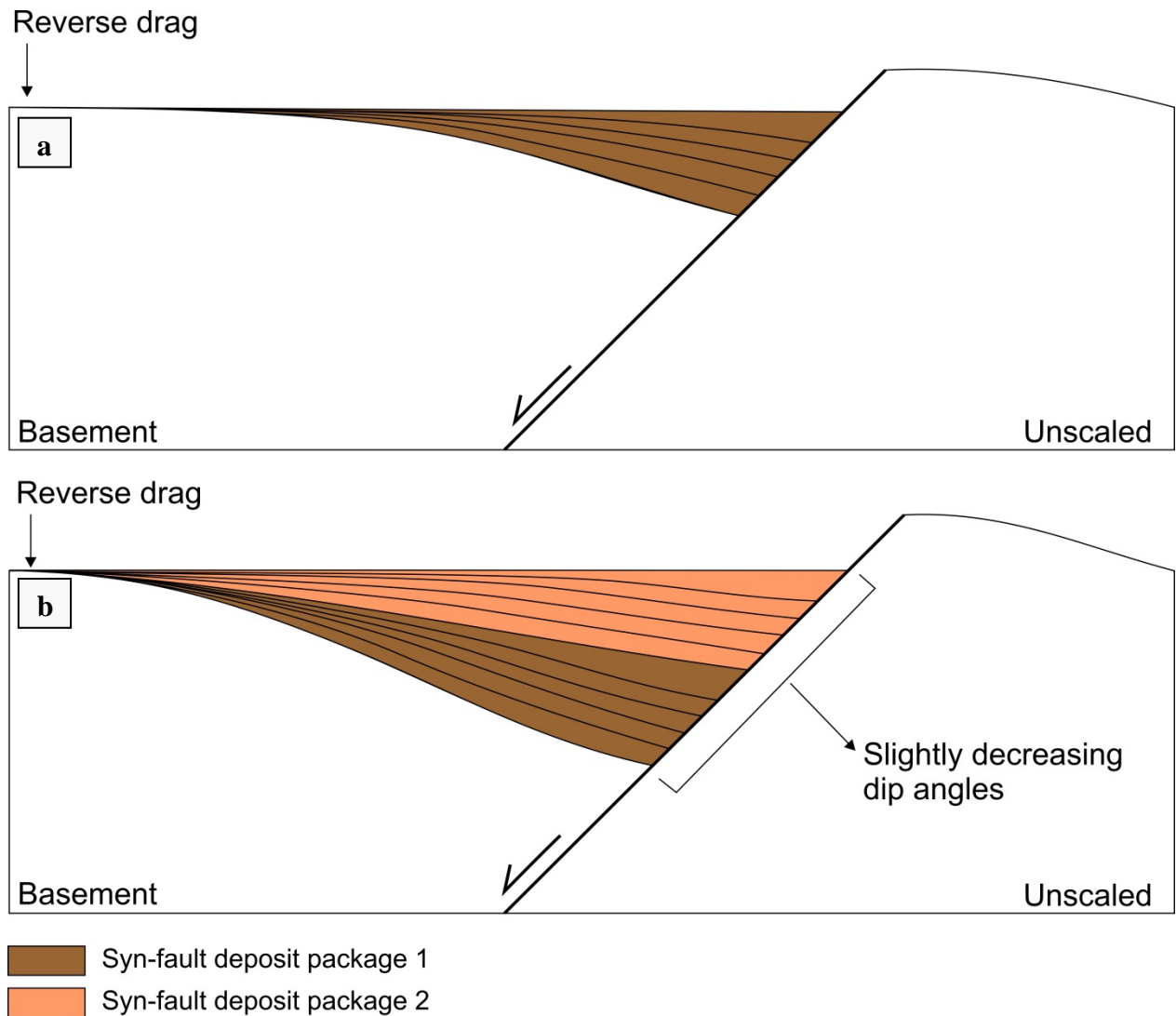


Figure 6.2: A schematic syn-fault configuration with reverse drag controls. This illustration is showing that with a longer reverse drag distance, the dip angles of syn-fault deposits are still decreasing towards the younger sediments. (a) The first step of fault movement and (b) the second step of the fault movement.

Syn-fault configuration with episodic movements

Another possible interpretation is that movement of the Kerpini Fault is episodic. An episodic movement means that the Kerpini Fault moved and stopped, then the sediments were deposited in the hanging-wall of the Kerpini Fault which is the depocentre in this half graben. After that, the Kerpini Fault moved, stopped, and the sediments are deposited again in the hanging-wall which produced a new package of syn-fault deposits. These processes might continue until the Kerpini

Fault completely ceases its movement. As a result, it should be expected to have different packages of syn-fault deposits in the Kerpini Fault block with unique dip angles for each package. It is also expected to have angular unconformity relationships between the sedimentary packages and onlap of syn-fault deposits package 1 to the basement.

As shown in Figure 6.3, the fault is moving episodically and the sediments are deposited as normal flat layers, fill the space, and form a syn-fault deposit package 1. The second phase is showing that the fault keeps moving and rotating the pre-existing sediments, followed by subsequent sedimentation above the syn-fault deposit package 1. A syn-fault deposit package 2 produces an angular unconformity on the top of syn-fault deposit package 1. Based on this interpretation, there is a possibility to have consistent dipping layers in the syn-faulting phase. The syn-fault package 1 may represent the Massive Conglomerate and Early Sandstone-Conglomerate units (unit 2 and 3) in the Kerpini Fault Block system, where they have slightly consistent dip angles. However, missing onlap relationship, angular unconformity, and syn-fault deposit package 2 may reduce the confidence to believe in this kind of theory for the Kerpini Fault Block; even though it is possible that those could have been eroded since they have been exposed for a long time

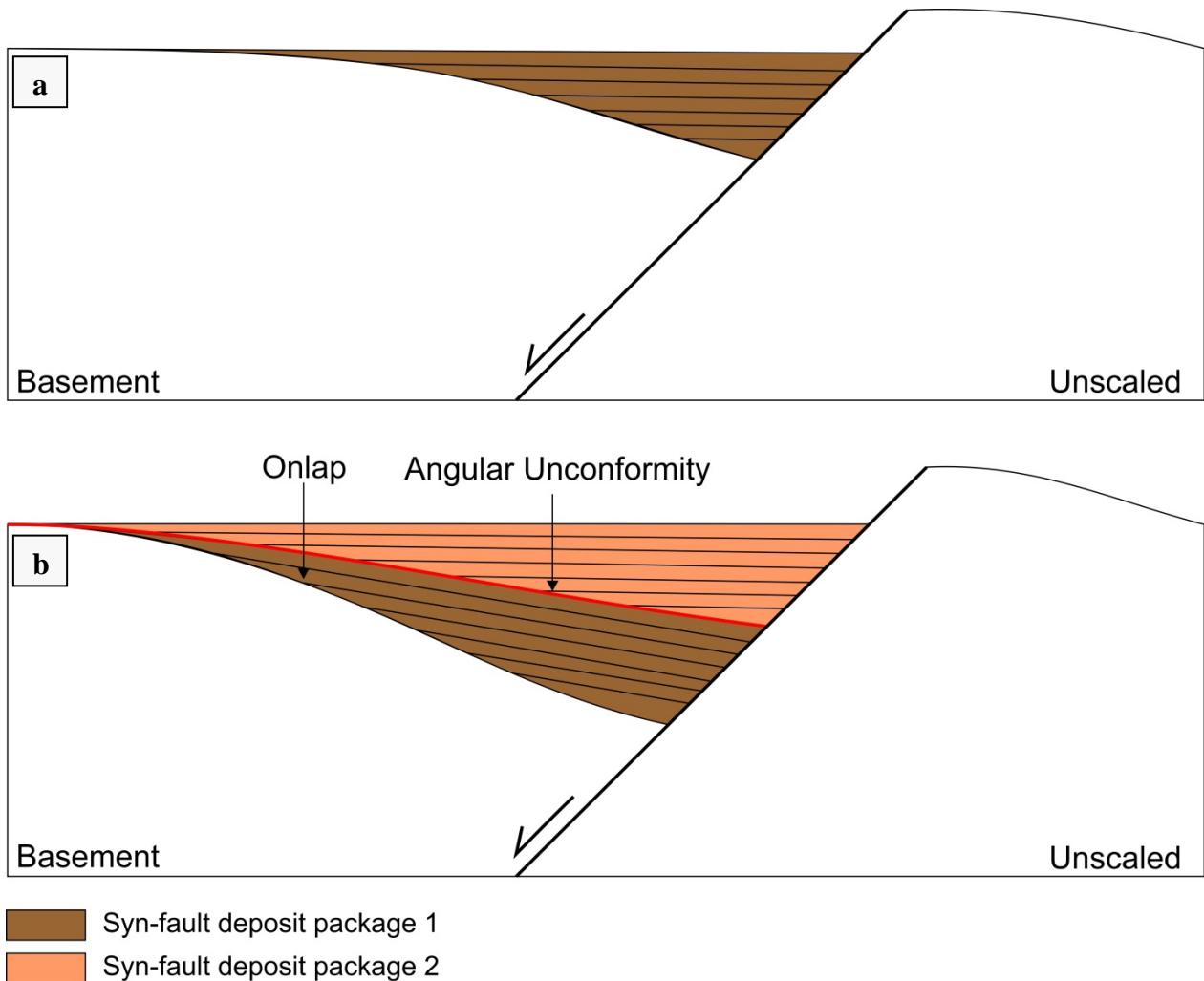


Figure 6.3: The schematic syn-faulting configuration with an episodic movement. A schematic model for consistent dip angle layers in syn-faulting phase, (a) first movement and (b) second movement. Syn-fault package 1 may represent the sediments in the Kerpini Fault Block, whilst the angular unconformity and package 2 may eroded due to significance exposure.

It could be assumed that all of the syn-fault deposits visible in the Kerpini Fault Block today are the result of one episodic movement and all of the other packages were eroded generating consistent dip angles. However, it is difficult to explain that the fault was moving for 800-1500m for one episodic movement and without sediments being deposited at the same time but after the movement.

6.2 Sedimentation of the Kerpini Fault Block

The sedimentation model of the Kerpini Fault Block has been generated based on the morphological evolution of a faulted block. In addition to that, the sedimentation model was

generated honoring the field data including strikes and dips, facies variations, and sedimentological observations. Combining these two aspects, the sedimentation model of the Kerpini Fault Block has been generated to approach the real condition in the field and to be an analogue model for hydrocarbon fields in similar geological settings (ie. North Sea).

Clast composition

Clast compositions of conglomerates in the Kerpini Fault Block in the western and eastern parts are slightly different. The eastern part is dominated by the limestone clast and a few appearances of chert and sandstone, whilst in the western part, there are several outcrops that show the composition of chert and sandstone is more dominant than their composition in the eastern part (Chapter 4, Stratigraphy sections).

The clast composition of the western Kerpini Fault Block is similar as the clast composition in the Kalavrita Fault Block. It suggests two different sources for the sediments in the eastern and western part of the Kerpini Fault Block.

Grain size variation

The observations show that the grain size distribution in the Kerpini Fault Block has fining northward (NNE) and westward (NWW) trends. It suggests that the sediments in the Kerpini Fault Block may have been transported from south to north. It explains the fining northward feature of grain size variation in the Kerpini Fault Block (Chapter 4, grain size section).

The anomalous grain size in the middle of Kerpini Fault Block (bigger grain size in the north) may suggest that there is a minor source of sediments. This feature is represented by two alluvial fan morphologies with finer grains to the south.

Controls of foot-wall uplift

As written before, the Kerpini Fault Block has a maximum displacement on the eastern tip and propagates to the west (WNW). The fault propagation to the west (WNW) affects the paleo-drainage development in the Kerpini Fault Block. The Vouraikos River which has been

interpreted as the ancient river and became the sediment source of the Kerpini Fault Block may also have developed during the fault propagation period.

Initially, the river might have an orthogonal paleo-drainage direction to the fault as it could follow the regional tilting of the area to the north. As the fault propagates, its foot-wall uplift becomes a barrier for the river. Therefore, the river was forced to step to the west gradually. It may become an implication of foot-wall uplift which could develop and control the direction of the paleo-drainage.

Paleo-drainage

Clast composition, grain size variation, and controls of footwall uplift on the sedimentation are the input parameters to building a schematic paleo-drainage map of the Kerpini Fault Block. Based on the previous discussions, the paleo-drainage that might become the sources of sediments in the Kerpini Fault Block comes from the south (Figure 6.4). The orthogonal direction of the Vouraikos River may have branches as the uplifted foot-wall becomes a barrier for the river to flow.

The rivers moved westward as the Kerpini Fault propagates to the west and reaches its tip. The anomalous grain size in the center of the Kerpini Fault Block has been interpreted as a result of Dhoumena Fault Block movement. The uplifted foot-wall of the Dhoumena Fault becomes an erosional area and source for the sediments at the central part of the Kerpini Fault Block. These sediments were transported from north to south (Figure 6.4).

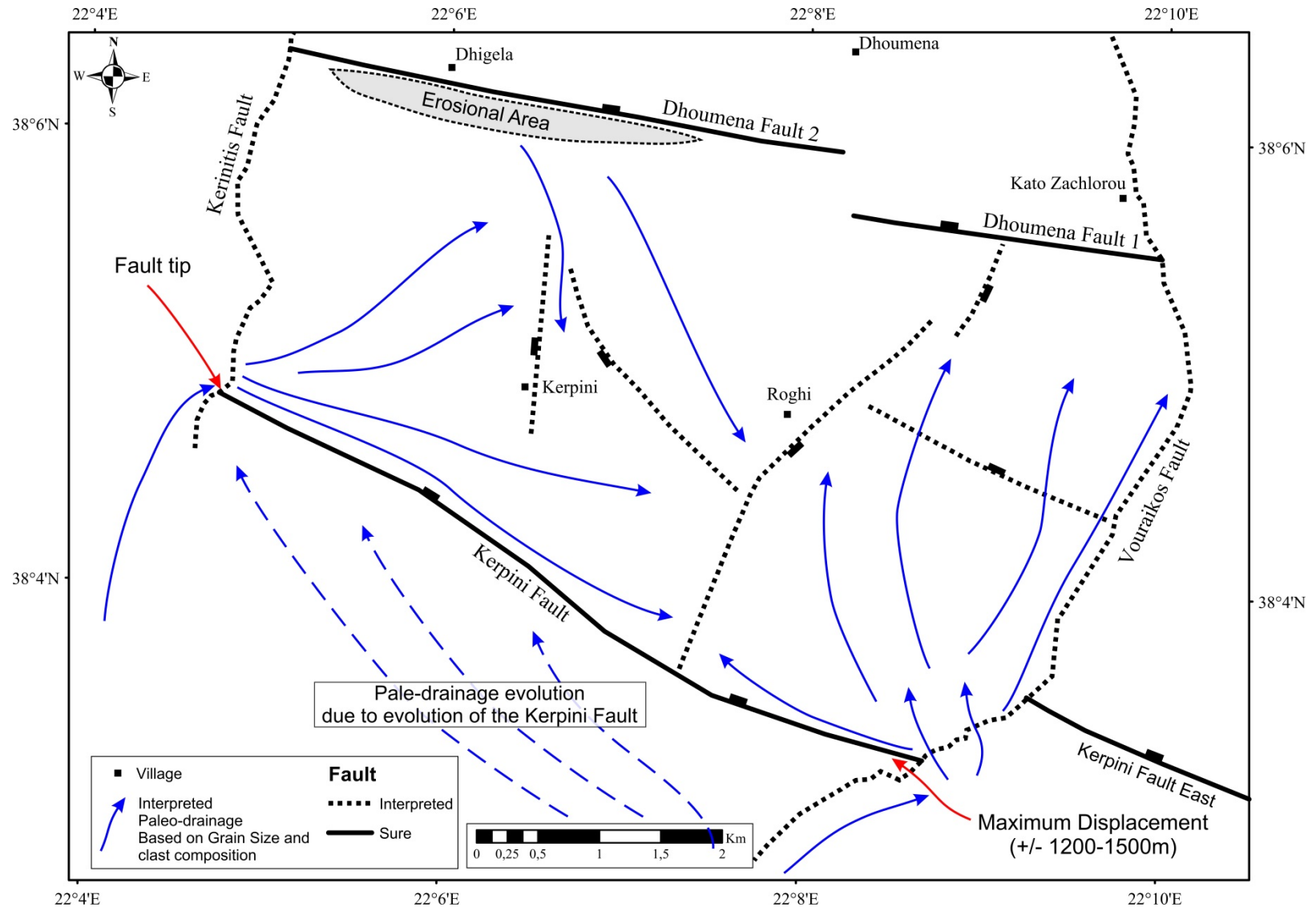


Figure 6.4: Paleo-drainage map based on facies, grain size, and clast components. Reconstructed paleo-drainage map shows the schematic analysis of source sediments in Kerpini Fault Block is dominated by the south to north source. However, there is still minor sediments came from north suggested by the anomaly grain size distribution.

6.3 Evolution of the Study Area

Evolution of the Kerpini Fault Block began with a Pre-fault phase, marked by the basements (limestone and red shale), as they were deposited as a regional basement. The limestone group is slightly metamorphosed and could be related to the limestone in Alps due to its orogeny. Moreover, the syn-fault phases can be divided into several steps.

Initial fault phase, after the stable condition in pre-fault phase, started from the east, the Kerpini Fault moved (Figure 6.5). The Kerpini Fault movement is an asymmetric fault displacement since it propagates gradually to the west. It provides an accommodation space in the hanging-wall of the fault. The Vouraikos River has been interpreted as an ancient river and sediments source for the Kerpini Fault Block flow to the hanging-wall of the Kerpini Fault. All the sediments which were transported by the Vouraikos River were deposited in the Kerpini Fault Block as alluvial fan deposit. At this time, the Dhoumena Fault had not yet moved.

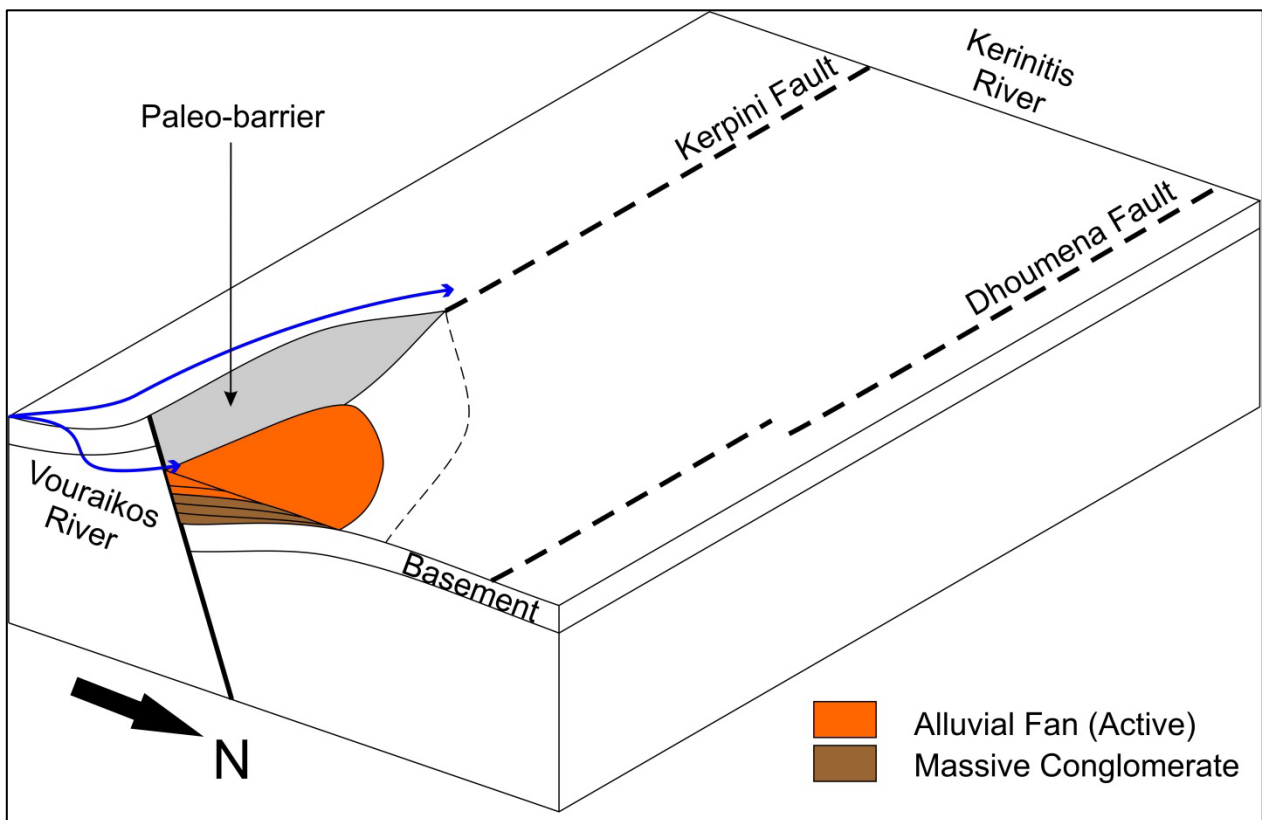


Figure 6.5: Structural and Sedimentation model of the Kerpini Fault Block; initial fault stage (without scale). The Kerpini Fault started to move and the Vouraikos River brought sediments to be deposited in the Kerpini Fault Block as alluvial fan deposits.

Syn-fault and Roghi Fault South development, the Kerpini Fault was continuously propagating to the west and provides a larger accommodation space through time whilst the Roghi Fault South started to move (Figure 6.6). The alluvial fan became bigger and distributed widely. The movement of the Roghi Fault South provided a larger accommodation space in the eastern area of the Kerpini Fault Block. This could explain the thick and massive conglomerate outcrop in the Roghi Mountain which has a significant difference in thickness with the sediment in central and western part of Kerpini Fault Block. The Vouraikos River is also interpreted to have evolved in response to Kerpini Fault movement. Uplifted foot-wall of the Kerpini Fault became a paleo-barrier for the Vouraikos River and stepping to the west followed the direction of the Kerpini Fault propagation.

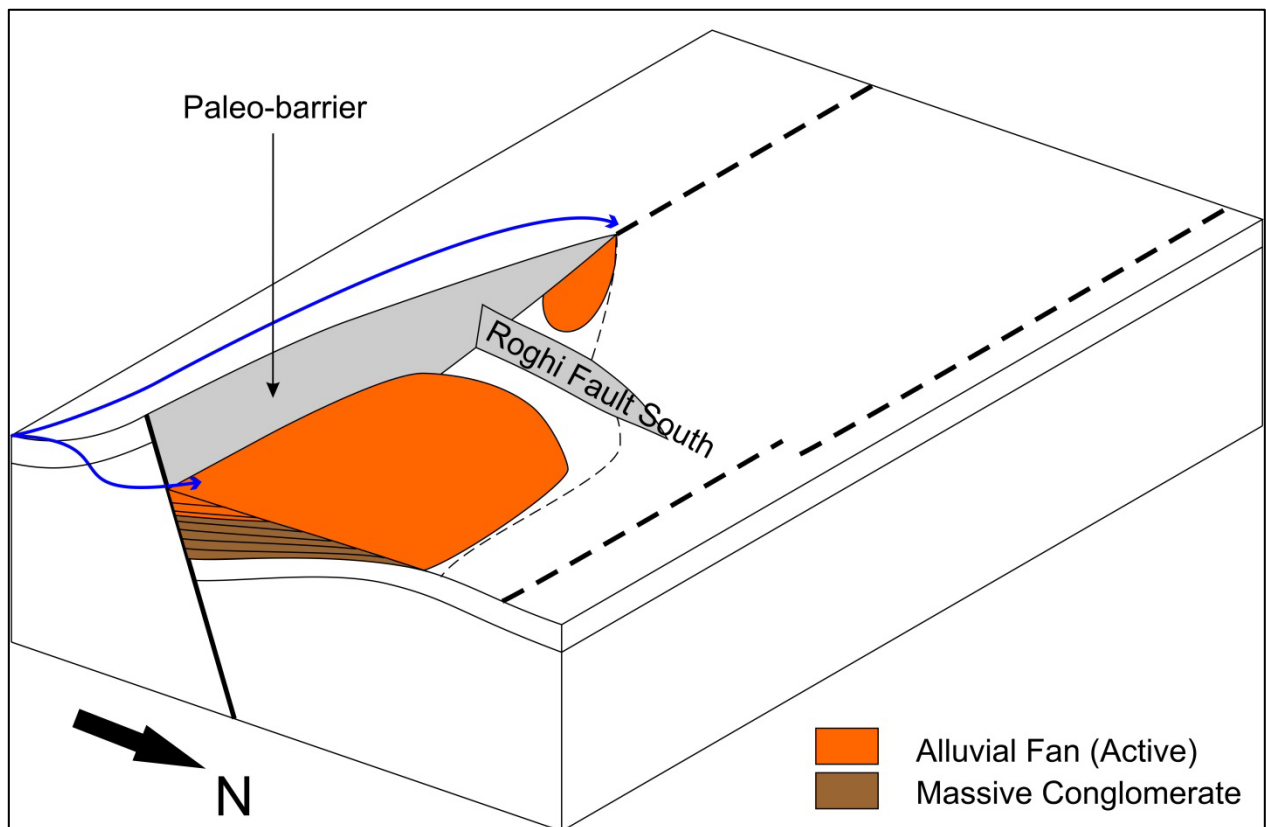


Figure 6.6: Structural and Sedimentation model of the Kerpini Fault Block; Syn-fault and Roghi Fault South development (without scale). *The Kerpini Fault continuously propagated and provided a bigger accommodation space for the sediments, at this step also the Roghi Fault South started to move.*

Syn-fault and western alluvial fan development phase. The Kerpini Fault continuously grew westward (Figure 6.7) and resulted in an arm of the Vouraikos River bypass to the hanging-wall in the western part of the Kerpini Fault Block towards the tip. It became a source of sediments in

the central and western part of the Kerpini Fault Block together with the alluvial fan in the Kalavrita Fault Block (behind the Kerpini Fault Block).

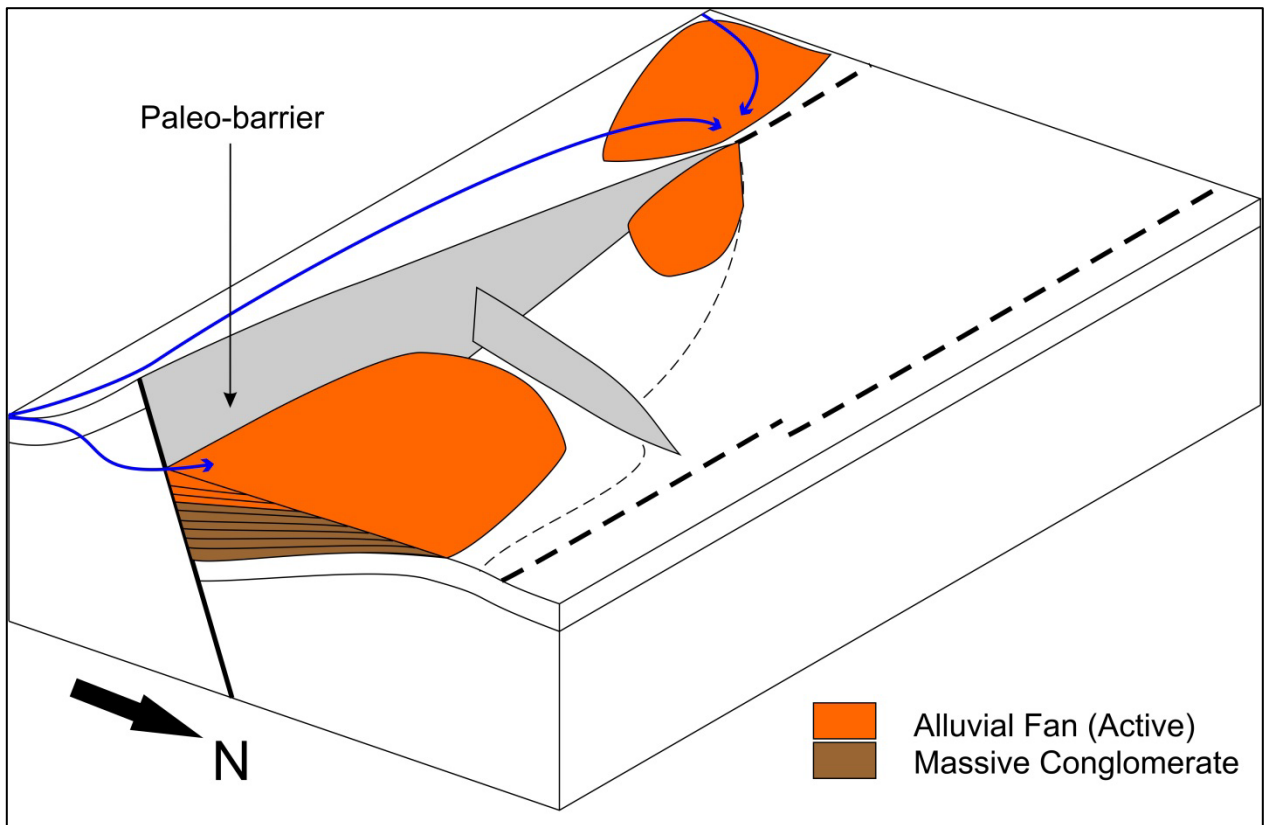


Figure 6.7: Structural and sedimentation model of the Kerpini Fault Block; syn-fault and western alluvial fan development phase (without scale). In this phase, the Kerpini Fault continuously grew; resulting in the accommodation space was getting bigger. The river and alluvial fan in the Kalavrita Fault Block (behind the Kerpini Fault) brought sediments to the central and western part of the Kerpini Fault Block and were deposited as alluvial fan and deposits.

Fault climax phase and development of the next fault block, the Kerpini Fault and Roghi Fault South were continuously growing and providing a maximum volume of accommodation space for the alluvial fan in the eastern part which is known as the Massive Conglomerate (unit 2) at the Roghi Mountain (Figure 6.8). The Dhoumena Fault also started to move together with the Roghi Fault West. The uplifted foot-wall of the Dhoumena Fault causes the drainage to step back and flow in the opposite direction. The Roghi Fault West provided accommodation space which was filled by the alluvial fan deposit with debris flow sediment structures. The grain size analysis indicates that in the central of the Kerpini Fault Block, the grain size is getting finer towards the south. The finer materials are situated close to foot-wall of the Roghi Fault South. This suggests the restricted basin which was controlled by the topographic expression of the uplifted Roghi

Fault South foot-wall. This restricted basin will then be filled by the finer material because of the low energy sedimentation regime.

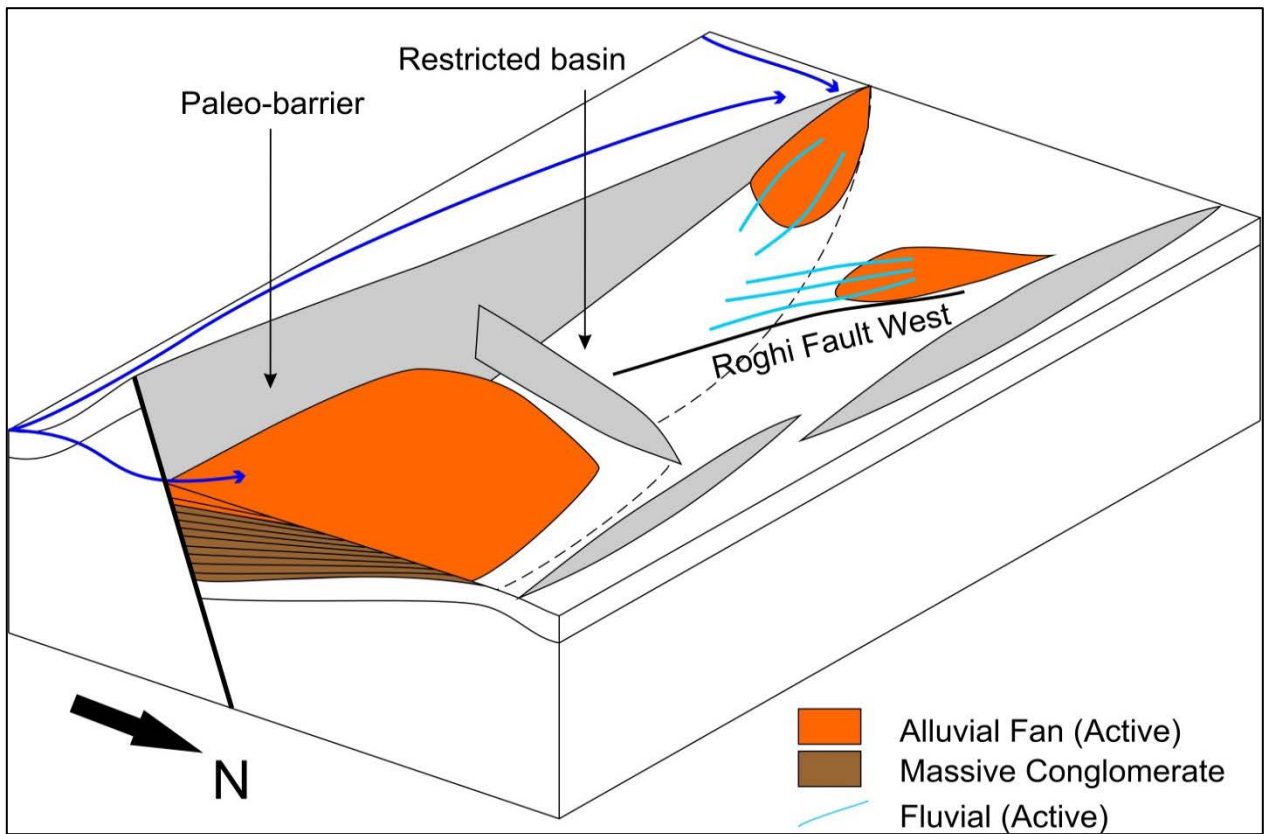


Figure 6.8: Structural and sedimentation model of the Kerpini Fault Block; Fault climax phase and development of the next fault block (without scale). *The Kerpini Fault and Roghi Fault South together form a greater accommodation space for the alluvial fan deposits in the eastern part of the Kerpini Fault Block. In this step, the Dhoumena Fault and Roghi Fault West started to move and resulted in development of an alluvial fan from the northern part of the area.*

Late syn-fault and channel incision, the initiation and peak of syn-faulting period has passed (Figure 6.9). The schematic model (Figure 6.9) shows that the units 2 and 3 of syn-fault deposits in the Kerpini Fault Block which are Massive conglomerate and Early Sandstone-Conglomerate have been deposited and filled the accommodation space within the Kerpini Fault Block. This phase was now showing the late syn-faulting events. It has been interpreted that the Vouraikos River bypassed the sediments to the next fault block to the north and no longer brought sediments into the Kerpini Fault Block. The rivers on the western part became active and there was a river which tried to incise unit 2 and unit 3. Since the flow direction of the rivers is always to find the weakest zone for them to flow, it was trying to flow to the east and was branching to the hanging-wall of the Dhoumena Fault Block, from its relay ramp which later formed alluvial fan deposits

in the Dhoumena Fault Block as the foot-wall uplift of the Dhoumena Fault became a barrier for them to flow northwards direction.

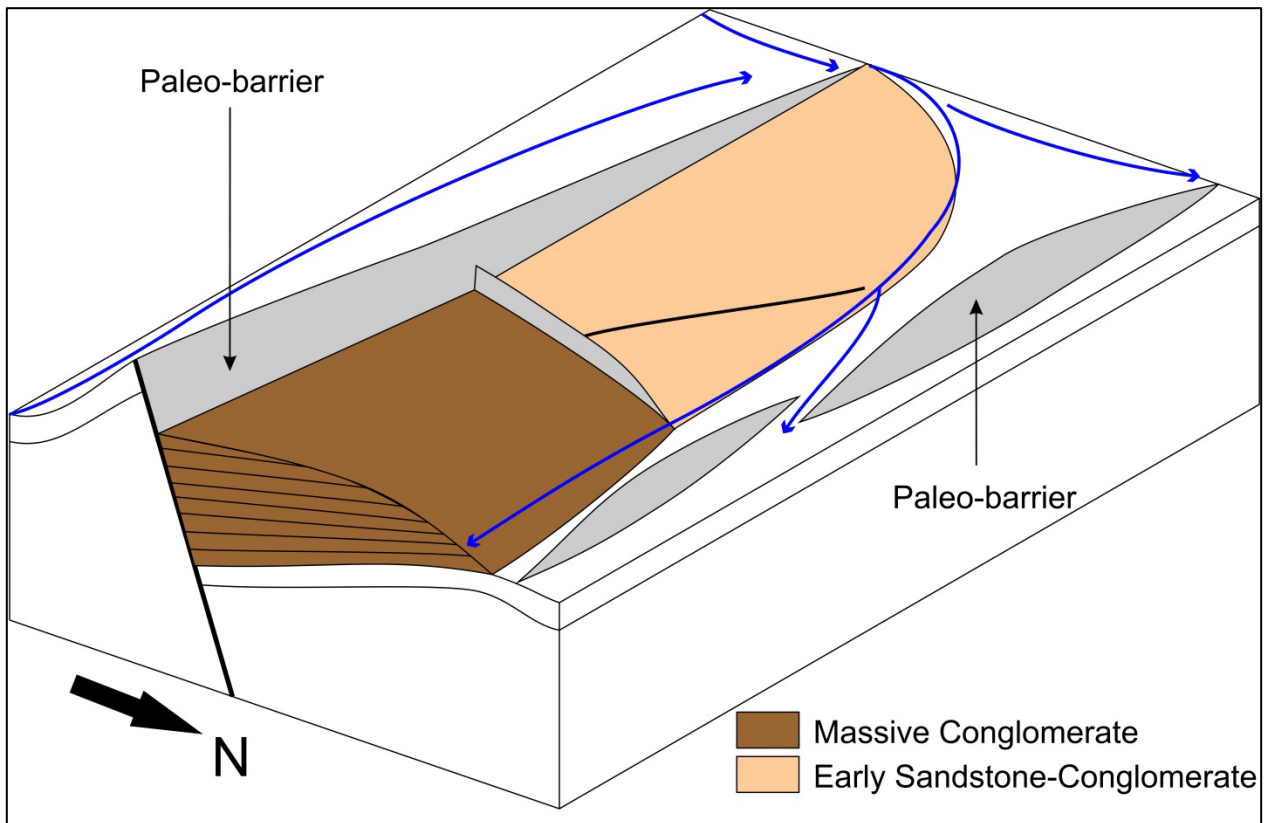


Figure 6.9: : Structural and sedimentation model of the Kerpini Fault Block; Late syn-fault and channel incision phase (without scale). This is the end of early and peak syn-faulting period whilst there is a river that was trying to flow to the east and incise the sediments of unit 2 and 3 because of the foot-wall uplift of the Dhoumena Fault topographic expression which became a boundary for the river to flow straight to the north. The river also has a branch in the relay zone of the Dhoumena Fault which later became the source of sediments of alluvial fan deposits in the Dhoumena Fault Block.

Post-fault phase, this is the final step of the syn-faulting period of the Kerpini Fault (Figure 6.10). In this step, the Kerpini Fault Block is interpreted to stop. The incised river deposited an Early Sandstone-Conglomerate (unit 4) in the immediate foot-wall of the Dhoumena Fault Block. The drainage of sediment source (rivers) moved and brought sediments to the next fault in the northern part of the area. The main event in this phase was erosion since the regional topography in this area is tilted to the north then the southern part may be exposed and become eroded away, producing what can be seen today in the Kerpini area.

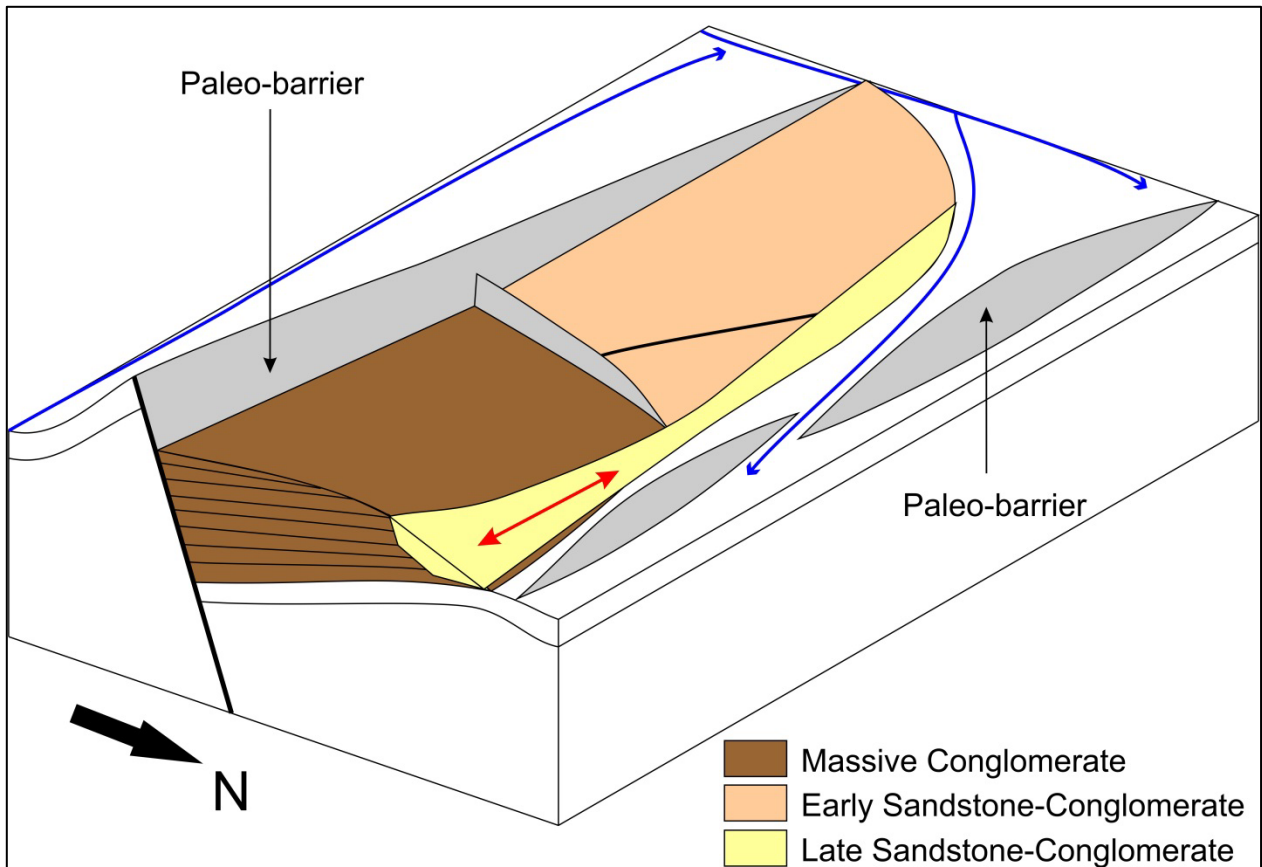


Figure 6.10: : Structural and sedimentation model of the Kerpini Fault Block; Post-fault phase (without scale). This is the final step of syn-faulting period in the Kerpini Fault Block. The Kerpini Fault Block has been interpreted to stop its movement and later on this area has been exposed until today and start to have an erosional period the produce what can be seen today in the field.

This evolution history has left questions; first, the position of unit 4 is now on elevation, they are sitting of the unit 2 and 3 close to the foot-wall of the Dhoumena Fault. Rotated fault block and long exposure time should have eroded them away. The second question is the configuration of the sedimentary layers which should not have consistent dip angles. The propagation concept, growth fault, and episodic fault still not answered the question as to why the dip angles of sedimentary layers in the Kerpini Fault Block are consistent. Future studies on the Kerpini Fault Block should attempt to address these questions.

Chapter 7 : CONCLUSIONS

The key conclusions of this surface geological study and modelling of Fault Controlled Sedimentation of the Kerpini Fault Block are:

- Fault movement has a big impact on the sedimentation of the intra fault block related to the reverse drag, fault propagation and evolution which may control the drainage of source sediments.
- The Kerpini Fault propagates to the west and the maximum throw is located in the east. The maximum fault displacement in the east is +/- 1200 to 1500m and gradually decreasing towards the tip in the west. The Kerpini Fault has been interpreted to be truncated by the Vouraikos Fault and also possibly by the Kerinitis Fault.
- There are 3 regional fault surround the area, Dhoumena Fault 1, Dhoumena Fault 2, and Kerpini Fault East. There are 5 intra block faults within Kerpini Fault Block which can be observed by looking at the unconformity relationship, facies and thickness variation of syn-fault deposits. Some of them may also be explained as the paleo-relief which is difficult to prove due to poor exposure and evidence.
- There are 4 lithology units which comprised the stratigraphy in the Kerpini Fault Block: basement, early sandstone-conglomerate, alluvial fan conglomerate, and late sandstone-conglomerate.
- Evolution of the growth of the fault would be expected to affect the sedimentary layers resulting in thickness and dip angles variations of syn-fault deposit. Lack of decreasing dip angle of sediments towards the younger deposits can be explained by the distance of reverse drag which might be far away from the fault (the modelling used 10km far away from the fault). However slight changes in dip angles (not completely consistent) may lead to another possibility that has been proposed to explain this feature. Episodic movement of the fault is another possible answer to explain the consistent dip angles within the Kerpini Fault Block.
- Sediment source for the Kerpini Fault Block are coming from the south and north. The southern sources are represented by the Vouraikos River in the eastern part, the Kerinitis River, also the branch of the Vouraikos River which bended due to the uplifted foot-wall of the Kerpini Fault. The northern source is represented by the erosion of uplifted foot-wall of Dhoumena Fault. The E-W river direction is special for Unit 4 sediment source.

REFERENCES

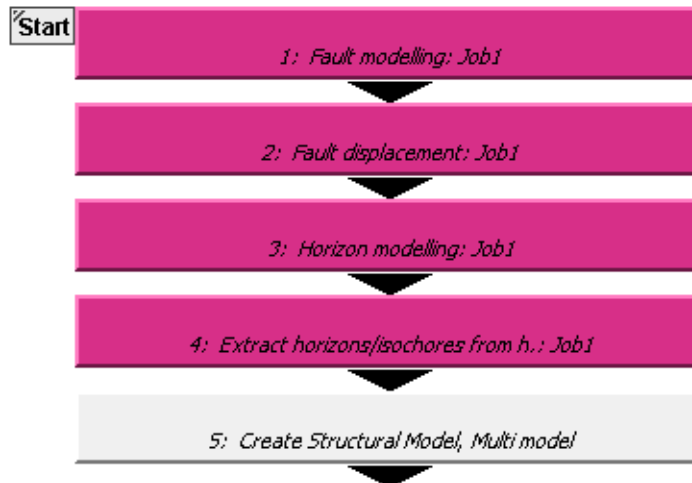
- Backert, N., Ford, M. and Malartre, F.** (2010) Architecture and sedimentology of the Kerinitis Gilbert-type fan delta, Corinth Rift, Greece. *Sedimentology*, **57**, 543-586.
- Barnett, J.A.M., Mortimer, J., Rippon, J.H., Walsh, J.J. and Watterson, J.** (1987) DISPLACEMENT GEOMETRY IN THE VOLUME CONTAINING A SINGLE NORMAL FAULT. *American Association of Petroleum Geologists Bulletin*, **71**, 925-937.
- Bell, R.E., McNeill, L.C., Bull, J.M. and Henstock, T.J.** (2008) Evolution of the offshore western Gulf of Corinth. *Geological Society of America Bulletin*, **120**, 156-178.
- Collier, R. and Jones, G.** (2004) Rift Sequences of the Southern Margin of the Gulf of Corinth (Greece) as Exploration / Production Analogues. *Search and Discovery*, **50007**.
- Doutsos, T. and Piper, D.J.W.** (1990) Listric faulting, sedimentation, and morphological evolution of the Quaternary eastern Corinth rift, Greece: First stages of continental rifting. *Geological Society of America Bulletin*, **102**, 812-829.
- Flotté, N. and Sorel, D.** (2001) Structural cross-sections through the Corinth–Patras detachment fault-system in northern Peloponnesus (Aegean arc Greece). *Bulletin Geological Society Greece*, **XXVI**, 235-241.
- Ford, M., Rohais, S., Williams, E.A., Bourlange, S., Jouselin, D., Backert, N. and Malartre, F.** (2013) Tectono-sedimentary evolution of the western Corinth rift (Central Greece). *Basin Research*, **25**, 3-25.
- Gawthorpe, R.L. and Leeder, M.R.** (2000) Tectono-sedimentary evolution of active extensional basins. *Basin Research*, **12**, 195-218.
- Ghisetti, F. and Vezzani, L.** (2005) Inherited structural controls on normal fault architecture in the Gulf of Corinth (Greece). *Tectonics*, **24**, TC4016.
- Gibson, J.R., Walsh, J.J. and Watterson, J.** (1989) Modelling of bed contours and cross-sections adjacent to planar normal faults. *Journal of Structural Geology*, **11**, 317-328.
- Goldsworthy, M. and Jackson, J.** (2001) Migration of activity within normal fault systems: examples from the Quaternary of mainland Greece. *Journal of Structural Geology*, **23**, 489-506.
- Groshong, R.H.** (2006) 3-D Structural geology "A Practical Guide to Quantitative Surface and Subsurface Map Interpretation". **Second Edition**.

- Gupta, S., Underhill, J.R., Sharp, I.R. and Gawthorpe, R.L.** (1999) Role of fault interactions in controlling synrift sediment dispersal patterns: Miocene, Abu Alaqa Group, Suez Rift, Sinai, Egypt. *Basin Research*, **11**, 167-189.
- Hamblin, W.K.** (1965) Origin of 'reverse drag' on the downthrown side of normal faults. *Bulletin of the Geological Society of America*, **76**, 1145-1163.
- Leeder, M.R., Mack, G.H., Brasier, A.T., Parrish, R.R., McIntosh, W.C., Andrews, J.E. and Duermeijer, C.E.** (2008) Late-Pliocene timing of Corinth (Greece) rift-margin fault migration. *Earth and Planetary Science Letters*, **274**, 132-141.
- Malatre, F., Ford, M. and Williams, E.A.** (2004) Preliminary biostratigraphy and 3D geometry of the Vouraikos Gilbert-type fan delta, Gulf of Corinth, Greece. *Comptes Rendus Geoscience*, **336**, 269-280.
- Moretti, I., Sakellariou, D., Lykousis, V. and Micarelli, L.** (2003) The Gulf of Corinth: an active half graben? *Journal of Geodynamics*, **36**, 323-340.
- Ori, G.G.** (1989) Geologic history of the extensional basin of the Gulf of Corinth (?Miocene-Pleistocene), Greece. *Geology*, **17**, 918-921.
- Ravnås, R. and Steel, R.J.** (1998) Architecture of Marine Rift-Basin Successions. *AAPG Bulletin*, **82**, 110-146.
- Schlische, R.W.** (1991) Half-graben basin filling models: new constraints on continental extensional basin development. *Basin Research*, **3**, 123-141.
- Schlische, R.W. and Anders, M.H.** (1996) Stratigraphic effects and tectonic implications of the growth of normal faults and extensional basins, **303**, pp. 183-203.
- Sorel, D.** (2000) A Pleistocene and still-active detachment fault and the origin of the Corinth-Patras rift, Greece. *Geology*, **28**, 83-86.
- Taylor, B., Weiss, J.R., Goodliffe, A.M., Sachpazi, M., Laigle, M. and Hirn, A.** (2011) The structures, stratigraphy and evolution of the Gulf of Corinth rift, Greece. *Geophysical Journal International*, **185**, 1189-1219.
- Walsh, J.J., Childs, C., Meyer, V., Manzocchi, T., Imber, J., Nicol, A., Tuckwell, G., Bailey, W.R., Bonson, C.G., Watterson, J., Nell, P.A.R. and Strand, J.A.** (2001) Geometric controls on the evolution of normal fault systems. *Journal of the Geological Society, London*, **186**, 157-170.
- Walsh, J.J. and Watterson, J.** (1987) Distributions of cumulative displacement and seismic slip on a single normal fault surface. *Journal of Structural Geology*, **9**, 1039-1046.
- Walsh, J.J. and Watterson, J.** (1988a) Analysis of the relationship between displacements and dimensions of faults. *Journal of Structural Geology*, **10**, 239-247.

- Walsh, J.J. and Watterson, J.** (1988b) Dips of normal faults in British Coal Measures and other sedimentary sequences. *Journal of the Geological Society, London*, **145**, 859-873.
- Walsh, J.J. and Watterson, J.** (1989) Displacement gradients on fault surfaces. *Journal of Structural Geology*, **11**, 307-316.

APPENDIX-1

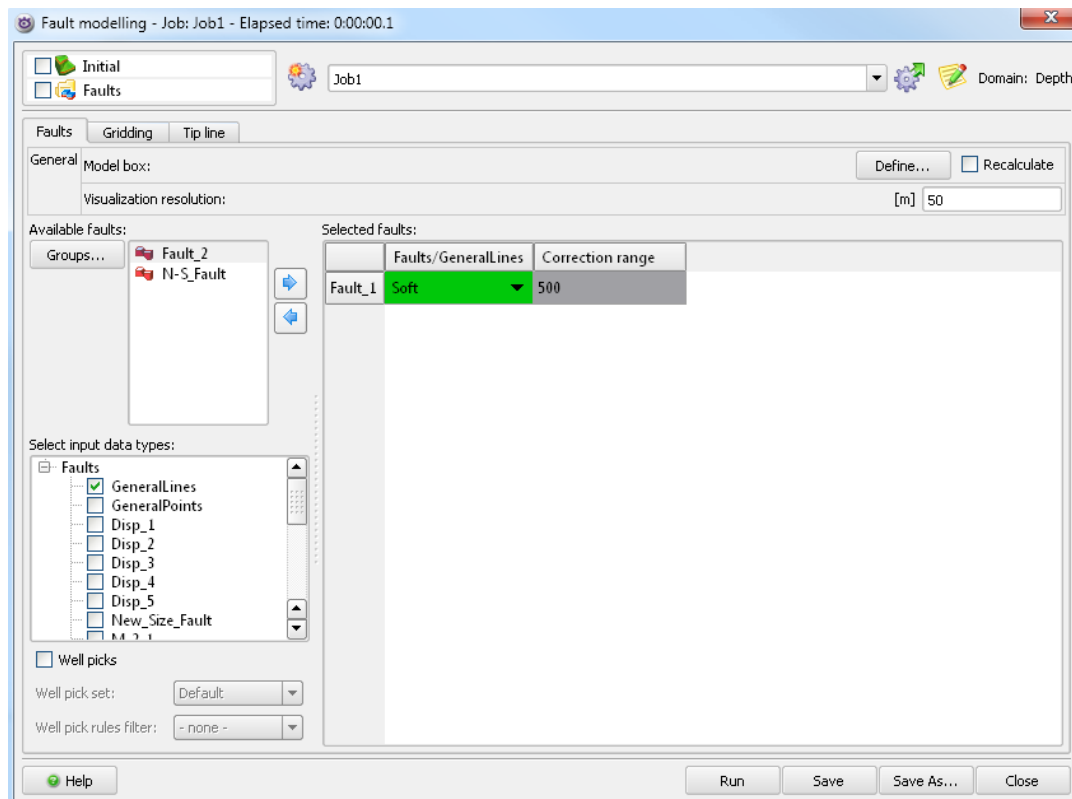
Structural model workflow in RMS 2013



Appendix 1: The workflow of modelling project.

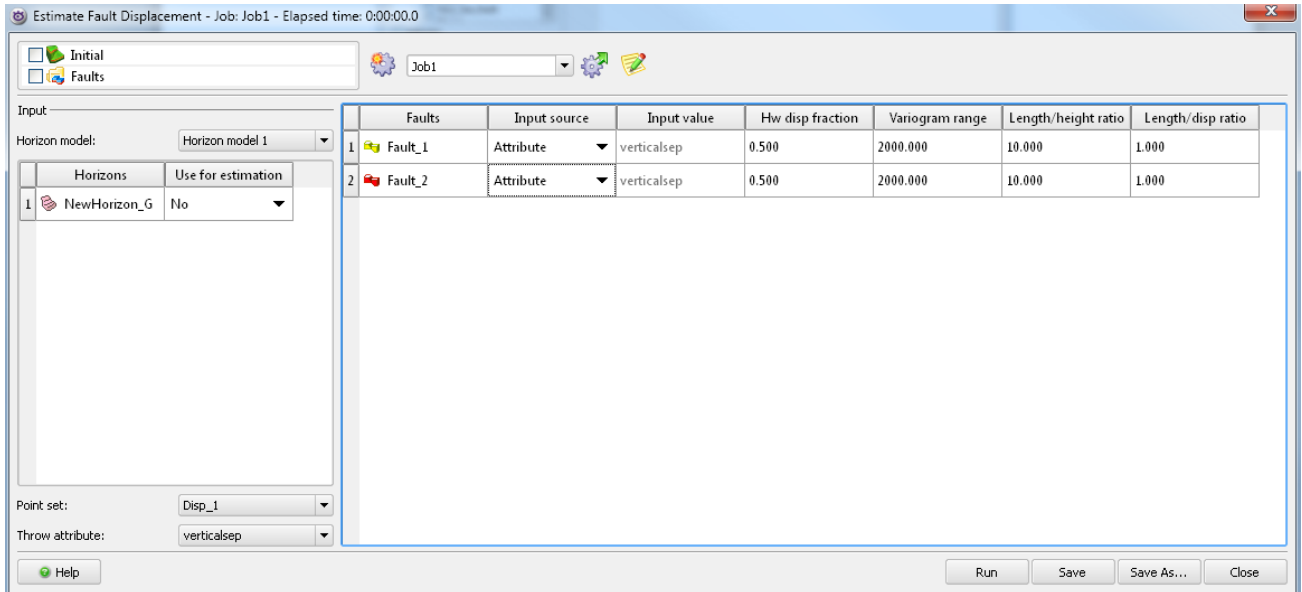
First, structural model must be created. Then, the modelling process can be continued by follow the workflow above:

1. Fault modelling; input the entire fault that you may want to include in the model, illustrated in the figure below.



Appendix 2: Fault modelling window in RMS 2013.

- Fault displacement; set the displacement distribution, you can use a horizon, maximum throw, or attribute (displacement points); in this case, attribute has been used for the modelling. The setting of this method can be seen in the figure below.



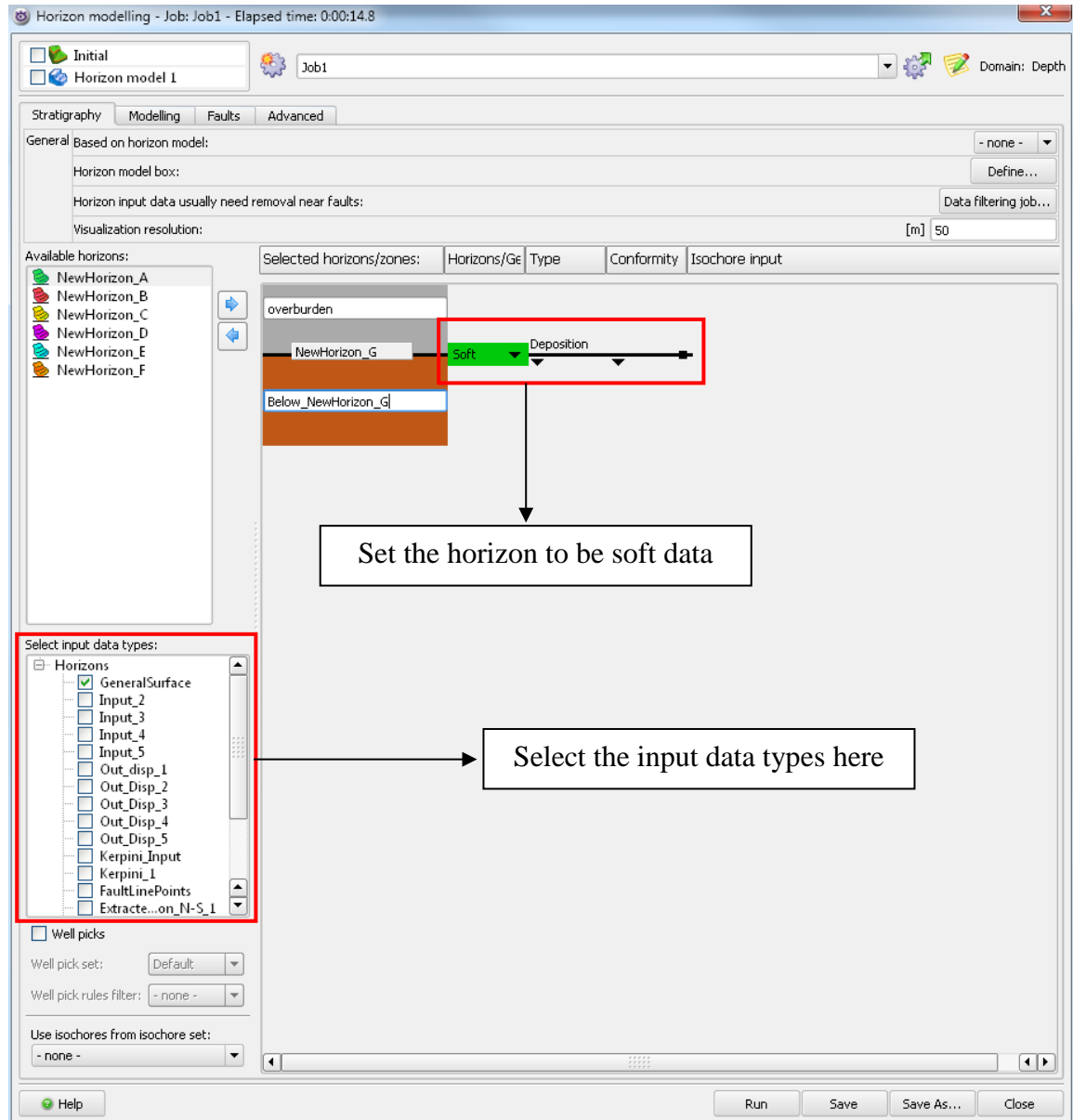
Appendix 3: Fault displacement window in RMS 2013.

X	Y	Z	Displacement (Throw)
180	-2300	0	1928
160	-2300	0	1936
140	-2300	0	1944
120	-2300	0	1952
100	-2300	0	1960
80	-2300	0	1968
60	-2300	0	1976
40	-2300	0	1984
20	-2300	0	1992
0	-2300	0	2000
-20	-2300	0	1992
-40	-2300	0	1984
-60	-2300	0	1976
-80	-2300	0	1968
-100	-2300	0	1960
-120	-2300	0	1952
-140	-2300	0	1944
-160	-2300	0	1936

The table beside is showing the example of how to build a displacement point set for certain fault. It should be specifying its X, Y, and Z positions as well as the amount of displacement.

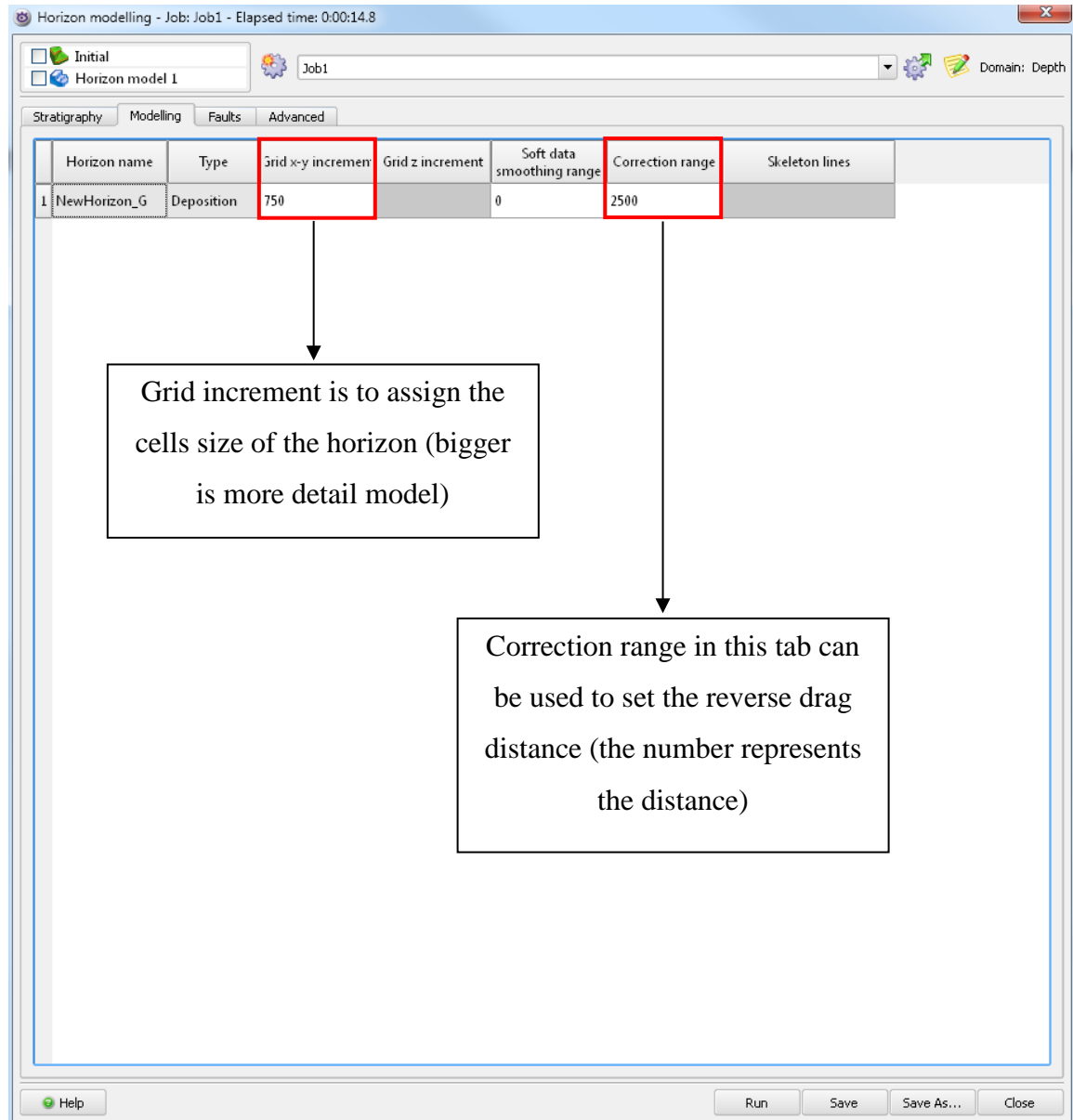
Appendix 4: Table is showing the example of displacement point set.

- Horizon modelling; the horizon modelling for this kind of workflow, must be done one by one for each horizon in each structural models. The figure below is showing the example for modelling the NewHorizon_G which is the oldest horizon in the model. In this tab below, the input data surface must be specified and it is recommended to using this horizon as the soft data instead of hard data.



Appendix 5: Horizon modelling window in RMS 2013. It is showing the stratigraphy tab of the process.

The next tab, Modelling tab, the parameters which are needed to be specified are the grid x-y increments, soft data smoothing range, and correction range. It depends on the standard to specify the grid x-y increment; in this case it was using 750. The correction range holds the important role for this modelling. This option is actually the way how the model can be built using different reverse drag. The number which is stated below represents the distance of zero displacement in the perpendicular direction to the fault.



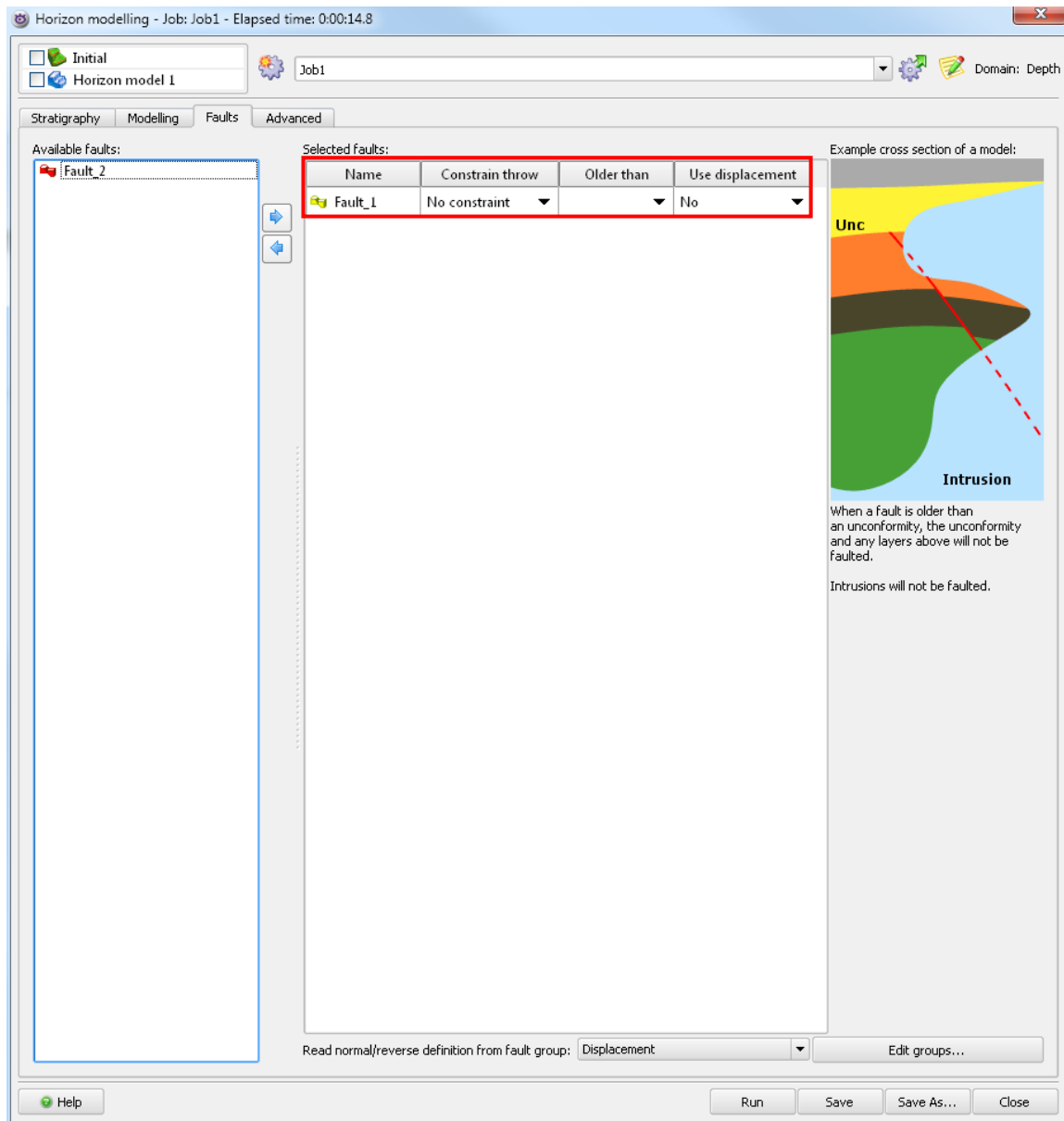
Horizon name	Type	Grid x-y increment	Grid z increment	Soft data smoothing range	Correction range	Skeleton lines
1 NewHorizon_G	Deposition	750		0	2500	

Grid increment is to assign the cells size of the horizon (bigger is more detail model)

Correction range in this tab can be used to set the reverse drag distance (the number represents the distance)

Appendix 6: Horizon modelling in RMS 2013. It is showing the modelling tab where the reverse drag and grid increment can be modified.

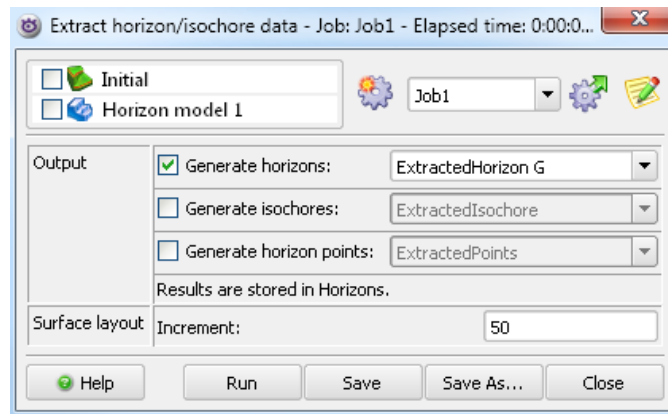
In Faults tab for horizon modelling below, all of the faults that want to be included into the model should be specified. After that, the using displacement option is also need to be clarified whether it should be modelled by using their displacements or not.



Appendix 7: Horizon modelling in RMS 2013. It is showing the faults tab, the incorporated fault should be specified.

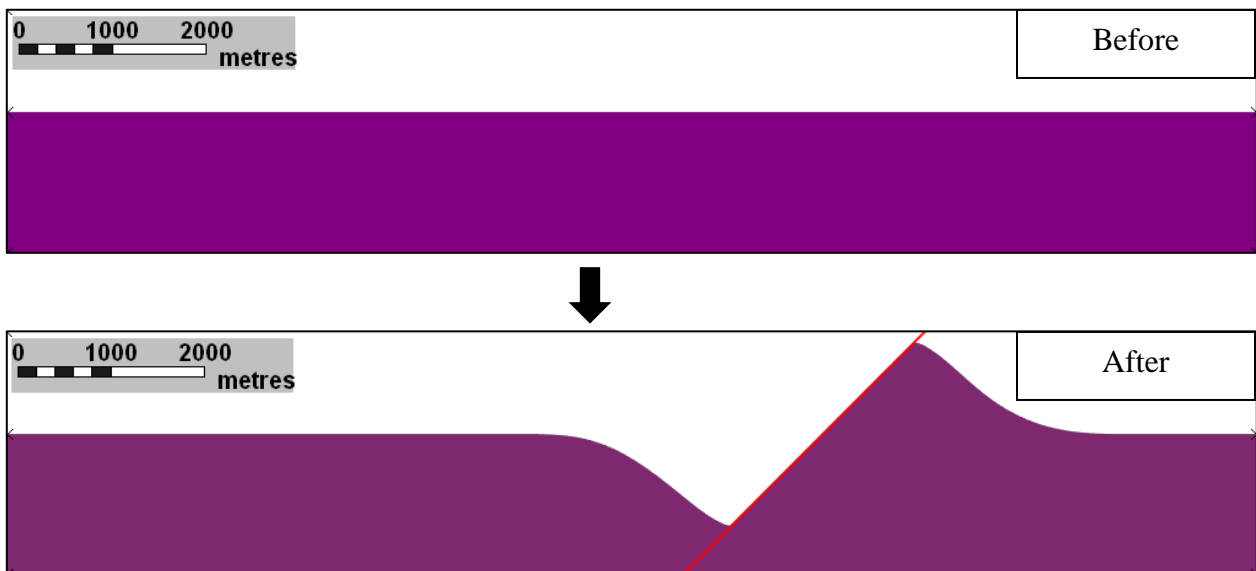
4. Extract horizons; this is kind of optional workflow if the modeler wants to extract the horizon from the modelling result for further works. By using this kind of task, it will try to extract the horizon from the modelling folder into the ordinary surface type of data.

Desired horizon should be selected and rename it whatever modeler wants and the increment of extraction should be specified in the task pane.



Appendix 8: Extract horizon window in RMS 2013. This is the tool to extract your horizons into surfaces.

After all these step have been done, the result will come up as a structural model including faults and horizon. The example result can be seen below.



Appendix 9: The result example of the modelling process showing the before (flat layer) and after (faulted horizon). All the steps must repeated by 4-5 times depend on how many horizons are needed into different structural models. Each structural model should have its own displacement point sets to model specific horizon. That is why; the important role in this modelling work is to build the displacement point sets because RMS 2013 is not designed to do the forward modelling of fault displacement, therefore, the creativity to build scenarios using the different displacement point sets is very important.